Evolution of the Geohydrologic Cycle During the Past 700 Million Years

Adam M. Angel

Dissertation submitted to the faculty of the Virginia Polytechnic Institute and State University in partial fulfillment of the requirements for the degree of

Ph.D. of Science
In
Geosciences

Robert J. Bodnar
Robert P. Lowell
Benjamin C. Gill
Alicia M. Wilson (University of South Carolina)

February 13, 2018
Blacksburg, VA

Keywords: geohydrologic cycle, numerical modeling, Earth history, cryosphere, biosphere, snowball Earth, global temperature

Evolution of the Geohydrologic Cycle During the Past 700 Million Years

Adam M. Angel

ABSTRACT

Water is a primary driver of the physical, geochemical and biological evolution of the Earth. The near-surface hydrosphere (exosphere) includes the atmosphere, cryosphere (glacial and polar ice), the biosphere, surface water, groundwater, and the oceans. The amounts of water in these various reservoirs of the hydrologic cycle have likely varied significantly over the past 700 Ma, with the cryosphere and continental biosphere reservoirs likely showing the most dramatic variations relative to the modern. For example, 700 Ma, during snowball-Earth conditions, the planet may have been almost entirely enveloped in ice, whereas throughout much of the Phanerozoic, greenhouse conditions predominately prevailed and the Earth had a much smaller cryosphere. Similarly, before about 444 Ma and the proliferation of land plants, the continental biosphere reservoir would have effectively non-existent. However, today, plants play a critical role in storage and transfer of water within the hydrologic cycle. Because the amount of water in the exosphere is thought to have remained relatively constant during the past 700 Ma, variations in the amounts of water held by the in the various exogenic reservoirs exert concomitant effects on other reservoirs in the exosphere.

We present a conceptual and numerical model that examines variations in the amount of water in the various reservoirs of the near-surface hydrologic cycle (exosphere) during the past 700 Ma and quantify variations in the rates of exchange of water between these reservoirs in deep time. We find that variations in the sizes of major reservoirs are primarily controlled by changes in global average temperature, and the flux of water between the atmosphere, surface water, and ocean reservoirs varies in concert with the waxing and waning of the cryosphere, with some fluxes decreasing to 0.0 kg/yr during snowball-Earth conditions. We find that the amount of water precipitated from the atmosphere to the cryosphere increases from greenhouse conditions to -10.5°C and decreases from -10.5°C to snowball-earth conditions, highlighting “tipping-point” behavior due to changes in temperature and cryosphere surface area. The amount of surface runoff to the oceans varies in proportion to the amount of water removed from the surface water reservoir and transferred into the continental biosphere. Variations in the movement of water between near-surface reservoirs that are driven by the waxing and waning of the cryosphere and emergence and growth of plant life thus have significant implications for the transfer of weathering products to the oceans and could contribute to short-term (<1 Ma) variations in seawater composition and isotopic signatures.

GENERAL ABSTRACT

Water drives the evolution of the planet, and the distribution of water throughout Earth's atmosphere and surface has varied during the geologic past. The amounts of water in the atmosphere, polar ice, the biosphere, surface water, groundwater, and the oceans have changed during the past 700 million years, and the polar ice and biosphere reservoirs have undergone the most significant changes during that time. For example, at extremely cold conditions the planet may have been covered in ice, and during warmer conditions the planet may have been covered in little to no ice. Similarly, before 444 million years ago, the biosphere on Earth's continental surface was almost non-existent. The evolution of land plants after 444 Ma resulted in an increase in the amount of water in the biosphere. Changes in the amounts of water in one reservoir of water over time will have effects on the other reservoirs of water in the water cycle.

We produce a numerical model that examines changes in the sizes of water cycle reservoirs and the movement of water between those reservoirs during the past 700 million years. Variations in reservoir sizes are primarily controlled by changes in global average temperature, and the movement of water between the atmosphere, surface water, and ocean reservoirs varies with changes in the amount of polar ice on Earth. We find that total annual precipitation to polar ice increases from greenhouse temperatures to -10.5°C and decreases from -10.5°C to cold snowball-earth temperatures due to changes in both temperature and the surface area of polar ice. The amount of surface runoff to the oceans varies in proportion to the amount of water removed from the surface water reservoir and transferred into the continental biosphere. Variations in the movement of water between reservoirs that are driven by the waxing and waning of polar ice and the growth of plant life have significant implications for the movement of dissolved material to the oceans and could contribute to short-term (<1 Ma) variations in seawater chemistry.

Table of Contents

List of Figures

List of Tables

List of Appendices

Introduction

1. Background

Water is arguably the most important natural resource on Earth. Without water, food could not be produced, resource extraction and manufacturing activity would cease and, indeed, humans and other life forms could not exist. Recent decades have witnessed a growing awareness and interest in the Earth's water resources as human population continues to expand and easily accessible clean water becomes more difficult to locate and produce. Moreover, recent increases in global average temperature are affecting the distribution of water within the exogenic hydrosphere, contributing to rising sea level, and catalyzing larger and more damaging storms. As such, there is a need to develop a better understanding of the linkages and feedbacks within the hydrologic cycle to better predict the future impacts of these changes and to gain a better understanding of the changes in the water cycle and their subsequent effects on other portions of the Earth the in the geologic past.

The geohydrologic cycle is comprised of various reservoirs on and near Earth's surface (the exosphere), and within the solid Earth (the geosphere) (Bodnar et al., 2013). The modern exosphere consists of six reservoirs, including the atmosphere (ATM), the cryosphere (CRYO), continental surface water (SW), groundwater (GW), the biosphere (BIO), and the oceans (Fig. 1A) (Berner and Berner, 2012 Drever, 1997. The largest of these reservoirs are the oceans that contain ~96.5% of all water in the near-surface hydrologic cycle. Ice on Earth (the cryosphere) contains ~1.75% of the total water in the exosphere and is the largest reservoir of fresh water on Earth. Plant life on Earth contains ~0.0003% of the total water in the exosphere and is the smallest of the six major

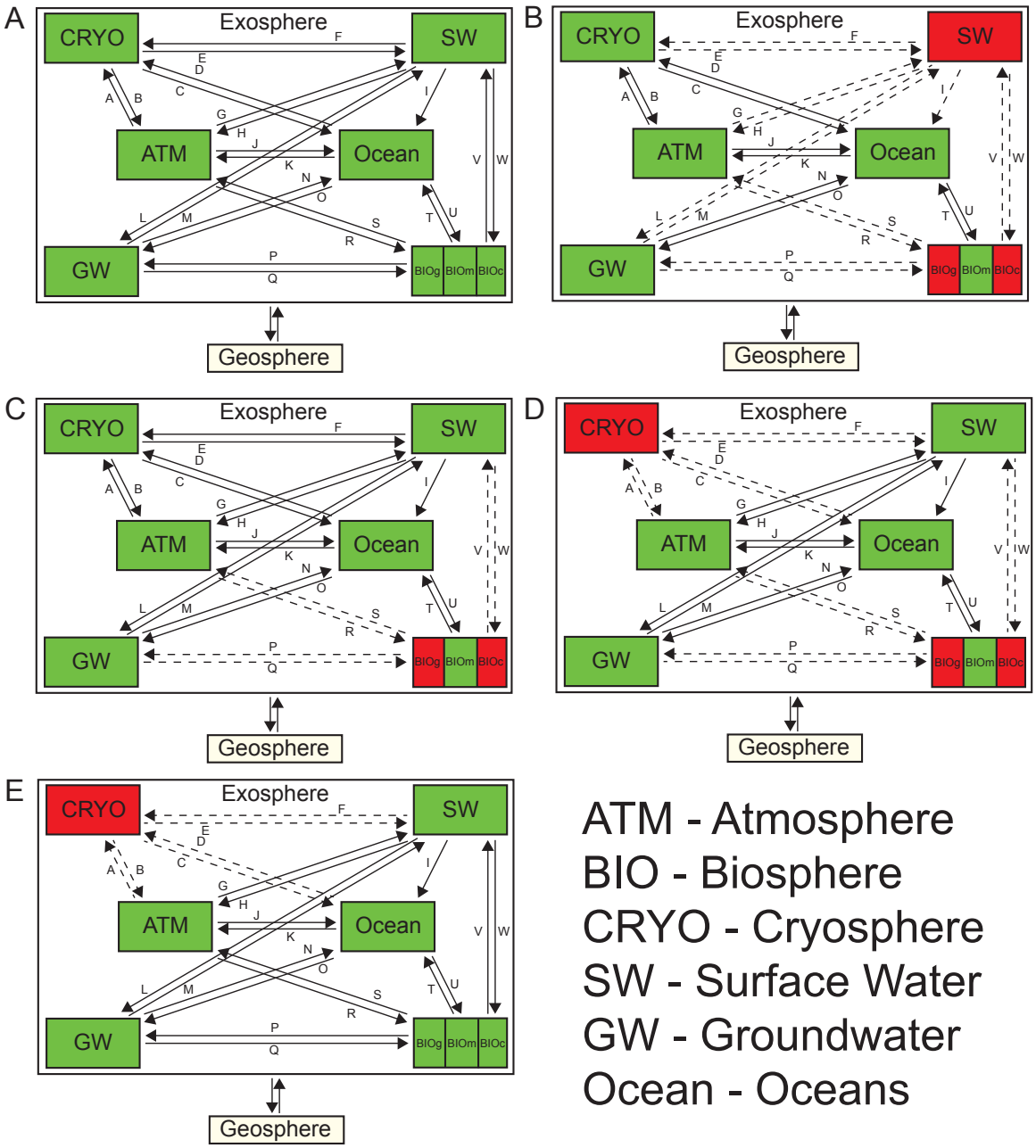

Figure 1: Box model of the exospheric hydrologic cycle showing the six major water reservoirs that comprise the exosphere, including the atmosphere (ATM), the cryosphere (CRYO), the biosphere (BIO), surface water (SW), groundwater (GW), and the oceans (Ocean). A green box indicates that the reservoir is part of the hydrologic cycle, and a red box indicates a reservoir that is absent and is not included in the hydrologic cycle. Solid lines connect reservoirs that exchange water, and arrows show the direction of water movement. Dashed lines originate or end at reservoirs that are not part of the hydrologic cycle at that time and, as such, water does not move into or out of that reservoir. Panel (A) represents the present hydrologic cycle with all six reservoirs included; panel (B) represents the water cycle during snowball Earth conditions when the Earth was enveloped in a shell of ice and the SW and continental BIO (BIOc) reservoirs were absent; panel (C) represents times in the late Proterozoic and early Phanerozoic (pre-444

Ma) when some ice existed on Earth but the continental biosphere had not yet developed; panel (D) represents greenhouse conditions during the late Ediacaran and early Cambrian before the continental biosphere had developed; panel (E) corresponds to the early Silurian when the continental biosphere had developed and greenhouse conditions applied.

exosphere reservoirs. The water in the geosphere consists of H_2O sequestered in the continental crust, oceanic crust, upper mantle, transition zone, lower mantle, and the core (Bodnar et al., 2013). The net flux of water between the exosphere and geosphere is small relative to fluxes between reservoirs within the exosphere. As such, during the past 700 Ma the amounts of water in both the exosphere and the geosphere remain essentially constant, but variation in relative amounts of water in the exosphere and geosphere over the history of the Earth is poorly constrained and a matter of debate (Bounama et al., 2001).

Owing to the numerous possible interactions between reservoirs, changes in either the amount of water in a given reservoir, or the amount of water transferred between any two reservoirs, will have a "ripple effect" on other reservoirs and processes in the exosphere. For example, melting of ice caps associated with increasing global temperature would lead to an increase in the amount of water in the ocean reservoir, causing sea level to rise. Rising temperature could change the areal proportion of the continents covered by glaciers and oceans and, thus, influences the amount of water in the SW reservoir and the amount of runoff from the continents to the oceans. Also increases in global temperature would influence the amount of water held in the atmosphere, as well as, rates of evaporation and precipitation.

In this study, we develop a numerical model that describes variations in the exosphere hydrologic cycle during the past 700 Ma, including temporal variations in the sizes of reservoirs (amount, or mass, of water contained in the reservoir) as well as temporal variations in fluxes between reservoirs. This is accomplished through a series of equations describing variations in physical parameters (such as global average temperature) that control and drive the distribution of water on Earth as a function of

time. These relationships are incorporated into a model that balances the amount of water in the hydrologic cycle. Such an approach is required because, as any single parameter describing the hydrologic cycle (such as the size of the CRYO reservoir) changes, by necessity the amount of water in one or more of the other reservoirs in the hydrologic cycle must change in order to maintain a constant total amount of water in the hydrosphere. This, in turn, necessitates changes in the fluxes between reservoirs to allow the amount of water in a given reservoir to increase or decrease with time. As such, the model involves a series of interdependent components (equations) that must be solved iteratively and simultaneously to arrive at a solution, and this is implemented using the commercially available STELLA™ dynamic system modeling package.

The two reservoirs within the hydrologic cycle that have experienced the largest relative variation during the past 700 Ma are the cryosphere (CRYO) and the continental biosphere (BIO_c) (discussed below), and we describe the evolution of these two reservoirs, and factors that drive the observed variations, in some detail. We then introduce these variations into the overall hydrologic cycle to develop a complete model for the hydrologic cycle during the past 700 Ma. We note that throughout the text we refer to these changes as occurring "during the Phanerozoic" for simplicity, recognizing that the 700 Ma time period includes both the Phanerozoic (541 Ma to today) as well as the end of the Neoproterozoic Era (1 Ga to 542 Ma).

2. Overview of the Numerical Model

The numerical model describing the evolution of the exosphere presented here includes all water present in the six major near-surface reservoirs: the atmosphere (ATM), the cryosphere (CRYO), the biosphere (BIO), surface water (SW), groundwater

(GW), and the oceans (Oceans). Previous workers have estimated that the total amount of water in the exosphere is 1.41×10^{21} kg (summarized in Bodnar et al., 2013). As discussed above, we assume that the amount of water in the exosphere has remained constant during the past 700 Ma, although some workers have suggested that the amount of water in the exosphere has gradually decreased with time as water is transferred to the interior of the Earth via subduction (Bounama et al., 2001). Given these uncertainties and the lack of information to rigorously test models related to variations in the total amount of water in the exosphere during the past 700 Ma, we assume that the total mass of water has remained constant and that the mass of water in the exosphere (M_{EXO}) equals the sum of the masses of water in the various reservoirs comprising the exosphere ($\Sigma M_{RES,t}$), and equals 1.41×10^{21} kg:

$$\Sigma M_{RES} = M_{ATM} + M_{BIO} + M_{ICE} + M_{SW} + M_{GW} + M_{OCEAN} = M_{EXO} = 1.41\text{x}10^{21}\ \text{kg} \quad (1)$$

We calculate the amount of water in any given reservoir at any time during the past 700 Ma based on the physical, chemical and/or biological factors that influence the capacity of the reservoir. These various factors have been quantified through a series of differential equations that describe the relationship between, for example, average global temperature and the various fluxes that control the movement of water through the exosphere. Thus, the amount of water in the cryosphere (CRYO) is a function of global average temperature, and we develop a relationship between global average temperature and the amount water in CRYO at any time in the past based on the amount of water in the CRYO reservoir at present, and the rate of change of this value as a function of global average temperature. The amount of water within a given reservoir in the exosphere (M_{RES}) at any time *t* during the past 700 Ma (t) is a function of those parameters that

control the amount of water in the reservoir ($f(g)$) and the manner in which they vary with time ($g(t)$):

$$M_{RES,t} = f(g(t)) \quad (2)$$

The amount (mass) of water in a reservoir at any given time ($M_{RES,1}$) is related to the amount of water in the reservoir at some earlier time ($M_{RES,0}$) and the rate of change in the amount of water in the reservoir with time ($\frac{d(M_{RES,0})}{dt}$) according to:

$$M_{RES,1} = M_{RES,0} + (\frac{d(M_{RES,0})}{dt} * \Delta t) \quad (3)$$

where Δt is the time increment of interest. Variations in the amount of water in a reservoir are directly related to fluxes of water into or out of that reservoir, and the processes that lead to temporal variations in the fluxes. For example, evaporation adds water to the atmosphere, and precipitation removes water from the atmosphere. At any specific time, the evaporation and precipitation fluxes are essentially equal, but their magnitudes will change over longer time periods in response to changing global average temperature. Accordingly, the rate of change in the amount of water in a reservoir ($\frac{d(M_{RES,0})}{dt}$) equals the sum of the fluxes of water into that reservoir ($\Sigma F_{RES,in,0}$), minus the sum of the fluxes of water out of that reservoir ($\Sigma F_{RES,out,0}$):

$$\frac{d(M_{RES,0})}{dt} = (\Sigma F_{RES,in,0} - \Sigma F_{RES,out,0}) \quad (4)$$

The amount of water in a reservoir at any time ($M_{RES,1}$) is related to the amount of water in the reservoir at some earlier time ($M_{RES,0}$), plus the sum of the fluxes of water into ($\Sigma F_{RES,in,0}$) and out of ($\Sigma F_{RES,out,0}$) the reservoir over some time interval (Δt), according to Equations 3 and 4:

$$M_{RES,1} = M_{RES,0} + [(\Sigma F_{RES,in,0} - \Sigma F_{RES,out,0}) * \Delta t] \quad (5)$$

117 In general, temporal variations in fluxes of water between most reservoirs described
118 below are reasonably well-understood, at least semi-quantitatively. However, some water
119 fluxes have not been previously quantified or are only poorly constrained. For these, we
120 have estimated a flux that varies in response to changing conditions based on our
121 understanding of the modern hydrologic cycle, or have chosen a flux that "balances" the
122 other fluxes linked to a common reservoir. As discussed above, the sum of the fluxes of
123 water into a reservoir over some time ($\sum Flux_{IN}$) minus the sum of the fluxes of water
124 out of a reservoir over that time ($\sum Flux_{OUT}$) must equal the change in the amount of
125 water in that reservoir over that same period of time ($\frac{dM_{RES}}{dt}$). For example, the change in
126 the size of the CRYO reservoir during the past 700 Ma is largely a function of global
127 average temperature. Moreover, water moves into the CRYO reservoir from the ATM,
128 SW and ocean reservoirs, and water moves out of the CRYO reservoir and into those
129 same reservoirs. The fluxes of water from the ATM and ocean reservoirs to the CRYO
130 reservoir (and vice versa), and the drivers that control temporal variations, are reasonably
131 well constrained based on analogs with the modern water cycle, whereas the flux of water
132 from the CRYO reservoir to the oceans is less well constrained (discussed below). As
133 such, the CRYO → Ocean flux was selected to balance those fluxes that are well
134 constrained and to be consistent with estimated variations in the size of the CRYO
135 reservoir, as described in detail below.
136 In a similar manner, variations in the size of the continental biosphere (BIOc) during
137 the past 444 Ma impact the amounts water contained in other reservoirs of the hydrologic
138 cycle as well as fluxes between reservoirs. Below we examine the impact of temporal
139 variations in reservoir sizes and fluxes associated with the cryosphere and the continental
140 biosphere and consider the impact of these variations on the movement and storage of

141 water in the hydrologic cycle. We first focus on variations in the cryosphere, followed by
142 an examination of temporal variations in the continental biosphere, recognizing that these
143 two reservoirs are linked indirectly through the surface water and atmosphere reservoirs.
144 Thus, a change in one of these reservoirs has the potential to affect the other because the
145 total amount of water in the hydrologic cycle remains constant.
146
147 **3. The Cryosphere**
148 **a. Role of the Cyrosphere in Earth's Modern Water Cycle**
149 Shrinking of the Earth's cryosphere as a result of global warming has captured both
150 the scientific and public interest for the past several decades. The Intergovernmental
151 Panel on Climate Change (2007) states *"Warming of the climate system is unequivocal,*
152 *as is now evident from observations of increases in global average air and ocean*
153 *temperatures, widespread melting of snow and ice, and rising global average sea level"*.
154 It is estimated that if all of the ice on Earth were to melt, and if all of that water flowed
155 into the oceans, sea level would rise by ~80 m (Poore et al., 2000). Coastal cities and
156 small-island developing states would be devastated by this worst-case scenario, where
157 even a relatively modest increase in sea level can impact, if not entirely decimate, the
158 economic viability of the community (Bloetcher and Romah, 2015; Arnall and Kothari,
159 2015; Betzold, 2015).
160 The recent melting of polar and glacial ice has also been linked to variations in
161 regional ocean chemistry and biological primary production. For example, an increase in
162 glacial melt runoff results in an increase in dissolved Fe transported to the oceans, which
163 promotes the growth of local algal blooms (Aguilar-Islas et al., 2008; Lyons et al., 2015;
164 Hawkings et al., 2015). Conversely, the seasonal freezing of sea ice locally produces

highly saline brines, which inhibits primary production (Gleitz et al., 1995). On a global scale, increasing imbalances in the amount of water exchanged between oceans and sea ice will dilute the concentrations of all constituents in seawater. Because marine primary producers are sensitive to variations in seawater chemistry, changes in global seawater composition related to variations in the amount of water held in the oceans and the cryosphere are likely to not only affect sea level and impact coastal areas, but has the potential to affect the marine biosphere and the global ocean ecosystem.

Variations in Earth's ice budget also influence the transport of water and other constituents that are linked to the CRYO reservoir. For example, the loss of Arctic sea ice is linked to increased regional evaporation and a subsequent increase in the proportion of Arctic-sourced moisture in the atmosphere (Kopec et al., 2015). This increase in evaporation, in turn, influences the amount of water precipitated from the atmosphere to the oceans, to the CRYO reservoir, and to the continental surface where the water is incorporated into the surface water reservoir. This, in turn, is likely to lead to increased surface runoff to the oceans (Kopec et al., 2016; Bintanja and Selten, 2014), resulting in an increase in sediment transport to the ocean basins. Furthermore, the melting of sea ice releases chlorine gas (Cl_2) to the atmosphere, where it catalyzes ozone degradation and mercury oxidation reactions (Liao et al., 2014). The increase in chlorine gas related to sea ice melting occurs on a diurnal basis; it is uncertain whether annual or longer-term sea ice loss is associated with a more significant increase in atmospheric chlorine concentration.

The cryosphere also plays a major role in the global circulation of heat (thermal energy) via oceanic currents. Warm water flows from the equator to the poles, and colder water is returned to the equator (Trenberth et al., 2001). Models of the Atlantic thermo-haline circulation system suggest that ocean currents become destabilized when the

amount of water in the cryosphere varies, and the destabilization of ocean circulation has been linked to Arctic climate variations over the past 21 ka (Schmittner et al., 2002).

b. Evolution of the Cryosphere during the past 700 Ma

The main control on the amount of water contained in the CRYO reservoir is average global temperature, and this in turn is a function of the amount of CO_2 (and other greenhouses gases) in the atmosphere, albedo, and long-term variations in the Earth's orbit (Milankovitch cycles) (Goddéris et al., 2014). The mass of water contained in the CRYO reservoir today has been estimated by various methods, with a general consensus that the CRYO reservoir contains ~3.32×10^{19} kg H_2O (Bodnar et al., 2013). The amount of water contained in the CRYO reservoir has been greater than and less than the modern value at various times in the past 700 Ma. The amount has been greater during major glaciation events during the past 700 Ma that include the Cryogenian Sturtian and Marinoan glaciations, the Late Ordovician event, and the Permo-Carboniferous glaciations, and the amount of water held by the CRYO reservoir has been less than the present amount during a significant portion of the Phanerozoic when average global temperatures were higher than today's value (14.6°C). During much of the Phanerozoic, an extensive cryosphere likely did not exist on Earth when greenhouse conditions prevailed, except perhaps as high elevation continental glaciers.

The Sturtian glaciation occurred during the Cryogenian from 720 to 660 Ma and is the first of two "snowball-Earth" events during the Cryogenian (Cohen et al., 2013). Previous workers have correlated paleogeographic reconstructions of continent distribution with dated glaciogenic formations to determine the global extent of the Sturtian glacial event (Prave, 1999). It is well accepted that atmospheric CO_2 estimates

213 can be used as a proxy for global average temperature, and previous workers have used
214 global carbon cycle models to estimate the conditions necessary to achieve low-latitude
215 glaciation (Hyde et al., 2000; Goddéris et al., 2003; Pollard and Kasting, 2004).
216 Furthermore, Swanson-Hysell et al. (2010) suggested that increased continental
217 weathering that sequesters CO_2 in carbonate promoted the decrease in atmospheric CO_2
218 during the Cryogenian. There is some debate regarding the latitudinal extent of the
219 Sturtian ice caps, with some workers suggesting that equatorial seas open to the
220 atmosphere existed even during snowball conditions (Pierrehumbert, 2005). Furthermore,
221 some models of snowball-Earth conditions suggest that the thickness of the ice was not
222 uniform, with some areas of the planet's surface covered by up to 5 km of ice (Hyde et
223 al., 2000). In our model we assume that polar ice extended to the equator and that
224 snowball earth conditions apply during the Cryogenian. This assumption affects the
225 movement of water between the oceans and atmosphere, whereby at snowball earth
226 conditions there is no ocean-atmosphere interaction, while at slushball earth conditions
227 some amount of water would be exchanged between the oceans and atmosphere. It is
228 thought that the end of the Sturtian glaciation occurred rapidly due to increased
229 submarine volcanic activity and a relatively rapid (<1 Ma) increase in the amount of CO_2
230 released to the atmosphere (Pierrehumbert, 2011; Gernon et al., 2016), as evidenced by a
231 carbon isotope excursion in the rock record (Halverson et al., 2005). The exact timing of
232 the submarine CO_2 release is unknown, and the extent of latitudinal ice cap retreat during
233 this period is also uncertain.
234 The Marinoan glaciation occurred during the late Cryogenian, from 650 to 635 Ma,
235 and is the second Cryogenian "snowball-Earth" event (Cohen et al., 2013). Glaciogenic
236 Marinoan formations occur near Sturtian-age formations, and Sturtian and Marinoan

237 formations are usually separated by thick cap limestones indicative of glacial retreat
238 between the two glacial events (Pierrehumbert et al., 2011). Paleogeographic
239 reconstructions suggest that the Marinoan glaciation was as extensive as the Sturtian,
240 with ice caps advancing to equatorial regions (Ewing et al., 2014). The debates and
241 uncertainties surrounding the Marinoan glaciation are similar to those concerning the
242 Sturtian glaciations. In addition, rifting of the Rodinia supercontinent occurred during the
243 Marinoan (Prave, 1999; Mahan et al., 2010). It is hypothesized that increased tectonic
244 activity associated with this event influenced the timing and extent of glacial advance and
245 retreat, although the magnitude of this influence is uncertain (Goddéris et al., 2003).
246 Furthermore, it is unclear whether the global ice caps fully melted and retreated to the
247 poles at the end of the Marinoan, or if some permanent ice remained (Ewing et al., 2014).
248 The Late Ordovician glaciation (~444 Ma) is thought to be a leading cause of the
249 Ordovician-Silurian extinction, one of the "big five" extinction events in Earth history
250 (Sheehan, 2001). Evidence in the rock record for this event includes glaciogenic deposits
251 beneath Silurian shales in North Africa, and oxygen isotopic excursions (both $\delta^{18}O$ and
252 clumped isotopes) in late Ordovician and early Silurian brachiopods suggest a brief
253 period of global cooling lasting ~0.5 Ma (Brenchley et al., 2001; Finnegan et al., 2011).
254 There is some debate regarding the duration of the glaciation, with earlier work
255 suggesting that the Late Ordovician glaciation lasted ~35 Ma (Frakes et al., 1992).
256 Furthermore, the mechanisms that triggered the onset of the glacial event remain
257 uncertain. Lenton et al. (2014) suggest that the evolution and radiation of primitive land
258 plants during the late Ordovician drew down atmospheric CO_2, resulting in global
259 cooling and subsequent glaciation. Others suggest that continental configuration
260 (Herrmann et al., 2004) or increased silicate weathering (Young et al., 2010; Lefebvre et

al., 2010) may have shifted climatic conditions to favor widespread glaciation. There is general consensus that the Late Ordovician glaciation ended quickly (over a period of <1 Ma), although the cause is debated. Many workers associate the end of the glaciation with an increase in atmospheric CO_2, which resulted in global warming and the collapse and retreat of the polar ice sheets (Saltzman and Young, 2005; Young et al., 2010).

The Permo-Carboniferous glaciation occurred from 350 to 290 Ma. Glacial deposits in the Karoo basin of South Africa are the primary evidence for global cooling and glacial advance (DuToit, 1956; Visser, 1987). It is largely accepted that the widespread radiation of land plants throughout the Carboniferous reduced atmospheric CO_2 and led to a decrease in average global temperature (Ronov, 1982). As discussed above, atmospheric CO_2 can be used as a proxy for global average temperature; the reduction of CO_2 in the atmosphere by incorporation into land plants is linked to a decrease in temperature, thus causing the onset of glaciation (Berner, 1994; Mii et al., 1999). There is uncertainty surrounding the latitudinal extent of glaciation and the exact timing of glacial retreat during and after this period. Gulbranson et al. (2010) used radiometric dating of glaciogenic deposits in Argentina to infer that the Permo-Carboniferous glaciation occurred in distinct "pulses" rather than as a singular onset of widespread glaciation.

The modern glacial period began at 35 Ma, shortly after the Paleocene-Eocene thermal maximum (Zachos et al., 2008) and has continued to the present day. This period includes the Last Glacial Maximum (LGM) that occurred approximately 100,000 years ago. The latitudinal extent of the LGM is evidenced by terminal moraines at low latitudes in North America and the widespread prevalence of glaciogenic lakes at higher latitudes (Ehlers and Gibbard, 2004). There is extensive debate regarding the exact timing of ice cap formation at the poles during the most recent glaciation, but it is well accepted that

285 the Antarctic ice sheet formed millions of years before the Arctic ice caps (Zachos et al.,
286 2008). Scher et al. (2014) analyzed chemical signatures in Antarctic coastal sediments
287 and suggested that the modern ice caps originally "flickered" into and out of existence
288 before the onset of permanent ice.
289
290 **c. Conceptual Model of the Cryosphere**
291 The modern cryosphere (CRYO) consists of all permanent ice on Earth and includes
292 the polar ice caps and glaciers that occur mostly at high elevations and/or high latitudes.
293 The amount of water in the CRYO reservoir today is estimated to be 3.32×10^{19} kg
294 (Bodnar et al., 2013). Within the hydrologic cycle, the CRYO reservoir exchanges water
295 directly with the atmosphere (ATM), oceans, and surface water (SW) reservoirs (Fig.
296 1A), and is indirectly linked to the groundwater (GW) and biosphere (BIO) reservoirs –
297 i.e., some water released from melting of ice flows into the SW reservoir and is
298 subsequently transferred into either the GW or into the BIOc reservoir.
299 The CRYO reservoir interacts directly with the ATM reservoir via precipitation onto
300 the Earth's surface, and some amount of H_2O is transferred directly from the CRYO
301 reservoir back into the ATM reservoir via sublimation (Fig. 1A). As average global
302 temperature increases and ice over the oceans melts, the resulting melt water is
303 transferred directly from the CRYO reservoir to the ocean reservoir. When ice on the
304 continents melts, the resulting water is transferred directly to the surface water reservoir.
305 Some water from the SW reservoir is transferred into the biosphere; note that before ~444
306 Ma the continental biosphere (BIOc) did not exist and this part of the cycle was absent
307 (Fig. 1B, C, D), However, before 444 Ma, a marine biosphere (BIOm) was present and
308 water was exchanged between the ocean biosphere and the oceans (Fig. 1C). As average

309 global temperature decreases and the CRYO reservoir grows, water from the oceans and
310 from the atmosphere are incorporated into the growing ice sheet, and on the continents
311 water from the atmosphere and surface water are transferred into the CRYO reservoir.
312 During the past 700 Ma Earth's climate has fluctuated from one in which permanent
313 ice sheets covered most of the Earth ("snowball-Earth" conditions during the
314 Cryogenian) to those in which ice was largely absent (greenhouse-Earth conditions), with
315 cyclical periods that allow for some ice caps on the Earth (similar to present-day
316 conditions) (Fig. 1A). Periods when average global temperature is greater than 18°C are
317 considered greenhouse periods (Oerlemans et al., 1998; Grénier et al., 2015) during
318 which no significant cryosphere existed on Earth. When average global temperature is
319 between +18°C and -27°C, some ice is present (mostly at polar latitudes and high
320 elevations). When average global temperature is less than -27°C, the planet is covered in
321 permanent ice to produce snowball Earth conditions (Hyde et al., 2000) (Fig. 2).
322 The Cryogenian Period lasted from 720-635 Ma (Cohen et al., 2013) and represents a
323 period of time when average global temperature was sufficiently low that the planet was
324 enveloped in a thick sheet of ice much of the time. During the Cryogenian the Earth's
325 near-surface water cycle would have been very different from the modern cycle, as the
326 continental biosphere and surface water reservoirs did not exist (Fig. 1B), and the flux of
327 water between the cryosphere and the oceans and atmosphere would have differed
328 significantly from the modern.
329 The beginning of the Ediacaran period at about 635 million years ago is associated
330 with dramatic increases in tectonic and volcanic activity at mid-ocean ridges, increasing
331 atmospheric CO_2 content, and increasing global temperature as snowball-Earth conditions
332 subsided (Gernon et al., 2016; Lund et al., 2016). This, in turn, exposed the continents

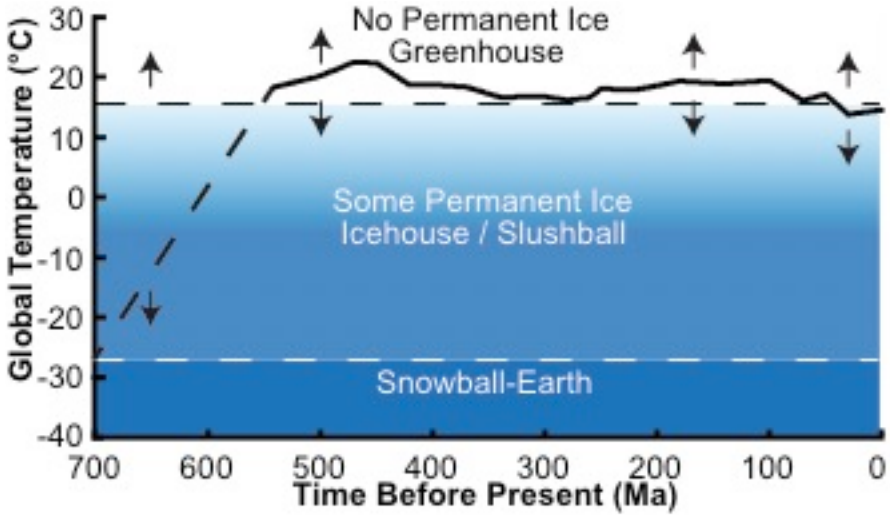

Figure 2: Relationship between global average temperature and waxing and waning of the cryosphere during the past 700 Ma. Periods when average global temperature is greater than 18°C are considered greenhouse periods (Grénier et al., 2015) when no polar ice exists on Earth and the cryosphere is not included in the hydrologic cycle. Periods when average global temperature is between 18°C and -27°C are periods when some ice is present (Hyde et al., 2000) and the cryosphere reservoir is included in the hydrologic cycle. Periods when average global temperature is less than -27°C represent snowball-Earth periods when the planet is completely covered in ice (Hyde et al., 2000). Temperature estimates from 542 Ma to the present are based on the global carbon cycle model of Godderis et al. (2014).

and oceans to the atmosphere and reintroduced the SW reservoir as a component of the exosphere, and water was exchanged between the SW reservoir and adjacent reservoirs in the hydrologic cycle (Fig. 1C). As global temperature continued to increase and the climate transitioned toward greenhouse conditions, Earth's cryosphere disappeared and no permanent ice existed on Earth for a significant portion of the Phanerozoic (Fig. 2). During greenhouse conditions, the amount of water in the CRYO reservoir and the transfer of water into and out of the CRYO reservoir were essentially nil (Fig. 1D). Note that during this period of the early Phanerozoic the continental biosphere had not fully developed and exchange of water between this portion of the biosphere and adjacent reservoirs also did not occur (Figs. 1B, C, D). As such, the reservoirs comprising the hydrologic cycle were limited to the oceans, atmosphere, surface water, groundwater and the marine and subsurface biospheres.

In the late Ordovician, the continental biosphere developed and plants began to exchange water with the atmosphere and SW reservoirs through transpiration and photosynthesis (Fig. 1E). Note that at this time greenhouse conditions prevailed, and no permanent ice was present on Earth (Figs. 1E, 2). As life radiated across the continental surface, plants began drawing down atmospheric CO_2, resulting in lower global average temperatures, leading to the onset of permanent ice at the poles during the late Pennsylvanian. Thus, the cryosphere reservoir and exchange of water between the CRYO reservoir and adjacent reservoirs again became a component of the hydrologic cycle (Fig. 1A). Since that time, Earth's climate and the hydrologic cycle have fluctuated from periods when some permanent ice was present (late Pennsylvanian-early Triassic glaciation and the Oligocene-present period) (Fig. 1A) to periods of greenhouse conditions when the Earth was ice-free (Fig. 1E).

357 The impact of the cryosphere on present-day, short-term geohydrologic processes is
358 easily recognized, and it is logical to assume that the waxing and waning of the
359 cryosphere on a much larger scale during the past 700 Ma has had a similar but more
360 pronounced influence on the Earth's hydrologic cycle, affecting both the sizes of the
361 other major water reservoirs and the amount of water moving between those reservoirs.
362 As discussed above, while the general timing of glacial events in the past is reasonably
363 well constrained, much uncertainty exists concerning the rate at which the CRYO
364 reservoir expanded or shrank, whether ice was present and grew at a constant rate during
365 the entire glacial event or if the CRYO reservoir expanded and shrank episodically during
366 the overall event. There is also uncertainty as to whether permanent ice extended to the
367 equator during snowball Earth conditions, or if some open ocean was present. While the
368 driver of CRYO expansion and shrinkage was global average temperature, some
369 uncertainty exists concerning the specific factors that resulted in temperature fluctuations.
370 Owing to these uncertainties, we assume that the CRYO reservoir size is a simple
371 function of global average temperature, without consideration of the drivers of global
372 temperature variations.
373
374 **4. The Continental Biosphere**
375 **a. Role of the Continental Biosphere in Earth's Modern Water Cycle**
376 The biosphere reservoir of the hydrologic cycle is comprised of three sub-reservoirs:
377 the continental biosphere (BIOc) which consists of all living organisms (primarily land
378 plants) on Earth's continental surface, the marine biosphere (BIOm) which consists of all
379 living organisms in Earth's oceans, and the subsurface biosphere (BIOg) which consists
380 of microorganisms in Earth's subsurface. The modern BIOc reservoir is estimated to

contain 2.9×10^{15} kg H_2O (Bodnar et al., 2013), while the amounts in the marine biosphere (BIOm) and in the subsurface biosphere (BIOg) are 2.3×10^{12} kg and 1.75×10^{15} kg, respectively. Recently, however, Kallmeyer et al. (2012) re-evaluated the amount of subseafloor biomass and, incorporating their new value into a global estimate, reported a total subsurface biomass that is 50-78% lower than that reported by Whitman et al. (1998). Accordingly, using this new estimate the total amount of water contained in the subsurface biosphere (BIOg) would be reduced by these same amounts.

Within the modern hydrologic cycle, the BIOc reservoir is directly linked to the atmosphere (ATM), and surface water (SW) reservoirs (Fig. 1A), and is indirectly linked to the cryosphere (CRYO), groundwater (GW) and ocean (Ocean) reservoirs. Plants take up water from the surface water reservoir through their root systems and incorporate a small amount of that water into biomass. Some plants (epiphytes) extract water vapor directly from the atmosphere through their leaves. The remaining water that is not used to build biomass is transpired back to the atmosphere as water vapor. As plants die, the water in the decaying biomass is transferred back into the surface water reservoir.

The continental biosphere plays a major role in critical zone geohydrologic processes. According to the National Research Council (2001), the critical zone is the *"heterogeneous, near surface environment in which complex interactions involving rock, soil, water, air, and living organisms regulate the natural habitat and determine the availability of life-sustaining resources"*. Indeed, the continental biosphere provides pathways for water between the atmosphere and continental surface waters. The distribution of land plants also influences surface runoff, where extensive root systems take up surface water and mediate the flow of water to the oceans via rivers and streams. Furthermore, deforestation and poor farming practices increase regional topsoil erosion,

405 which can reduce the arability of farmland and hinder agricultural efforts (Pimentel et al.,
406 1995; Zheng, 2006). Recently, concerns have been raised concerning the effects of rapid
407 deforestation on climate change (Shukla et al., 1990; Gash et al., 1996). The removal of
408 plants from the global biome reduces the amount of CO_2 that is removed from the
409 atmosphere by plants during photosynthesis, which in turn results in an increase in
410 atmospheric CO_2 and an increase in global average temperature (Bala et al., 2006).
411 During the last few centuries especially, anthropogenic activities have contributed
412 substantial amounts of CO_2 to the atmosphere (Zimen and Altenhein, 1973), and
413 deforestation has reduced the ability of the biosphere to buffer this rapid change in
414 atmosphere chemistry.
415
416 **b. Evolution of the Continental Biosphere during the past 700 Ma**
417 Before the Silurian (~444 Ma), sophisticated land plants did not exist, and Earth's
418 continents were covered in mosses and other primitive, low-biomass plants that required
419 a nearby source of water to survive (Koslowski and Greguss, 1959). Here, we define the
420 beginning of the continental biosphere at 444 Ma, and assume that before this time the
421 BIOc reservoir was not a significant component of the hydrologic cycle. Note, however,
422 that a biosphere was present in the oceans and water was exchanged between the marine
423 biosphere and the oceans before 444 Ma (Fig. 1B, C, D). It is uncertain if a significant
424 subsurface biosphere existed on the continents before the development of land plants.
425 The diversity of plant flora, as well as the emergence and dominance of particular
426 groups of flora, has varied since the beginning of the Silurian. Progymnosperms, conifer-
427 like trees with fern-like leaves, formed the planet's first forests during the middle
428 Devonian (Algeo and Scheckler, 1998). Pteridosperms, or "seed ferns", became the most

diverse plant group during the Carboniferous, and the proliferation of these plants led to a drawdown of pCO_2 and a period of global cooling (DiMichele et al., 2001). During the early Mesozoic, proper ferns were the most diverse and abundant flora on Earth (Hallam, 1985) and shortly thereafter conifers became the dominant group during the early Cretaceous (Harris, 1976; Hallam, 1985). Following the dominance of conifers and since the beginning of the Cenozoic, angiosperms have been the most diverse group of plants on Earth (Martin, 2006; Crisp and Cook, 2011; Graham, 2011).

Five major extinctions that destroyed a significant fraction of life on Earth (and, presumably, reduced the amount of water in the BIO reservoir) have been recorded during the Phanerozoic. During these events a majority of life was rapidly (<1 Ma) destroyed (Jablonski and Chaloner, 1994). Diversity of both marine and continental organisms sharply decreased during these extinction periods (Sepkoski, 1993), but marine taxa and continental taxa were affected differently by these events (Benton, 1993, 1995). The amount of time needed to recover taxon diversity depends on the severity of the extinction event (Sepkoski, 1994). Recent studies of deforested Amazon jungle suggest that biomass can recover 90% of its diversity in about 66 years, depending on the extent of devastation and availability of water (Poorter et al., 2016). This rapid recovery suggests that land plant biomass likely recovered very quickly (instantaneously in a geologic sense) following a major extinction event.

The Ordovician-Silurian extinction occurred at the end of the Ordovician (~444 Ma) and destroyed ~26% of all family taxa (Jablonski and Chaloner, 1994) (Table 1). The extinction occurred in two phases that coincide with the onset and offset of the Hirnantian glaciation; the first phase coincides with the growth of ice caps and lowering of seawater temperature, and the second phase coincides with the melting of ice caps and a brief

		BIO H_2O (kgx10^{14})		Percent change in fluxes					
Event	Extinction	Total	Destroyed	BIO fluxes	ATM->Ocean,SW	GW->Ocean	GW->SW	SW->GW	SW->Ocean
Late Devonian	27%	5.49	1.48	-27%	-0.045%	-1.66%	-0.023%	-0.045%	0.16%
End Permian	55%	12.5	6.88	-55%	-0.21%	-7.16%	-0.11%	-0.21%	0.77%
End Triassic	43%	15.8	6.79	-43%	-0.20%	-6.85%	-0.10%	-0.20%	0.72%
KT Impact	11%	24.8	2.73	-11%	-0.091%	-2.51%	-0.047%	-0.091%	0.34%

Table 1: The impact of Phanerozoic extinction events on the amount of water contained in the continental biosphere and changes in fluxes of

period of continental shelf anoxia (Brenchley et al., 2001). Owing to the small number of primitive land plants on Earth before the Silurian, this event mostly affected marine life, and the fossil record does not show a decrease in the number of continental plant family taxa during this event (Benton, 1993). Thus, land plants were not significantly influenced by the late Ordovician extinction and, as a result, this event had little impact on the role of the continental biosphere (BIOc) in the global hydrologic cycle.

The Late Devonian extinction occurred at the end of the Devonian period (~360 Ma) and destroyed ~22% of all family taxa (Jablonski and Chaloner, 1994) (Table 1). Benton (1995) estimated that perhaps 23 plant family taxa were eliminated during this event, which comprised 27% of all land plant families. There is some debate regarding the timing of the Late Devonian extinction, with some workers suggesting that the extinction consisted of multiple distinct events occurring over a 25 Ma time period (McGhee, 1988; Sole and Newman, 2002). Various explanations for the decline in biodiversity have been offered, including ocean anoxia (Bond et al., 2004), extraterrestrial impact (Claeys et al. 1992; McGhee, 2001), or a general decrease in speciation (Bambach et al., 2004).

The End Permian extinction occurred at 252 Ma and marks the transition from the Paleozoic Era to the Mesozoic Era. It is estimated that ~51% of all family taxa (Jablonski and Chaloner, 1994) and ~70% of all land species (Retallack et al., 2006) and up to 55% of all land plant taxa were destroyed during this most extensive extinction event in Earth's history (Benton, 1995; Benton and Twitchett, 2003) (Table 1). Erwin (2000) discussed several mechanisms that could have triggered the extinction, including plate tectonic and volcanic activity, variations in seawater chemistry, ocean anoxia, and bolide impact. Benton and Twitchett (2003) attributed catastrophic "runaway greenhouse" changes in atmosphere and ocean chemistry to large igneous province formation and

477 contemporaneous ash bed deposition. Ecological niches opened after the extinctions, and
478 the evolution and radiation of ferns and conifers occurred shortly after this event
479 (McElwain and Punyasena, 2007).
480 The End Triassic extinction event occurred at ~201 Ma and destroyed ~22% of all
481 family taxa (Jablonski and Chaloner, 1994) and up to 43% of all land plant taxa (Benton,
482 1995) (Table 1). Recently, Blackburn et al. (2013) associated the event with the
483 emplacement of the Central Atlantic Magmatic Province (CAMP) and a concomitant
484 rapid (~600 ka) release of CO_2 to the atmosphere (Schaller et al., 2011) and decrease in
485 ocean pH at this time (Hönisch et al., 2012). Blackburn et al. (2013) also note that the
486 biological recovery from this extinction occurred ~100 ka after the extinction; the number
487 of land plant family taxa continued to increase after this event (Benton, 1995).
488 The K-T Impact occurred at 65 Ma and destroyed the dinosaurs as well as 16% of all
489 family taxa worldwide (Schulte et al., 2010; Jablonski and Chaloner, 1994). Seventy-five
490 (75) plant family taxa were destroyed during the extinction event, making up 11% of all
491 land plant families (Benton, 1995). D'Hondt et al. (1998) used carbon isotope excursions
492 in marine sediments to estimate that the marine biosphere recovered from the K-T Impact
493 within ~3 Ma after the event. It is uncertain how rapidly the continental biosphere
494 recovered from the impact event.
495
496 **c. Conceptual Model of the Continental Biosphere**
497 The amount of H_2O contained in continental plant biomass on Earth has varied from
498 essentially nil before the Silurian to the present-day value, although the factors that
499 control how that amount has varied over time are poorly understood. To our knowledge,
500 there are no defensible estimates of the rate at which biomass on the continents increased

501 during the Phanerozoic, and here we assume a linear increase with time for reasons
502 discussed below. The manner in which the size of the continental biosphere grows
503 influences variations in the amounts of water transferred between the biosphere and other
504 reservoirs within the exosphere, and thus has implications for the entire water cycle. The
505 impact of the biosphere on present-day, short-term (< 10 ka) geohydrologic processes is
506 easily recognized, and it is logical to assume that the growth and decline of the biosphere
507 during the past 444 Ma has had a similar influence on Earth's hydrologic cycle. In our
508 model we also examine the short-term (instantaneous to 10 ka) modifications to the
509 hydrologic cycle associated with each of the five major extinction events, assuming
510 instantaneous loss of biomass followed by gradually recovery.
511
512 **Algorithms Describing Variations in Sizes of Exosphere Reservoirs in Deep Time**
513 Here we describe the manner in which the amount of water contained in the various
514 reservoirs in the exosphere has varied during the past 700 Ma, as well as the rationale
515 behind the algorithms employed to achieve these estimates (summarized in Table 2 and
516 Table 3). In the following, the size of a reservoir indicates the mass of water (in kg)
517 contained in the reservoir.
518
519 **1. Variations in the CRYO reservoir**
520 Presently, it is estimated that the CRYO reservoir contains ~3.32×10^{19} kg of H_2O
521 (Bodnar et al., 2013). The manner in which the size of the CRYO reservoir varies with
522 average global temperature is uncertain, but various studies indicate that no permanent
523 ice existed on Earth when the average global temperature was ≥18°C (Grénier et al.,
524 2015). Thus, we develop a relationship between the size of the cryosphere and average

Reservoir	Modern Amount (kg H_2O)	Equation
Cryosphere	3.32×10^{19}	$M_{CRYO} = (-1.04x10^{19} * T_{AVG}) + 1.85x10^{20}$
Atmosphere	1.3×10^{16}	Eqns. 5-9 (see text)
Continental biosphere	2.9×10^{15}	Before 444 Ma: 0 kg H_2O After 444 Ma: $M_{BIOc,T} = M_{BIOc,T-1} + (6.5x10^{12}\ kg\ H_2O)$
Surface water	2.07×10^{17}	$M_{SW,T} = \left(2.23x10^{17} * SA_{exposed\ continent\ fraction,T}\right)$
Groundwater	1.05×10^{19}	1.05×10^{19} kg H_2O
Oceans	1.37×10^{21}	$M_{OCEAN} = M_{EXO} - (M_{CRYO} + M_{ATM} + M_{BIOc} + M_{SW} + M_{GW})$

Table 2: Summary of relationships that describe variations in the amounts of water in major exospheric reservoirs on Earth.

Flux	Modern Flux (kg H_2O/yr)	Drivers	Equation
ATM➔CRYO	2.51×10^{15}	T, CRYO SA	$F_{CRYO\ Pptn.,T} = F_{Total\ Pptn.,T} * (SA_{CRYO\ fraction,T}{}^2)$
CRYO➔ATM	2.00×10^{14}	CRYO SA	$F_{Sublimation,T} = F_{Sublimation,modern} * \frac{SA_{CRYO\ fraction,T}}{SA_{CRYO\ fraction,modern}}$
OCEAN➔CRYO	1.50×10^{16}	T	$F_{Sea\ Ice\ Freeze,T} = F_{Sea\ Ice\ Freeze,modern} * \frac{M_{CRYO,T}}{M_{CRYO,modern}}$
CRYO➔OCEAN	1.73×10^{16}	Balance	$F_{Sea\ Ice\ Melt,T} = (F_{CRYO\ Pptn.,T} + F_{Sea\ Ice\ Freeze,T} + F_{Glacial\ Advance,T}) - (F_{Sublimation,T} + F_{Deglaciation,T})$
CRYO➔SW	4.10×10^{14}	T	$F_{Deglaciation,T} = (9.855x10^{12} * T) + 2.66x10^{14}$
SW➔CRYO	4.10×10^{14}	Balance	$F_{Glacial\ Advance,T} = F_{Deglaciation,T}$
ATM➔SW	1.43×10^{17}	T, CRYO SA	$F_{SW\ Pptn.,T} = F_{Total\ Pptn.,T} * 0.29 * (1 - SA_{CRYO\ fraction,T}{}^2)$
ATM➔OCEAN	3.50×10^{17}	T, Balance	$F_{Ocean\ Pptn.,T} = F_{Total\ Pptn.,T} - F_{CRYO\ Pptn.,T} + F_{SW\ Pptn.,T}$
SW➔ATM	3.34×10^{16}	T, Balance	$F_{SW\ Evaporation,T} = 0.2608 * F_{SW\ Pptn.,T}$
OCEAN➔ATM	4.53×10^{17}	Balance	$F_{Ocean\ Evaporation,T} = (F_{Total\ Pptn.,T} + F_{ATM\rightarrow BIOc,t}) - (F_{Sublimation,T} + F_{SW\ Evaporation,T} + F_{BIOc\rightarrow ATM,t})$
SW➔OCEAN	1.00×10^{17}	T, CRYO SA	$F_{Runoff,T} = F_{SW\ Pptn.,T} - F_{SW\ Evaporation,T} - F_{SW\rightarrow BIOc}$
SW➔GW	3.35×10^{16}	Balance	$F_{SW\rightarrow GW,T} = (F_{Deglaciation,T} + F_{SW\ Pptn.,T} + F_{GW\rightarrow SW,T} + F_{BIOc\rightarrow SW,t}) - (F_{Glacial\ Advance,T} + F_{SW\ Evaporation,T} + F_{Runoff,T} + F_{SW\rightarrow BIOc,t})$
GW➔SW	3.34×10^{16}	T, Balance	$F_{GW\rightarrow SW,T} = 0.333 * F_{Runoff,T}$
OCEAN➔GW	2.60×10^{14}	-	$F_{OCEAN\rightarrow GW,t} = Perimeter_{Coastline,t} * F_{OCEAN\rightarrow GW,t}$
GW➔OCEAN	3.50×10^{14}	Balance	$F_{SGD,T} = (F_{SW\rightarrow GW,T} + F_{SGR,T}) - F_{GW\rightarrow SW,T}$
SW➔BIOc	5.56×10^{16}	BIO	$F_{SW\rightarrow BIOc,t} = F_{SW\rightarrow BIOc,modern} * \frac{M_{BIOc,t}}{M_{BIOc,modern}}$
BIOc➔ATM	5.50×10^{16}	BIO	$F_{BIOc\rightarrow ATM} = 0.99 * F_{SW\rightarrow BIOc}$
BIOc➔SW	9.00×10^{13}	BIO	$F_{BIOc\rightarrow SW,t} = F_{BIOc\rightarrow SW,modern} * \frac{M_{BIOc,t}}{M_{BIOc,modern}}$
ATM➔BIOc	3.44×10^{13}	Balance	$F_{ATM\rightarrow BIOc,t} = (F_{BIOc\rightarrow SW,t} + F_{BIOc\rightarrow ATM}) - F_{SW\rightarrow BIOc,t}$

Table 3: Summary of mathematical expressions that describe variations in the amounts of water in major exospheric reservoirs on Earth. See text for complete description of individual terms.

global temperature using a linear extrapolation from 0 kg water in the cryosphere at 18°C to 3.32×10^{19}kg of water in the cryosphere at 14.6°C (the current average global temperature), and linearly extrapolate this relationship to -27°C to provide an estimate of the size of the CRYO reservoir during snowball Earth conditions (Fig. 3):

$$M_{CRYO} = (-9.76x10^{19} * T_{AVG}) + 1.76x10^{20} \quad (6)$$

where M_{CRYO} is the amount of water in the CRYO reservoir (kg) and T_{AVG} is average global temperature. We note that the actual manner in which the CRYO reservoir "grows" with decreasing temperature is uncertain, but the exact relationship between the amount of polar ice and temperature is of secondary concern because we are examining the effect that changing the size of one reservoir has on the other reservoirs in the cycle, and the effects on adjacent reservoirs will scale with actual size of the CRYO reservoir. Accordingly, the amount of water in the cryosphere at snowball Earth conditions (global average temperature ≤ -27°C) is calculated to be 4.39×10^{20} kg. This amount of ice corresponds to an ice sheet averaging ~1 km thick covering the entire Earth. This ice thickness is consistent with the Ashkenazy et al. (2013) model of latitudinal ice flow during cooling climate periods, whereby ~26% of all water in both the cryosphere and ocean reservoirs is sequestered in polar ice during snowball-Earth conditions. We also note that Hyde et al. (2000) estimated that polar ice sheets up to 5 km thick could have been present on landmasses during snowball-Earth conditions. For comparison, the mean thickness of the Antarctic ice sheet today is ~2.2 km, with a maximum thickness of ~4.8 km (http://nsidc.org/data/seaice_index/).

The physical location of the CRYO reservoir on the surface of the Earth influences which other reservoirs exchange water with the CRYO reservoir. For example, during glacial growth and retreat on the continents the CRYO reservoir exchanges water with

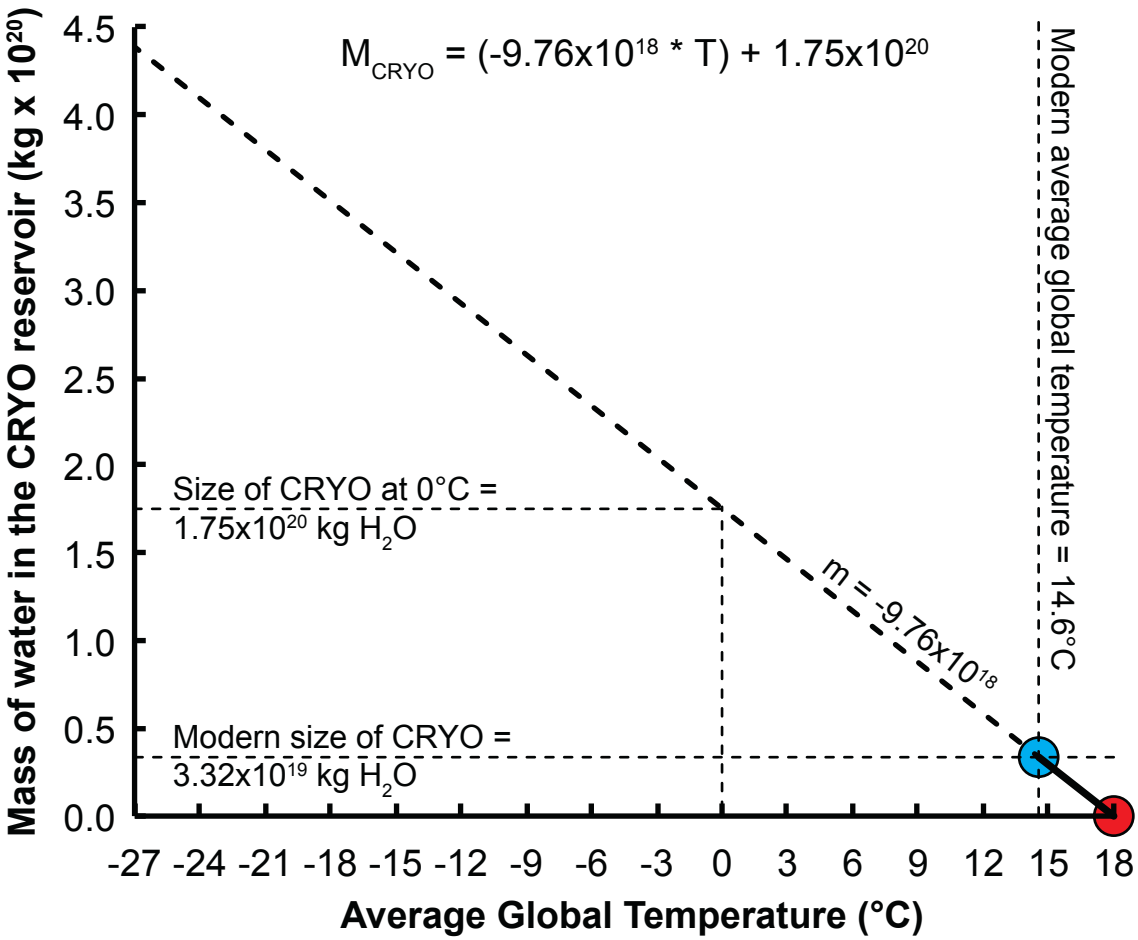

Figure 3: Graphical description of the method used to estimate the amount of water in the cryosphere as a function of average global temperature. The filled blue circle represents the amount of water in the cryosphere (3.32x10^{19} kg H_2O) at the present time (average global temperature =14.6°C). The filled red circle represents the amount of water in the cryosphere (0 kg H_2O) at the beginning of greenhouse conditions (18°C; Grénier et al., 2015). Assuming a linear relationship between the amount of water in the cryosphere and global average temperature between these two values defines a slope of -9.76x10^{18} kg H_2O/°C. A line with this slope (dashed line) extrapolated to -27°C (representing the global average temperature corresponding to snowball Earth conditions) predicts a cryosphere containing 4.39x10^{20} kg H_2O at snowball earth conditions.

549 the SW reservoir. Because the surface water (SW) reservoir consists of lakes, rivers, and
550 soil moisture, it is logical to assume that, as the amount of continental area covered by
551 polar ice increases, the continental area that can accommodate lakes, rivers, and soil
552 moisture decreases (we ignore any liquid water that might occur at the bottom of the ice
553 sheet). Thus, the size (amount of water) of the SW reservoir is linked to the area of
554 exposed continental surface. If the continental surface is completely covered by ice
555 (snowball-Earth), lakes, rivers, and streams (not including lakes and fluvial activity on
556 the surface of the glaciers themselves), and soil moisture would no longer be present on
557 the continents and, therefore, the SW reservoir (and the processes linked to the SW
558 reservoir) would no longer be included in the water cycle (Fig. 1B). Conversely, if the
559 CRYO reservoir is absent (greenhouse Earth), the continents would be ice-free and the
560 area of exposed continental surface capable of hosting the surface water reservoir would
561 be equal to the total continental area. As such, the amount of water contained in the SW
562 reservoir can be related to exposed continental surface area. Today, ~10% of the land
563 surface (~14.8×10^6 km^2) is covered by glacial and polar ice
564 (http://water.usgs.gov/edu/watercycleice.html). Modern sea ice makes up ~60% (by
565 mass) of the CRYO reservoir and covers ~23.1×10^6 km^2 of the Earth's surface
566 (http://nsidc.org/data/seaice_index/). As such, ~40% of the total mass of water held in the
567 CRYO reservoir is located on the continents.
568 Using variations in the amounts of water in the CRYO reservoir during the
569 Phanerozoic, we can estimate variations in the amount of the land surface covered by the
570 CRYO reservoir during the Phanerozoic, assuming that the relative proportion of
571 cryosphere on land and on the oceans is similar to that observed today. During the
572 Phanerozoic, the total continental area has fluctuated with time, with relatively more land

573 area above sea level at about 600 Ma, at 200 Ma and present day, and relatively less
574 continental area during periods of rifting and high sea level at ~450 and 100 Ma, but the
575 average has remained relatively constant (Tardy et. al., 1989). Similarly, compared to the
576 average land mass distribution during the Phanerozoic, a relatively larger proportion of
577 the continental land mass today is located at higher latitudes (Tardy et al., 1989). As a
578 result, a relatively larger proportion of polar ice should be located on the continents today
579 compared to the proportion on the continents for the same average global temperature
580 during most of the Phanerozoic when a larger proportion of the land surface was at low
581 latitudes. Recognizing these variations in continental surface area and the distribution of
582 the continents on the Earth during the Phanerozoic, for simplicity we assume that the
583 total area and relative distribution is comparable to modern values – as with the variation
584 in the CRYO reservoir described above, the actual relationship between amount of
585 continental surface area covered by ice and temperature is of secondary importance as we
586 are examining impacts on the water cycle as the covered area increases or decreases
587 during the Phanerozoic. Correspondingly, the area of continental (land) surface covered
588 by ice has varied from 0 km^2 during most of the Phanerozoic, when greenhouse
589 conditions prevailed, to ~1.48×10^8 km^2 at 700 Ma when snowball Earth conditions
590 prevailed.

591 We assume that the total area and relative distribution of the oceans are comparable to
592 modern values, and that the amount of Earth's ocean surface covered by ice has varied
593 from 0 km^2 during most of the Phanerozoic to ~3.62×10^8 km^2 (at 700 Ma). If the CRYO
594 reservoir is located over the oceans, the growth and retreat of sea ice will influence
595 atmosphere-ocean interactions. When the ocean surface is completely covered by ice,
596 exchange of water between the atmosphere and oceans does not occur. Conversely, when

597 the CRYO reservoir is absent (greenhouse conditions) atmosphere-ocean exchange is not
598 affected by ice coverage. Thus, the movement of water between the atmosphere and the
599 oceans can be related to exposed ocean surface area. Variations in the surface area of the
600 oceans during the Phanerozoic have been estimated in a manner similar to that described
601 above for surface area of the continents.

602 To estimate variations in the proportion of Earth's surface covered by the cryosphere
603 as a function of global average temperature, we assume that polar ice on Earth is
604 contained within a uniformly thick ice mass that extends northward and southward from
605 the poles in proportion to average global temperature. We recognize, however, that the
606 thickness of the ice caps varies geographically, and the variation is related to latitude
607 (Pierrehumbert, 2011) as well as the distribution and position of the continents. As global
608 average temperature decreases, the amount of water sequestered in the CRYO reservoir
609 increases as the average thickness of the ice caps increases. As such, the amount of water
610 transferred into the CRYO reservoir from adjacent reservoirs must increase to
611 accommodate the growing CRYO reservoir, and the sizes of the source reservoirs would
612 decrease proportionally.

613 During snowball-Earth conditions, we assume that the 0°C average annual
614 temperature isotherm is located along the equator, and that the average temperature
615 decreases with distance north and south of the equator. Here, we assume that the change
616 in temperature with distance north of the equator is equal to the change in temperature
617 with distance south of the equator, recognizing that there are differences owing to the
618 obliquity of Earth's rotational axis. During greenhouse conditions, we assume that the
619 0°C average annual temperature isotherm is located at the poles and that average
620 temperature increases linearly with distance from the poles towards the equator. The

621 global average temperature range between snowball-Earth conditions (-27°C) and
622 greenhouse conditions (18°C) represents a 45 degree Celsius range in temperature. As
623 noted above, we assume that permanent ice on Earth is represented by an ice layer of
624 uniform thickness such that the amount of water in the cryosphere increases as the area of
625 the Earth covered by ice increases with decreasing temperature. Thus, the mass of
626 permanent ice (H_2O), or the size of the cryosphere, varies with temperature in proportion
627 to the variation in the surface area of the Earth in which the average annual temperature is
628 <0°C, i.e., the amount of surface area that is located north or south of the 0 degree
629 Celsius isotherm corresponding to some global average temperature. The average
630 temperature at polar latitudes (80° to 90° north and south of the equator) today is
631 approximately -24°C and the average temperature at equatorial latitudes straddling the
632 equator (0° to 20°) is approximately 25°C. Along a traverse from the equator to the poles,
633 the distance on the surface of the Earth separating each one degree Celsius change in
634 temperature is fairly constant between latitudes 20-80°. However, near the poles (80-90°
635 latitude) and near the equator (0-20° latitude) the temperature remains reasonably
636 constant at ~-24°C and ~25°C, respectively (New et al., 2000; Reynolds et al., 2002;
637 Kalnay et al., 1996). Today, owing to the distribution of land and oceans, the southern
638 extent of the boreal ice cap varies from about 70° to 38° north latitude, whereas the
639 austral icecap around Antarctica is relatively symmetrical and extends to about 75° south
640 latitude. Here, we assume that during the Phanerozoic polar ice was present at all
641 locations on Earth where the average global temperature was ≤0°C. Our linear
642 extrapolation of the amount of water contained in the cryosphere as a function of global
643 average temperature (Fig. 3) assumes a uniform thickness of the ice sheet. As such, as the
644 amount of water in the cryosphere increases, the latitudinal extent of the ice sheet (and

thus the surface area of the ice sheet) must increase proportionally. Thus, we calculate the surface area S of a spherical ice cap using the relationship between the height h of a spherical cap and the radius r of the Earth (6370 km):

$$S_{cap} = 2\pi rh \quad (7)$$

A spherical ice cap (the region of a sphere above a particular plane) with h=r represents a complete hemisphere of ice from the poles to the equator, i.e., snowball-Earth conditions. Furthermore, a spherical ice cap with h=0 represents conditions during which permanent ice is absent, i.e., greenhouse conditions. We assume that the height (vertical distance from a horizontal surface passing through the Earth at the equator) of the polar ice caps increases linearly as global average temperature changes. Thus, we define the height h of the ice caps as a function of global average temperature T at some time t:

$$h = (18 - T_t) * (\frac{r}{45}) \quad (8)$$

where 18 represents the average global temperature (°C) above which polar ice does not exist on Earth, r is the radius of the Earth (6370 km), and 45 is the range in temperature (degrees Celsius) between snowball-Earth and greenhouse conditions. Thus, for every 1°C decrease in temperature, the height of the spherical cap of ice increases by ~141 km. It is important to note that latitude is measured by the angle between an imaginary line from the center of the Earth and an imaginary plane through the equator, and the linear increase in the height of the ice caps with changes in temperature does *not* correspond to a linear decrease in the latitudinal extent of the ice caps.

The surface area of the earth corresponding to each 141 km increment in ice cap height variation north or south of the equator is ~5.67×10^6 km^2 (Eqn. 7, 8). Thus, for each 141 km increment of migration of the polar ice cap height north and south of the equator (corresponding to a 1 degree Celsius increase in average global temperature), the amount

669 of surface area covered by polar ice decreases by 11.34×10^6 km^2 (5.67×10^6
670 km^2/increment × 2 increments to account for both the boreal and austral poles). Using the
671 relationship between the area of the cryosphere compared to the total area of the Earth
672 and average global temperature, the fraction of Earth's surface occupied by the CRYO
673 reservoir as a function of average global temperature is described as follows:

674 $$SA_{CRYO\ fraction,T} = (-0.0222 * T_{AVG}) + 0.4 \quad (9)$$

675 As discussed above, during periods when the global average temperature was greater
676 than 18°C, permanent ice did not exist, and at temperatures lower than -27°C, the Earth is
677 completely covered in ice. Thus, at temperatures ≥18°C, the fraction of the Earth's
678 surface covered by cryosphere is 0, and at temperatures ≤-27°C, the fraction of Earth's
679 surface covered by ice is 1. As the surface area of the Earth covered by ice increases at
680 temperature decreases, the relative areas of the exposed oceans and continents decrease in
681 proportion to the relative proportions of ocean (71%) and continents, or land (29%),
682 today (Fig. 4).

683 To summarize, we assume that the amount of water in the cryosphere varies linearly
684 with temperature. Moreover, the decrease in continental surface area covered by
685 permanent ice scales with the migration of the ice caps away from the equator as global
686 average temperature increases. As a result, the amount of H_2O contained in the
687 cryosphere increases with decreasing average global temperature over the range -27°C to
688 +18°C.

689

690 **2. Variations in the BIOc reservoir**

691 At present, the BIOc reservoir contains 2.9×10^{15} kg of H_2O (Bodnar et al., 2013), and
692 before 444 Ma plant life was essentially non-existent on the continents. The manner in

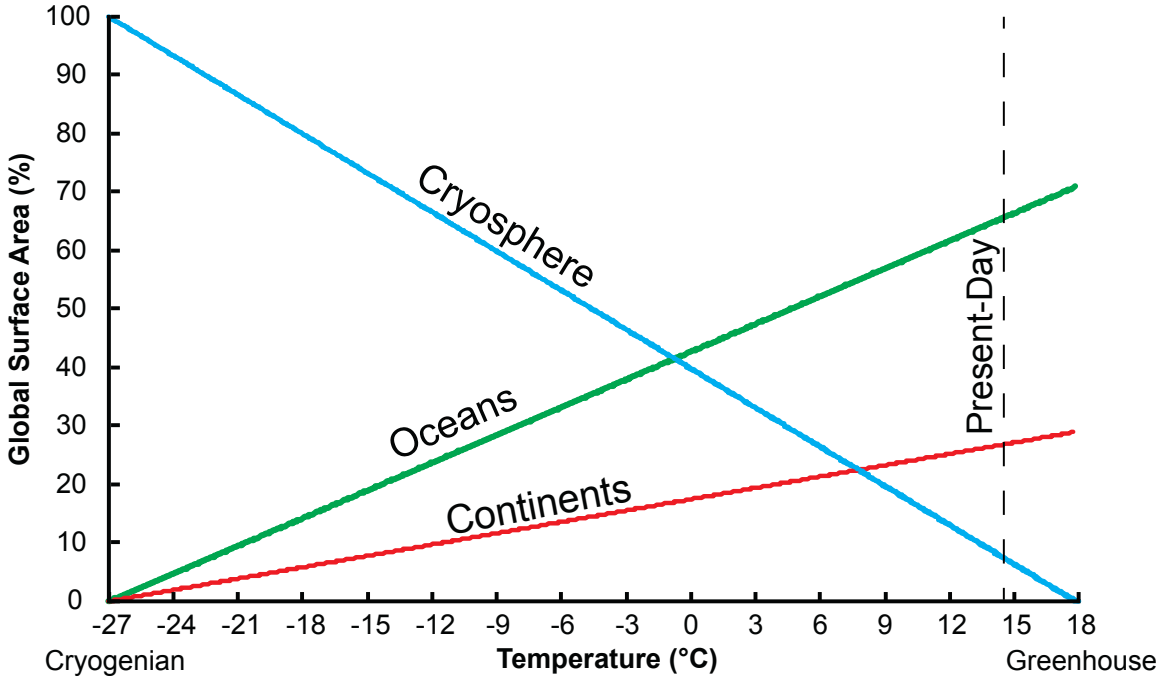

Figure 4: Relationship between the relative amount of the Earth's surface covered by ice (Cryosphere), oceans, and continents as a function of average global temperature. These areas, in turn, constrain the relative sizes of the cryosphere, oceans and surface water reservoirs that are available to interact with and exchange water with other reservoirs in the hydrologic cycle. "Cryogenian" refers to snowball-Earth conditions at ~700 Ma when the planet's surface is completely covered in ice and the continents and oceans are not exposed to the atmosphere. "Greenhouse" refers to conditions when polar ice did not exist. "Present-Day" indicates the proportions of the Earth's surface covered by cryosphere, oceans, and continental surface area at the present-day temperature of 14.6°C. For simplicity, we assume that the oceans and continents are distributed evenly across the entire surface of the Earth. Thus, as the surface area of polar ice linearly decreases from 100% starting at -27°C, the surface areas of both the continents and the oceans linearly increase.

693 which the size (amount of water) of the BIOc reservoir has varied over time is uncertain,
694 and here we describe several plausible scenarios to estimate the amount of water
695 contained in the continental biosphere during the Phanerozoic. We assume that no
696 significant biomass existed on the continental surface before the Silurian (~0.0 kg wet
697 biomass; 444 Ma) and that the amount of biomass on the continents today is ~2.9×10^{15} kg
698 wet biomass. The simplest case for growth of the size of the continental biosphere is to
699 assume that the amount of biomass has increased linearly, starting from 0 (zero) at 444
700 Ma to the present value (Fig. 5). Alternatively, we might assume that the rate of change
701 in the amount of water contained in the continental biosphere during the Phanerozoic is
702 related to the temporal change in size of organisms during the Phanerozoic. Various
703 workers have noted an increase in average organism size during the Phanerozoic and
704 conclude that if organism size increases and the abundance of organisms remains
705 constant over time, then the total amount of biomass contained in the organisms increases
706 (Bambach, 1993; Cope, 1887). Other workers observe that the biomass of Cenozoic
707 mammals increases to a particular optimum mass, depending on the species (Alroy,
708 1998). Kingsolver and Pfennig (2004) report that this qualitative pattern of selection on
709 size and other traits holds for all taxonomic groups, including plant life. Several
710 mechanisms have been proposed to explain the increase in biomass, including an increase
711 in available nutrients (Bambach, 1993; Martin, 1996) and an increase in nutrient uptake
712 efficiency (McMenamin and McMenamin, 1994). Other workers suggest that the
713 mechanisms and constraints associated with the increase in organism size with time vary
714 between different organisms (Hone and Benton, 2005).
715 As one means to estimate the increase in the amount of water in the continental biosphere
716 that is consistent with observations related to organism size, we can assume that the

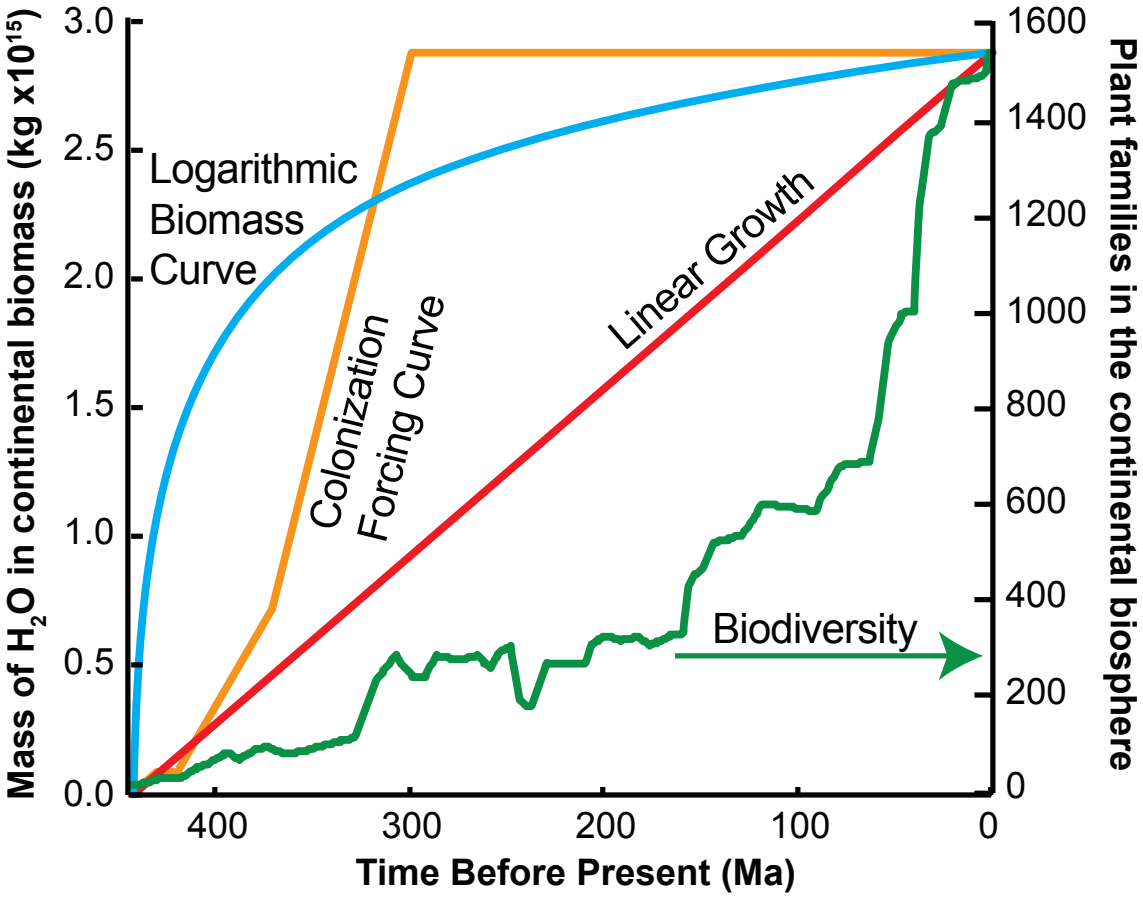

Figure 5: Effect of different models for growth of the continental biosphere over the past 444 Ma. All four scenarios assume that the continental biosphere contains 0.0 kg of H_2O at 444 Ma and increases to the present value of 2.9×10^{25} kg H_2O. The red line labeled "Linear Growth" assumes a constant (linear) rate of biomass increase and corresponds to an increase in the amount of H_2O in the continental biosphere of 6.5×10^{12} kg/Ma during the past 444 Ma. The blue curve labeled "Body Mass Optimization" assumes that the increase in the amount of H_2O in the continental biosphere follows the biological optimum for all continental organisms (Alroy, 1998). Accordingly, the rate of growth of the amount of H_2O in the continental biosphere is high during the early Phanerozoic and decreases towards the present. The green irregular growth curve labeled "Biodiversity" assumes that the increase in the amount of H_2O in the continental biosphere is proportional to variations in the number of plant family taxa during the Phanerozoic (Benton, 1993; 1995). This scenario indicates that the amount of water in the continental biosphere was significantly less than the modern value for most of the Phanerozoic and increased rapidly to present values over about the past 150 Ma. The orange curve labeled "Colonization Curve" assumes that the increase in the amount of H_2O in the continental biosphere is proportional to the influence or "forcing" of land plant colonization on global chemical cycles. This model suggests that the size of amount of water contained in the continental biosphere increased rapidly from about 444 to 300 Ma and then remained fairly constant to the present time (after Bergman et al., 2004).

717 current amount of water in the continental biosphere is the “optimum” wet biomass, and
718 then calculate the rate of change in the amount of water in the continental biosphere
719 required to achieve the current value, starting from 0.0 kg at 444 Ma (Fig. 5). This results
720 in a rapid increase in the amount of water in the continental biosphere early, and a more
721 gradual increase later.

722 A third approach to estimate the growth of the continental biosphere during the
723 Phanerozoic is to relate the increase in continental biomass to biological diversity (Fig.
724 5). The total number of land plant taxonomic families preserved in the fossil record has
725 increased since the beginning of the Silurian. The number of major flora family taxa has
726 increased from 19 at 444 Ma to 1,519 today (Sepkoski, 1993; Benton, 1993). We
727 recognize that the diversity of plant taxa may not equate to plant biomass abundance
728 (Smith, 2007) because the fossil record is sampled from geographically (and
729 geologically) accessible rock, and some areas are better preserved in the rock record and
730 are studied in more detail than others. The fossil record also contains many
731 unconformities representing missing strata and, therefore, does not provide a continuous
732 record of life on Earth. Furthermore, each available part of the fossil record represents a
733 local environment at a discrete time, which may not faithfully represent the average
734 global environment. Thus, the abundance and diversity of fossils found in a specific
735 location may not accurately represent the global abundance of life at that time. Smith
736 (2007) also argues that inconsistent taxonomic categorization affects our understanding
737 of biological diversity. Previous workers have shown that certain species of
738 morphologically similar crinoids are given different names depending on the epoch in
739 which the fossil is discovered (Ausich and Peters, 2005); a species may be “extinct” in
740 one epoch while another species “originates” in the next epoch without changing

741 morphology. This mis-categorization skews our understanding of extinction and species
742 origination over time. Also, as the taxonomic classification of organisms becomes more
743 specific (e.g., family to genus to species), the average duration of an organism's existence
744 decreases (Peters, 2006), i.e., the duration of a particular species within a family will be
745 shorter than that of the family itself. Furthermore, the number of species in a given family
746 varies by either biological diversification or sampling bias; previous workers show that
747 more species are assigned to later families than earlier families (Flessa and Jablonski,
748 1985). Recognizing all of these limitations and uncertainties, if we assume that the
749 amount of water scales with the variation in diversity, the continental biosphere would
750 have contained little water early in the development of plant life on the continents and the
751 amount of water in the BIOc reservoir would have increased slowly from about 444 Ma
752 to about 150 Ma, followed by a dramatic increase during about the past 150 Ma (Fig. 5).
753 A fourth approach to estimate the growth of the continental biosphere on Earth during
754 the past 444 Ma is to assume that plant biomass correlates with other geochemical cycles.
755 The COPSE model of biogeochemical cycling during the Phanerozoic examines the role
756 of land plant evolution and colonization on the global carbon, oxygen, phosphorus and
757 sulfur cycles (Bergman et al., 2004). In this scenario, land plants represent a "forcing"
758 value where 0 indicates that plants do not influence geochemical cycles (and would
759 represent times when no land plants were present), and a value of 1 correlates with the
760 modern impact of plants on geochemical cycles. The results of Bergman et al. (2004)
761 suggest that land plant forcing increases from zero during the late Ordovician to 1.0
762 during the late Carboniferous and remains constant throughout the remainder of the
763 Phanerozoic (Fig. 5). As such, the amount of water contained in the continental biosphere
764 increases rapidly from nil to modern values during the late Ordovician to late

765 Carboniferous, and is then constant for the remainder of the Phanerozoic. These results
766 are consistent with the global spread of vegetation and the development of forests in the
767 fossil record (Benton, 1993).

768 Some workers have suggested that rather than increasing, plant biomass has
769 decreased during the last 500 Ma (Franck et al., 2006). Based on analysis of the carbon
770 cycle, these workers report that biomass will continue to decrease and that all biomass
771 will disappear from Earth in about 1.6 Gy.

772 Owing to an incomplete understanding of how plant biomass and the related size of
773 the continental biosphere portion of the hydrologic cycle have evolved during the past
774 444 Ma, we assume a linear growth model. Thus, the size of the continental biosphere has
775 increased linearly from 0 at 444 Ma to 2.9×10^{15} kg of H_2O today. This growth
776 corresponds to an increase in the amount of water contained in biomass on the continents
777 of ~$6.5x10^{12}$ kg H_2O/Ma during the past 444 Ma (Fig. 5). Thus, the amount of water in
778 the continental biosphere at any time during the past 444 Ma is given by:

779 $$M_{BIOc} = 6.5x10^{12} * (444 - t) \quad (10)$$

780 where t is the time of interest (Ma), i.e., millions of years before the present.

781 It is plausible that other environmental and evolutionary factors also influence the
782 impact of plant life during the Phanerozoic. For example, extinction events destroy a
783 significant portion of plant life, reducing plant biomass and likely modifying the effect
784 that plants have on geochemical cycles. However, owing to the observation that the
785 amount of plant biomass returns to pre-extinction values "instantly" (over hundreds of
786 thousands of years), the loss and recovery of plant biomass during and after extinction
787 events is too rapid to observe on the 1 Ma time steps of our model. In order to refine how
788 variations in continental biomass influence the whole-Earth hydrologic cycle requires a

789 better understanding of variations in plant abundances and biomass over shorter time
790 scales (10^4 – 10^5 years).
791
792 **3. Variations in the Atmosphere Reservoir (ATM)**
793 The atmosphere reservoir (ATM) consists of all water from the surface of the Earth to
794 the edge of the troposphere at ~12 km altitude (Barry and Chorley, 2009). Previous
795 workers (Trenberth and Smith, 2005) estimated that the total mass of the atmosphere
796 (including all volatile components) is ~5.6×10^{18} kg, and that the modern atmosphere
797 contains ~1.3×10^{16} kg H_2O (Berner and Berner, 1987; Drever, 1988; Bodnar et al., 2013).
798 The water-carrying capacity of the atmosphere (for a given relative humidity) is
799 controlled mainly by temperature (c.f., Lawrence, 2005), and increases exponentially as
800 temperature increases, doubling for approximately every ten degree Celsius increase in
801 temperature. At constant temperature, the amount of water in the atmosphere also
802 increases with increasing relative humidity (Fig. 6). The current average global
803 temperature is 14.6°C (NOAA National Climatic Data Center, 2015) and the relative
804 humidity on Earth today varies over a wide range. In Antarctica and in the Amazon rain
805 forest the relative humidity is typically about 80-90%, although the "carrying capacity"
806 of the atmosphere in the Amazon is much higher than that of Antarctica owing to the
807 large average temperature difference. The Sahara desert and other higher temperature
808 desert regions typically have relative humidity in the range 25-50 %. The NOAA
809 National Climatic Data Center (2015) reports that global average relative humidity has
810 decreased by an average of ~3.1% per degree Celsius as global average temperature
811 increased during the period from 1981 to 2010. The variation in average global relative
812 humidity with temperature will also vary depending on the distribution of land and

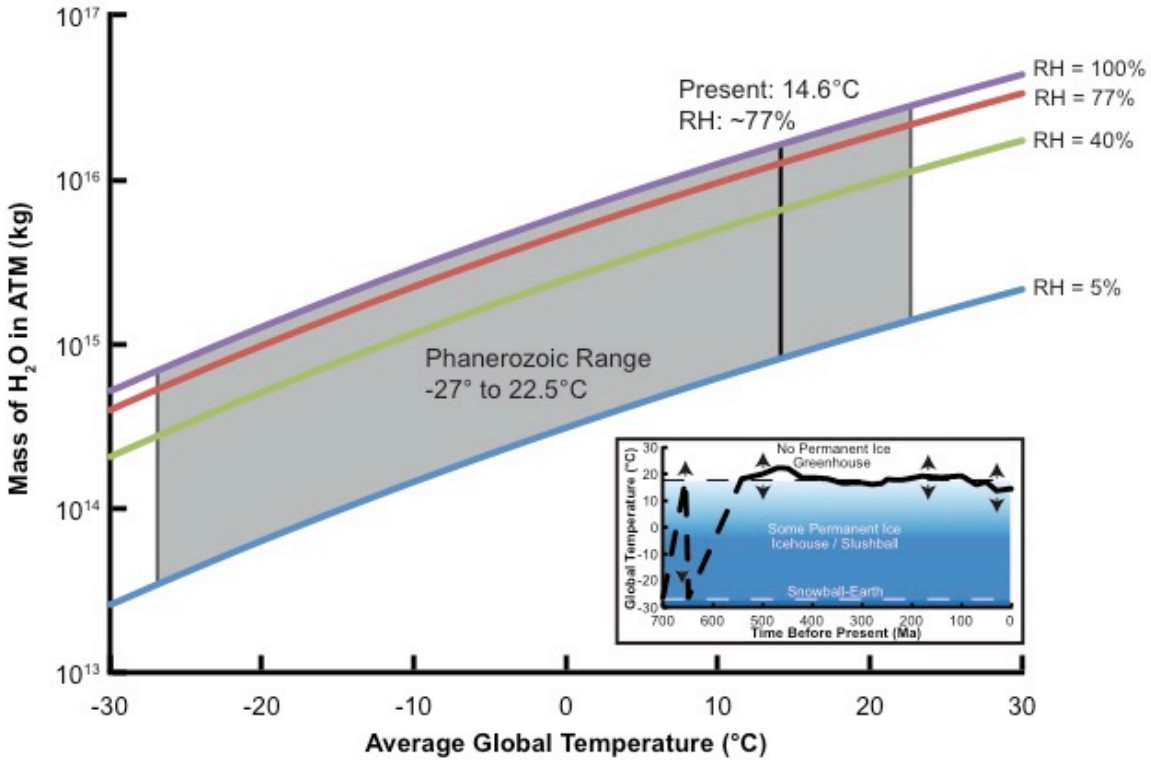

Figure 6: Relationship between the amount (mass) of water in the atmosphere as a function of global average temperature and relative humidity (RH). Inset: Variations in global average temperature and climatic conditions during the past 700 Ma (see Figure 2). Individual curves show the amount of water in the atmosphere as a function of temperature for various choices of relative humidity, ranging from 5 to 100%. The modern global average relative humidity is 77%. The vertical line at 14.6°C represents the current average global temperature, and the shaded area represents the possible range in temperature and relative humidity, and corresponding amount of water in the atmosphere, during the Phanerozoic.

813 oceans relative to the equator, as well as on the distribution of land masses, i.e., presence
814 of a supercontinent versus multiple separated continental land masses. Here, we have
815 assumed a constant average relative humidity during the past 700 Ma that is equal to the
816 current average relative humidity on Earth (see further justification for this below), owing
817 to our inability to offer defensible and realistic estimates of how average relative
818 humidity might have varied in the geologic past.

819 Willett et al. (2014) have shown that the average relative humidity over landmasses is
820 ~70%, and the average relative humidity over the oceans is ~80%. Approximately 29% of
821 Earth's surface is covered by land and the remaining 71% of the planet is covered by
822 oceans, ignoring parts of the oceans and continents that are covered by permanent ice.
823 Tardy et al. (1989) estimated that continental area has varied from about 125×10^6 km^2 to
824 187×10^6 km^2 during the Phanerozoic and that the ocean area has varied from 323×10^6
825 km^2 to 385×10^6 km^2 during this time. Thus, continents (area above sea level) has varied
826 from ~24.5% to ~36.7% of the Earth's surface during the Phanerozoic, with relatively
827 more land area at 600 Ma, 200 Ma and at the present, and relatively less continental area
828 at 450 Ma and 100 Ma. Tardy et al. (1989) note that, while the proportions of land and
829 ocean have varied during the Phanerozoic, the average land area during the Phanerozoic
830 has been about 30%, or the same as the modern value. Thus, we use the modern
831 proportion of land surface to ocean surface to estimate a modern average global relative
832 humidity of 77% (Fig. 6).

833 To estimate variations in the amount of water in the atmosphere as global average
834 temperature varies during the Phanerozoic, we use the relationships between temperature,
835 the vapor pressure of water, relative humidity, and the molar masses of water and dry air

to calculate the specific humidity of the atmosphere. The vapor pressure of water in air (e; hPa) can be quantified as a function of temperature (T) (Lowe and Ficke, 1974):

$$e(T) = 6.1078 + 0.433\,T + 1.42x10^{-2}\,T^2 + 2.65x10^{-4}\,T^3 + 3.031x10^{-6}\,T^4 + 2.034x10^{-8}\,T^5 + 6.137x10^{-11}\,T^6 \quad (11)$$

We relate the vapor pressure of water in air to relative humidity (RH), representing the percentage of water vapor needed to saturate air at a given temperature. RH is related to the partial pressure of water in air (P_{H2O}) and the vapor pressure of water at a given temperature (Eqn. 11) as follows:

$$RH = \frac{P_{H_2O}}{e(T)} * 100 \quad (12)$$

For a given temperature, we calculate P_{H2O} and relate that to the volume mixing ratio of water in air (x_{H2O}), which is also related to the nominal pressure of the atmosphere at sea level (1013.25 hPa):

$$x_{H_2O} = \frac{P_{H_2O}}{P} \quad (13)$$

Using Equations 11, 12, and 13, we relate the volume mixing ratio of water vapor in air to relative humidity and vapor pressure as a function of temperature according to:

$$x_{H_2O} = \frac{RH*e(T)}{P*100} \quad (14)$$

and use the volume mixing ratio of water in air to calculate specific humidity (q), which represents the mass ratio of water vapor to the total mass of air in a given system (kg H_2O/kg air). Specific humidity is then described by the volume mixing ratio of water in air (x_{H2O}) as follows:

$$q = \frac{kg\ H_2O}{kg\ air} = \frac{x_{H_2O}*M_{H_2O}}{(x_{H_2O}*M_{H_2O})+[(1-x_{H_2O})*M_{dry}]} \quad (15)$$

where M_{H2O} is the molar mass of water (18.015 g/mol) and M_{dry} is the molar mass of dry air (28.96 g/mol). Above we have described x_{H2O} as a function of temperature. Thus, we

859 can calculate variations in specific humidity as a function of temperature, specific
860 humidity, and the amount of air in the atmosphere (5.6×10^{18} kg; Trenberth and Smith,
861 2005) to estimate the amount of water in the atmosphere as a function of global average
862 temperature (Fig. 6).
863 To summarize, we assume that the total mass of the atmosphere and the average
864 global relative humidity remain constant through time, and we use variations in
865 temperature to calculate the specific humidity of the atmosphere and estimate the amount
866 of water in the ATM reservoir. As average global temperature increases, the amount of
867 water in the atmosphere increases, as expected, and varies from 5.24×10^{14} kg at -27°C to
868 2.14×10^{16} kg at 22.5°C (Fig. 6).
869
870 **4. Variations in the Surface Water Reservoir (SW)**
871 The surface water reservoir (SW) includes all water above the water table (and land
872 surface) that is not contained in the ocean reservoir, and includes lakes, rivers, swamp
873 water, and soil moisture (Gleick, 1996; Bodnar et al., 2013). The size of the surface water
874 reservoir has been estimated by various methods, with a general consensus that the SW
875 reservoir contains ~2.07×10^{17} kg H_2O (Berner and Berner, 1987; Gleick, 1996; Bodnar et
876 al., 2013). We relate variations in the amount of H_2O contained in the surface water
877 reservoir during the Phanerozoic to the area of the continents that is open to the
878 atmosphere, i.e., continental surface that is not flooded by oceans nor covered by glaciers
879 and polar ice. This assumes that the amount of water in the surface water reservoir varies
880 linearly with continental surface area. The current subaerial surface area of the continents
881 is ~1.4×10^{8} km^2 (with a current ocean surface area of ~3.6×10^{8} km^2 and a current CRYO
882 reservoir surface area of ~1.63×10^{7} km^2). We recognize that the amount of surface water

per unit area of continental surface area varies widely across the globe, depending on the location of the continent relative to the equator, and the location on the continents relative to the oceans (or other large bodies of water) and/or physiographic features such as mountains that affect global atmospheric circulation patterns. However, in the absence of detailed information concerning how these factors varied in the geologic past, we relate the fraction of exposed continental surface to the fraction of Earth's surface area covered by polar ice (Eqn. 9) as average global temperature varies from -27°C to 18°C:

$$SA_{exposed\ continent\ fraction,T} = \begin{cases} 0 & T \leq -27^\circ C \\ 1 - SA_{CRYO\ fraction,T} & -27^\circ C \leq T \leq 18^\circ C \\ 1 & T > 18^\circ C \end{cases} \quad (16)$$

Thus, at temperatures ≥18°C, the fraction of exposed continental surface area is 1, and at temperatures ≤-27°C, the fraction of exposed continental surface is 0. Additionally, as described above, while the proportion of the Earth's surface occupied by subaerial land masses has varied from about 25-37% during the Phanerozoic, the average is similar to the modern value. As such, we apply this relationship to the size of the SW reservoir accommodated by exposed continental surface (Eqn. 16):

$$M_{SW,T} = \left(2.23x10^{17} * SA_{exposed\ continent\ fraction,T}\right) \quad (17)$$

where M_{SW} is the amount of water in the SW reservoir (kg). The variation in size of the surface water reservoir (amount of water) with changing average global temperature, plotted as the percent difference relative to the modern value, is shown on Figure 7. During snowball-Earth conditions (≤-27°C), the amount of water in the SW reservoir is zero because the entire continental surface is covered by ice. As temperature increases, the amount of water in the SW reservoir increases as more continental surface is exposed

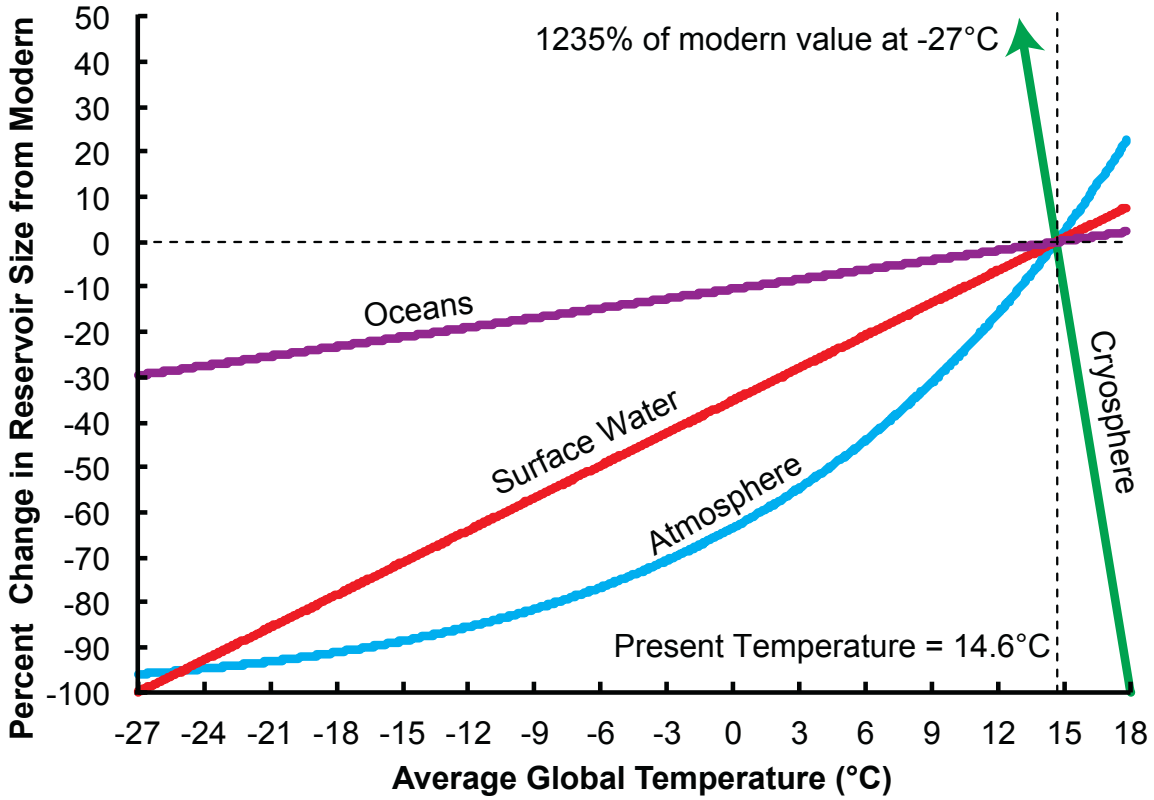

Figure 7: Relationship between global average temperature and the relative amounts of water in the atmosphere, cryosphere, oceans, and surface water reservoirs, all shown relative to the amount of water in each reservoir today. At -27°C, "snowball-Earth" conditions prevail and the CRYO reservoir contains 4.39×10^{20} kg H_2O, or 1,235% more than the amount of water in the CRYO reservoir at present (3.32×10^{19} kg H_2O). As global average temperature decreases and the CRYO reservoir grows, water added to the cryosphere is removed from the oceans, resulting in a ~-30% decrease in the amount of water in the oceans compared to the modern value. During snowball Earth conditions, the continental surface is completely covered by ice and the amount of water in the surface water reservoir is zero, or -100% of the modern value. The amount of water in the atmosphere decreases as global average temperature decreases, and the atmosphere contains 96% less water at -27°C compared to the modern value. As global temperature increases, polar ice melts and returns to the oceans. Also, continental ice masses shrink and expose the continental surface, increasing the area that can accommodate the surface water reservoir. Thus, as global average temperature increases to greenhouse conditions (18°C), the amount of water in CRYO decreases to zero and the amounts of water in the oceans, surface water, and atmosphere reservoirs increase by 2%, 8%, and 24%, respectively, compared to their present values.

905 until it reaches a maximum value of 2.23×10^{17} kg H_2O at 18°C when the fraction of
906 exposed continents is 1 (i.e., when no permanent ice covers the land surface).
907
908 **5. Variations in the Groundwater Reservoir (GW)**
909 The groundwater reservoir (GW) contains all pore and fracture-bound water in the
910 Earth's crust between the water table and an arbitrarily depth of 4 km (Berner and Berner,
911 1987; Bodnar et al., 2013). Below this depth, rock porosity is generally very low, the
912 temperature is elevated, and the water is often very saline. Thus, water below this depth
913 in the crust is considered to be part of the continental crust reservoir rather than the GW
914 reservoir, as described by Bodnar et al. (2013), and is included in the geosphere water
915 cycle rather than the exosphere described here. The amount of water in the groundwater
916 reservoir between the water table and 4 km depth has been estimated by various methods,
917 with a general consensus that the groundwater reservoir contains about $1.05\text{x}10^{19}$ kg H_2O
918 (Berner and Berner, 1987; Shiklomanov, 1993; Gleick, 1996; Bodnar et al., 2013).
919 Temporal variations in the amount of water in the GW reservoir are largely unknown; for
920 simplicity, we assume that the amount of water in the GW reservoir remains constant
921 throughout the Phanerozoic. The GW reservoir has no direct interaction with the CRYO
922 reservoir and also does not interact directly with the continental biosphere (Fig. 1). Thus,
923 assuming that the size of the GW reservoir has remained constant during the past 700 Ma
924 is expected to have little impact on the overall water cycle as the CRYO reservoir waxes
925 and wanes during the past 700 Ma and as the BIOc reservoir grows over the past 444 Ma.
926
927 **6. Variations in the Ocean Reservoir (Oceans)**

928 The amount of water in the modern oceans is ~1.37×10^{21} kg (Bodnar et al., 2013).
929 While changes in global sea level during a portion of the Phanerozoic have been
930 estimated, the variations are influenced not only by the amount (mass) of water in the
931 oceans but also by changes in ocean bathymetry related to seafloor spreading rates
932 (Müller et al., 2008). As such, estimates of relative sea level cannot be related directly to
933 the total amount of water in the oceans. Owing to this, the total amount of water in the
934 exosphere is assumed to be constant in our model, with water either added to or removed
935 from the oceans to maintain a constant total mass of water in the exosphere during the
936 Phanerozoic. Accordingly, the amount of water in the ocean reservoir (M_{OCEAN}) equals
937 the total amount of water in the exosphere (M_{EXO}) minus the sum of the amounts of water
938 in other five reservoirs comprising the exosphere:

939 $$M_{OCEAN} = M_{EXO} - (M_{CRYO} + M_{ATM} + M_{BIOc} + M_{SW} + M_{GW}) \quad (18)$$

940 As discussed above, the surface area of the oceans is influenced by the areal extent of
941 the CRYO reservoir and can be linked to the movement of water between the atmosphere
942 and ocean reservoirs. We describe relationships between the surface areas of the CRYO
943 and SW reservoirs as functions of temperature, and we use a similar relationship between
944 the surface area of the oceans and temperature that is related to the growth and retreat of
945 permanent ice caps. We relate the fraction of exposed ocean surface to the fraction of
946 Earth's surface area covered by permanent ice (Eqn. 9) in the range of -27°C and 18°C,
947 according to:

948 $$SA_{exposed\ ocean\ fraction,T} = \begin{cases} 0 & T \leq -27^\circ C \\ 1 - SA_{CRYO\ fraction,T} & -27^\circ C \leq T \leq 18^\circ C \\ 1 & T > 18^\circ C \end{cases}$$

949 (19)

During periods when the global average temperature was greater than 18°C, permanent ice did not exist, and at temperatures lower than -27°C, the Earth is completely covered in ice. Thus, at temperatures ≥18°C, the fraction of exposed ocean surface area is 1, and at temperatures ≤-27°C, the fraction of exposed ocean surface is 0. We will later link this relationship to variations in the amounts of water transferred between the atmosphere and ocean reservoirs.

7. Summary

During the past 700 Ma the amount of water contained in the various reservoirs comprising the exosphere has varied (Fig. 8). Much of the variation can be directly related to changes in average global temperature (Fig. 8, top panel). Thus, as average global temperature increases, the size of the ATM, SW and ocean reservoirs increase, whereas the size of the CRYO reservoir decreases (Fig. 8). The size of the continental biosphere is not linked directly to temperature and is assumed to increase linearly from zero at 444 Ma to the present value, with minor and short-lived decreases in the size of the BIOc reservoir associated with extinction events (Fig. 8).

Algorithms Describing Variations in the Fluxes of Water Between Exosphere Reservoirs in Deep Time

1. Water flux from the atmosphere to the cryosphere

The total amount of water that falls from the atmosphere to the Earth's surface as precipitation today is ~4.96×10^{17} kg/yr (Berner and Berner, 1987; Schlesinger, 1997; Reeburgh, 1997). For purposes of this study we describe the total amount of precipitation to Earth's surface as the sum of precipitation to the cryosphere, the non-ice-covered

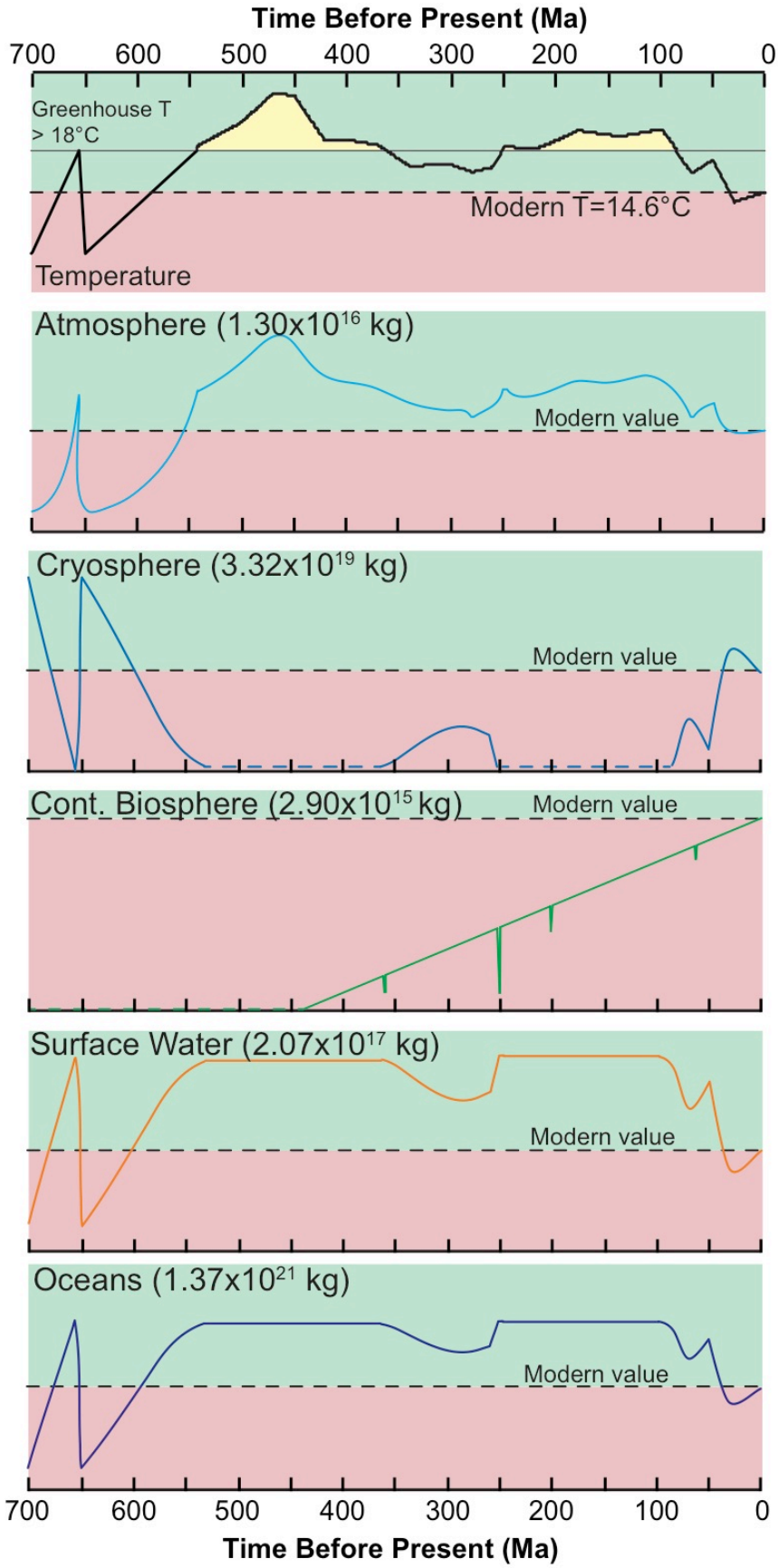
Time Before Present (Ma)
700
600
500
400
300
200
100
0
Greenhouse T
> 18°C
Modern T=14.6°C
Temperature
Atmosphere (1.30x10^16 kg)
Modern value
Cryosphere (3.32x10^19 kg)
Modern value
Cont. Biosphere (2.90x10^15 kg)
Modern value
Surface Water (2.07x10^17 kg)
Modern value
Oceans (1.37x10^21 kg)
Modern value
700
600
500
400
300
200
100
0
Time Before Present (Ma)

Figure 8: Schematic representation of the variation in the sizes (mass of water) contained in the various reservoirs of the hydrologic cycle during the past 700 Ma, all compared to the size that reservoir today (Modern value). On the temperature plot (A) the yellow shaded areas correspond to periods when the average global temperature was ≥18°C and greenhouse conditions prevailed and polar ice did not exist (see the dashed lines on the CRYO panel C). Note that each panel is schematic and not to scale – the lines are only intended to highlight times during the past 700 Ma when the amount of water in a given reservoir was greater than or less than modern values, and when those changes occurred. Dashed lines in the CRYO and continental biosphere panels represent times when those reservoirs were absent and not included in the hydrologic cycle.

974 continents (whereby the water becomes part of the surface water reservoir), and the
975 oceans:

976 $$F_{Total\ Pptn.} = F_{CRYO\ Pptn.} + F_{SW\ Pptn.} + F_{Ocean\ Pptn.} \quad (20)$$

977 While some portion of the total global precipitation falls onto glaciers and polar ice
978 (mostly as solid H_2O) and is incorporated into the CRYO reservoir, most earlier studies
979 only described precipitation over the continents and over the oceans, and did not consider
980 the amount of water that is transferred directly from the ATM to the CRYO reservoir as a
981 separate flux. Based on estimates by Bentley and Giovinetto (1992) and Ohumura and
982 Reeh (1991) concerning annual snow accumulations in Antarctica and Greenland, Bodnar
983 et al. (2013) estimated a modern flux of water from the atmosphere to the CRYO
984 reservoir of 2.2×10^{15} kg/yr. The proportion of total precipitation that falls onto glaciers
985 and polar ice is expected to vary as a function of global average temperature and the
986 portion of Earth's surface area covered by ice. Previous workers have included estimates
987 of global precipitation during the Phanerozoic in global CO_2 cycle models (Tardy et al.,
988 1989). Other workers have observed that precipitation increases by ~23% for every 1°C
989 increase in average global temperature (Liu et al., 2009). The change in amount of
990 precipitation with temperature reported by Liu et al. (2009) is an order of magnitude
991 greater than that estimated by other climate models (reported by Sun et al., 2007).
992 However, the aforementioned models underestimate precipitation flux relative to the 7%
993 per °C increase estimated by Trenberth et al. (2003). Here, we assume that precipitation
994 increases by 7% per degree Celsius, as proposed by Trenberth et al. (2003). Thus, the
995 flux of water from the atmosphere to the Earth's surface ($F_{Total\ Pptn.}$; kg/yr) is related to
996 average global temperature (T) as follows:

997 $$F_{Total\ Pptn.,T} = 1.785x10^{17}\ e^{0.07\bullet(T)} \quad (21)$$

where 1.75×10^{17} represents the flux at 0°C (i.e., when T=0, $e^{0.07\cdot(T)} = 1$).

Precipitation rate varies as a function of latitude (Tardy et al., 1989), regional geography and topography (Fawcett and Barron, 1998) and local temperature (Liu et al., 2009), and Tardy et al. (1989) report that the amount of precipitation per unit area increases from the poles to the equator. Above we estimated the manner in which the latitudinal extent of permanent ice varies with temperature. As temperature decreases to -27°C and permanent ice extends to the equator, the area of Earth's surface occupied by the cryosphere reservoir increases. Here, the fluxes of water from the atmosphere to the CRYO reservoir, to the continents (SW), and to the oceans are functions of the relative surface areas of those reservoirs. We express global precipitation rate as a function of temperature, and we define the areal extent of the CRYO reservoir on the surface of the Earth as a function of the amount of water in the CRYO reservoir, which, in turn, is a function of temperature. Thus, the flux of water from the atmosphere to the CRYO reservoir at a given temperature ($F_{CRYO\ Pptn.,T}$) is a function of the fraction of Earth's surface area covered by the CRYO reservoir at that temperature ($SA_{CRYO\ fraction,T}$; Eqn. 9) and the flux of water from the atmosphere to the Earth's surface at that temperature ($F_{Total\ Pptn.,T}$; Eqn. 17) (Fig. 9):

$$F_{CRYO\ Pptn.,T} = F_{Total\ Pptn.,T} * (SA_{CRYO\ fraction,T})^2 \quad (22)$$

Here, the modern flux of water from the atmosphere to the CRYO reservoir is 2.83×10^{15} kg/yr, consistent with the estimate of Bodnar et al. (2013). The variation in flux of water from the atmosphere to the cryosphere as a function of temperature is shown on Figure 9, plotted as percent change in flux relative to the modern flux. Note that the flux reaches a maximum at about -10°C and decreases at temperatures above and below -10°C. This behavior reflects the competing effects of temperature and surface

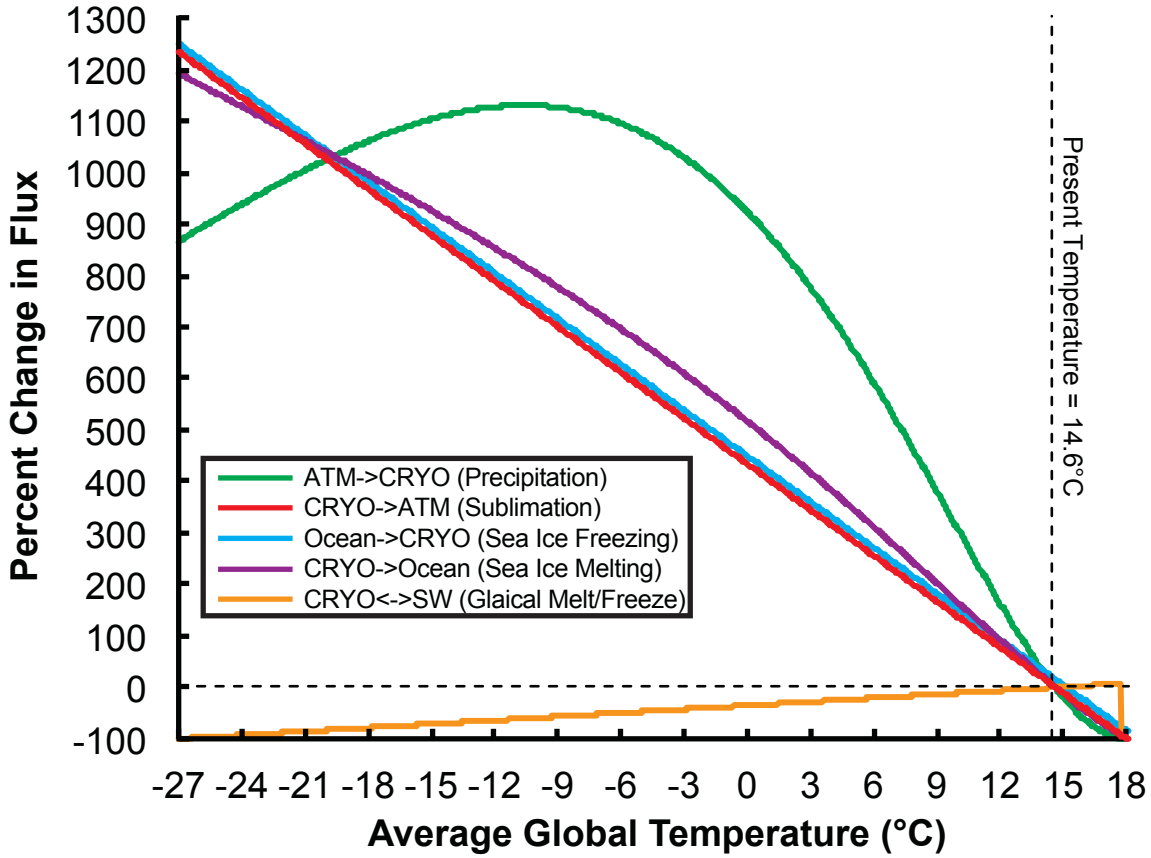

Figure 9: Relationship between the global average temperature and the fluxes of water into and out of the cryosphere, relative to the fluxes into and out of the cryosphere today (average global temperature 14.6°C). During the "Cryogenian" (T≤ -27°C) the planet is covered in an ~1 km thick shell of ice and at temperatures above 18°C, no polar ice exists on Earth. The amount of water that is transferred from the atmosphere to the cryosphere is a function of both global average temperature and the surface area of the cryosphere. As temperature increases from -27°C, the amount of precipitation per unit area of the CRYO reservoir increases, while at the same time the total surface area of the cryosphere decreases. Thus, as temperature increases from -27°C to ~-10.5°C, the total flux of water from the atmosphere to the cryosphere is dominated by the temperature effect, whereas at higher temperatures (>-10.5°C) the decreasing surface area of the cryosphere dominates. As a result, the total flux of water from the atmosphere to the cryosphere reaches a maximum at ~-10.5°C and decreases as temperature increases or decreases from this tipping point. See text for additional details.

1022 area of the CRYO. As temperature increases the flux per unit area increases, but as
1023 temperature increases the total area of the CRYO reservoir decreases. Thus, as
1024 temperature increases from -27°C, the flux from the atmosphere to the cryosphere
1025 increases as the effect of increasing temperature is greater than the effect of decreasing
1026 CRYO surface area. At temperatures above -10°C the effect of decreasing surface area of
1027 the CRYO reservoir is greater than that of increasing temperature, and the flux
1028 continuously decreases until the CRYO reservoir is completely gone at 18°C. Also note
1029 that, as discussed above, permanent ice did not exist during greenhouse periods; i.e., the
1030 amount of water in the CRYO reservoir was zero. As such, during periods when polar ice
1031 did not exist, there would be no flux of water into and out of the (non-existent) CRYO
1032 reservoir . The variation in the flux of water from the atmosphere to the CRYO reservoir
1033 during the past 700 Ma is shown in Figure 10.
1034
1035 **2. Water flux from the cryosphere to the atmosphere**
1036 Sublimation occurs when solid ice transitions directly into the gas phase at low
1037 temperature, in the absence of melting to produce a liquid phase. Previous workers have
1038 estimated that the amount of water transferred from the CRYO reservoir to the
1039 atmosphere via sublimation today is ~2.0×10^{14} kg/yr (Bodnar et al., 2013). The rate of
1040 sublimation (or ablation) from the CRYO reservoir is controlled by relative humidity,
1041 wind speed, ice surface area and, to a lesser extent, temperature (Wagnon et al., 1999;
1042 Bliss et al., 2011). Variations in these driving factors in the geologic past are unknown
1043 and not easily estimated without large uncertainties. As discussed above, we estimate
1044 variations in the surface area of the CRYO reservoir in the past as a function of the
1045 amount of water in the CRYO reservoir, and we assume that average global relative

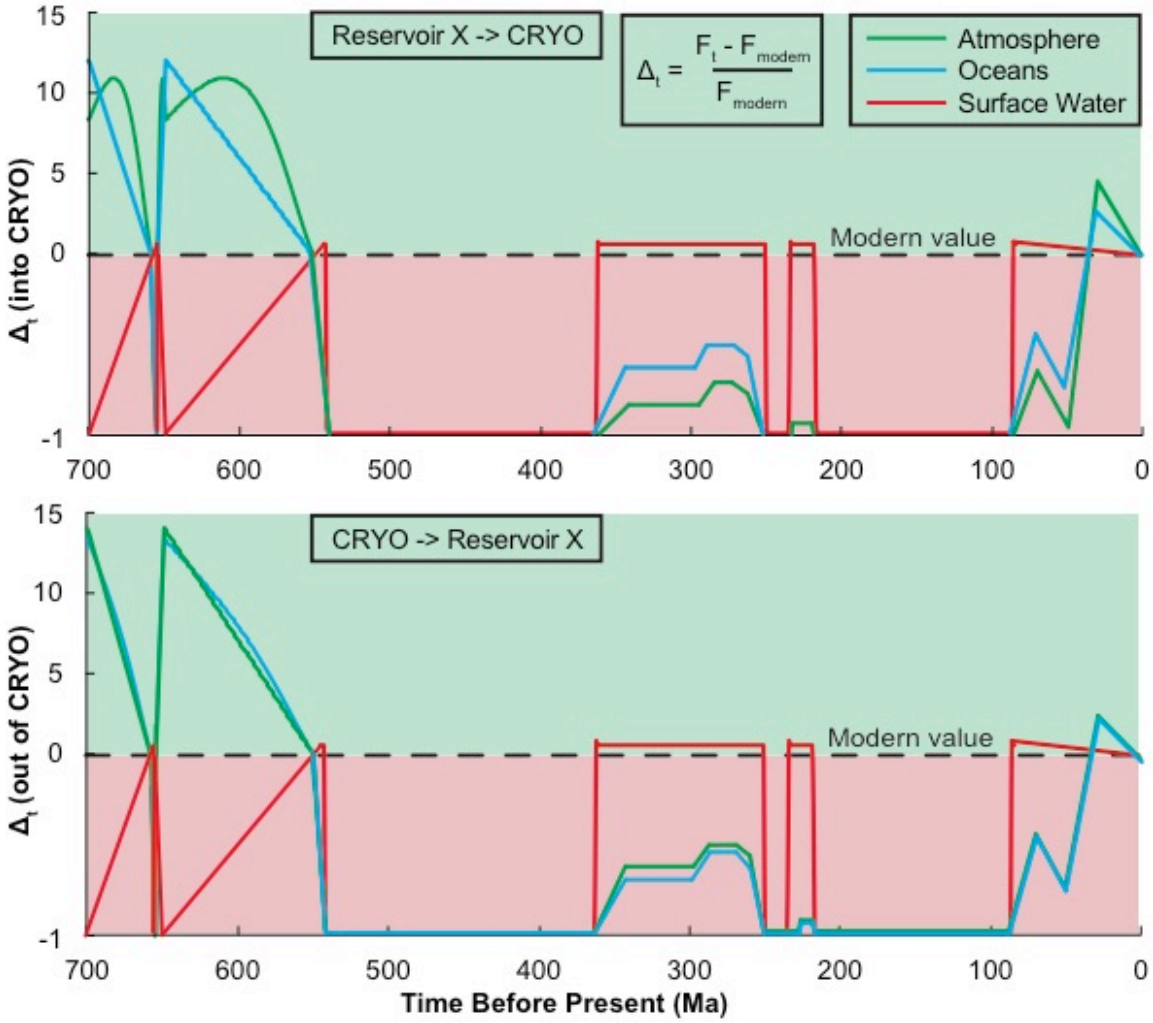

Figure 10: Variations in fluxes of water into and out of the CRYO reservoir, all calculated as the change in flux relative to the modern value.

humidity is similar to the modern value. Here, the flux of water from the CRYO reservoir to the atmosphere ($F_{Sublimation,T}$) is related to the modern water flux from the CRYO reservoir to the atmosphere ($F_{Sublimation,modern}$) and is assumed to vary in proportion to the fraction of the earth's surface area occupied by the CRYO reservoir ($SA_{CRYO\ fraction,T}$; Eqn. 9) compared to the modern CRYO surface area ($SA_{CRYO\ fraction,modern}$):

$$F_{Sublimation,T} = F_{Sublimation,modern} * \frac{SA_{CRYO\ fraction,T}}{SA_{CRYO\ fraction,modern}} \quad (23)$$

As discussed above, the flux of water from the CRYO to the ATM is zero during greenhouse conditions (T≥18°C) when permanent ice is absent. The variation in the flux of water from the CRYO reservoir to the atmosphere during the past 700 Ma is shown in Figure 10.

3. Water flux from the oceans to the cryosphere

Seawater freezes to form sea ice during polar winters and melts into the oceans during polar summers. Due to this seasonal cycling, the net amount of water transferred between the cryosphere and oceans on an annual basis is zero as long as the average global temperature remains constant. We recognize, however, that during the past few decades there has been a net transfer of water from the cryosphere to the oceans in response to increasing average global temperature. Workers have measured the decrease in Antarctic sea ice cover during summer and estimated that ~1.5×10^{16} kg/yr of water is transferred from the CRYO reservoir to the oceans via sea ice? melting (Parkinson, 1996). Here, we use this value and assume that the amount of water transferred from the oceans to the CRYO reservoir today is 1.5×10^{16} kg/yr.

While the history of glaciations during the Phanerozoic is reasonably well-understood (Soreghan et al., 1999; Zachos et al., 2008), temporal variations in water fluxes related to the CRYO reservoir are difficult to constrain. As the amount of water in CRYO increases, the extent of sea ice coverage away from the poles also increases. This means, in turn, that the change in surface area covered by ice corresponding to a one degree Celsius decrease in temperature increases with decreasing temperature. Stated differently, the amount of ice that undergoes seasonal melting/freezing at an average global temperature of 10°C is much less than the amount that undergoes seasonal melting at an average global temperature of 0°C. Thus, we relate variations in the flux of water from oceans to the CRYO reservoir to the amount of water present in the CRYO reservoir which, in turn, is related to the surface area covered by ice. Above, we described how the amount of water in the CRYO reservoir varies as a function of average global temperature. Here, the flux of water from the oceans to the CRYO reservoir at a given temperature ($F_{Sea\ Ice\ Freeze,T}$) is a function of the relative amount of water in CRYO at that temperature ($M_{CRYO,T}$; Eqn. 6), the modern amount of water in CRYO ($M_{CRYO,modern}$), and the modern flux of water from the oceans to CRYO ($F_{Sea\ Ice\ Freeze,modern}$) (Fig. 9).

$$F_{Sea\ Ice\ Freeze,T} = F_{Sea\ Ice\ Freeze,modern} * \frac{M_{CRYO,T}}{M_{CRYO,modern}} \quad (24)$$

As discussed above, this flux approaches zero when the CRYO reservoir is absent during greenhouse periods. The variation in the flux of water from the oceans to the CRYO reservoir during the past 700 Ma is shown in Figure 10.

4. Water flux from the cryosphere to the oceans

Sea ice annually melts into the oceans during polar summers, and we assume that the amount of water removed from the oceans and incorporated into ice at one pole during its winter season is balanced by the amount of ice melted into the oceans during summer at the other pole (see above). Previous workers have measured the decrease in Antarctic sea ice cover during the austral summer and estimated that ~1.5×10^{16} kg/yr of water is transferred from CRYO to the oceans via melting (Parkinson, 1996). Other workers (Bodnar et al., 2013) have examined fluxes of water from the Antarctic continent to the oceans via glacial calving (~2×10^{15} kg/yr; Allison, 1996) and estimated that the amount of water transferred from CRYO to the oceans by this process is 1.7×10^{16} kg/yr.

As discussed above, estimates of temporal variations in fluxes of water into and out of the CRYO reservoir are highly uncertain. Here, we follow the method of Bodnar et al. (2013) and calculate the flux of water from the CRYO reservoir to the oceans by mass balance, assuming that the sum of the fluxes into the CRYO reservoir (precipitation, sea ice freezing, and continental glacial advance; Eqns. 22, 24, 27) minus the sum of fluxes out of the CRYO reservoir (sublimation and continental glacial retreat; Eqns. 23, 26) equals the flux of water from the cryosphere to the oceans:

$$F_{Sea\ Ice\ Melt,T} = \left(F_{CRYO\ Pptn.,T} + F_{Sea\ Ice\ Freeze,T} + F_{Glacial\ Advance,T}\right) - \left(F_{Sublimation,T} + F_{Deglaciation,T}\right) \quad (25)$$

As such, we estimate a modern flux of water from CRYO to the oceans of 1.73×10^{16} kg/yr, consistent with the estimate of Bodnar et al. (2013). As discussed above, the flux of water from the cryosphere to the oceans approaches zero as the amount of water in the CRYO reservoir approaches zero during greenhouse conditions. The variation in the flux of water from the CRYO reservoir to the oceans during the past 700 Ma is shown in Figure 10.

1115

1116 **5. Water flux from the cryosphere to surface water**

1117 As polar ice melts during warming periods, water is transferred to the continental
1118 surface (and thus the SW reservoir) as melt water runoff. The Greenland ice sheet is the
1119 largest body of continental ice in the Northern Hemisphere and discharges ~400 km^3
1120 (4×10^{14} kg) of freshwater annually (Hawkings et al., 2015). Other bodies of continental
1121 ice (reported in Meier and Bahr, 1996) are orders of magnitude smaller than the
1122 Greenland ice sheet and discharge concomitantly less water annually, and we do not
1123 include fluxes of water from those smaller bodies in our melt water estimate. We
1124 recognize, however, that smaller subpolar glaciers have been decreasing in area and mass
1125 over the past several decades and increasing the flux of water from the cryosphere to SW
1126 (Dyurgerov and Meier, 2005).

1127 Janssens and Huybrechts (2000) modeled mass balance variations in the Greenland
1128 ice sheet and reported an annual melt water runoff of ~2.81×10^{14} kg/yr. Helm et al.
1129 (2014) report an annual ice loss of ~375 km^3/yr, or 3.75×10^{14} kg/yr, from the Greenland
1130 ice sheet during the past three years. Meier and Bahr (1996) estimate an annual flux from
1131 the Greenland ice sheet to surface melt water of 5.4×10^{14} kg/yr. Hanna et al. (2008)
1132 analyzed runoff data from 1958 to 2006 and estimated that melt water runoff has
1133 increased from ~2.75×10^{14} kg/yr in 1958 to ~ 3.88×10^{14} kg/yr in 2006. Here, we use a
1134 linear extrapolation of the trend over time reported by Hanna et al. (2008) to estimate a
1135 modern flux of water from the CRYO reservoir to the SW reservoir of 4.1×10^{14} kg/yr.
1136 This value is consistent with current observations of Greenland ice sheet melt water
1137 discharge (~400 km^3, Hawkings et al., 2015).

Previous workers have linked increases in melt water runoff to increases in global temperature (Hanna et al., 2008). As discussed above, the amount of H_2O contained in the cryosphere decreases linearly with increasing average global temperature over the range -27°C to +18°C. During snowball-Earth conditions, all landmasses on Earth are covered by ice, thus there is no water transferred from ice to surface water. As global temperature increases from snowball-Earth conditions (-27°C), permanent ice recedes and exposes continental surface and the amount of water transferred from ice to surface water increases. During greenhouse conditions, no permanent ice exists on Earth and thus no water is transferred from the cryosphere to surface water. We use a linear extrapolation of the data reported by Hanna et al. (2008) to determine the amount of water transferred from the cryosphere to the surface water reservoir as a function of average global temperature. We then estimate variations in the flux of water from the CRYO reservoir to the SW reservoir over the temperature range -27°C to 18°C (Fig. 9):

$$F_{Deglaciation,T} = (9.855x10^{12} * T) + 2.66x10^{14} \quad (26)$$

As discussed above, when the average global temperature is -27°C or lower, the flux of water from the cryosphere to the surface water reservoir is zero. The variation in the flux of water from the CRYO reservoir to the surface water reservoir during the past 700 Ma is shown in Figure 10.

6. Water flux from surface water to the cryosphere

Glacial ice annually melts during polar summers and local surface water freezes during the winter and is incorporated into glacial ice. Here, we relate the flux of water from the surface water reservoir to the CRYO reservoir to glacial advance and melt water retention on the surface of the continents. Extensive discussion has taken place regarding

1162 the decrease in volume of glaciers over the past several decades. Most studies of glacial
1163 expansion and retreat examine the mass balance of ice sheets as a function of
1164 precipitation, sublimation, melt water runoff, and melt water retention over the short term
1165 (<1 Ma) (Janssens and Huybrechts, 2000; Dyurgerov and Meier, 2005; Luthcke et al.,
1166 2006; Hanna et al., 2008; Helm et al., 2014). To estimate the effect of glacial expansion
1167 and retreat on fluxes of water between the cryosphere and surface water over longer (>1
1168 Ma) time scales, we assume that the flux of water from the SW reservoir to the CRYO
1169 reservoir is equal to the flux of water from the CRYO reservoir to the SW reservoir (see
1170 above) at any average global temperature (Fig. 9):

1171 $$F_{Glacial\ Advance,T} = F_{Deglaciation,T} \quad (27)$$

1172 Here, the modern flux of water from the SW reservoir to CRYO is 4.1×10^{14} kg/yr, which
1173 balances the modern flux of water from CRYO to SW. The variation in the flux of water
1174 from the surface water reservoir to the CRYO reservoir during the past 700 Ma is shown
1175 in Figure 10.
1176

1177 **7. Water fluxes from the atmosphere to surface water and to the oceans**

1178 Precipitation onto the continents weathers exposed rock and transfers the products of
1179 weathering to surface runoff. Bodnar et al. (2013) estimated that the modern annual flux
1180 of water from the atmosphere to SW is 1.1×10^{17} kg/yr. Today, the continents (SW
1181 reservoir) occupy ~29% of Earth's total surface (including ice covered surface), but the
1182 relative subaerial surface area of the continents has varied with changes in sea level
1183 during the Phanerozoic. Furthermore, because global precipitation varies with latitude
1184 (Tardy et al., 1989), the latitudinal position and arrangement of the continents influences
1185 the amount of annual continental precipitation (Fawcett and Barron, 1998). We describe

1186 the relationship between the surface areas of the continents and the size of the cryosphere
1187 as functions of global average temperature, such that as the surface area of polar ice
1188 linearly decreases from complete coverage of the planet at temperatures of -27°C (and
1189 lower) to zero coverage at temperatures of 18°C (and higher). Concomitantly, the surface
1190 areas of both the continents and the oceans that are not covered by ice linearly increase
1191 with increasing temperature (Fig. 4). Furthermore, as discussed above, as global average
1192 temperatures decrease and permanent ice extends toward the equator, the mid-latitudes at
1193 which the continents receive relatively higher precipitation per unit area are covered by
1194 ice. Thus, the amount of water transferred from the atmosphere to the continents further
1195 decreases as global average temperature decreases (Fig. 11). We describe the flux of
1196 water from the atmosphere to the SW reservoir (the continents) as a function of the total
1197 precipitation to Earth's surface (Eqn. 20), the fraction of Earth's surface occupied by the
1198 continents (29%, excluding ice coverage), and the fraction of Earth's surface occupied by
1199 the CRYO reservoir (Eqn. 9):

1200 $$F_{SW\ Pptn.,T} = F_{Total\ Pptn.,T} * 0.29 * (1 - SA_{CRYO\ fraction,T}{}^2) \quad (28)$$

1201 Here, the annual amount of water transferred from the atmosphere to the surface water
1202 reservoir today is 1.43×10^{17} kg/yr, consistent with previous estimates (Bodnar et al.,
1203 2013). The variation in the flux of water from the atmosphere to the surface water
1204 reservoir during the past 700 Ma is shown in Figure 12.

1205 Most global precipitation falls onto the oceans. Bodnar et al (2013) estimated that the
1206 modern annual flux of water from the atmosphere to the oceans is 3.85×10^{17} kg/yr. As
1207 discussed above, we relate variations in the total amount of precipitation to Earth's
1208 surface to changes in global average temperature. Furthermore, the total amount of
1209 precipitation to Earth's surface is related to the amounts of precipitation to the CRYO and

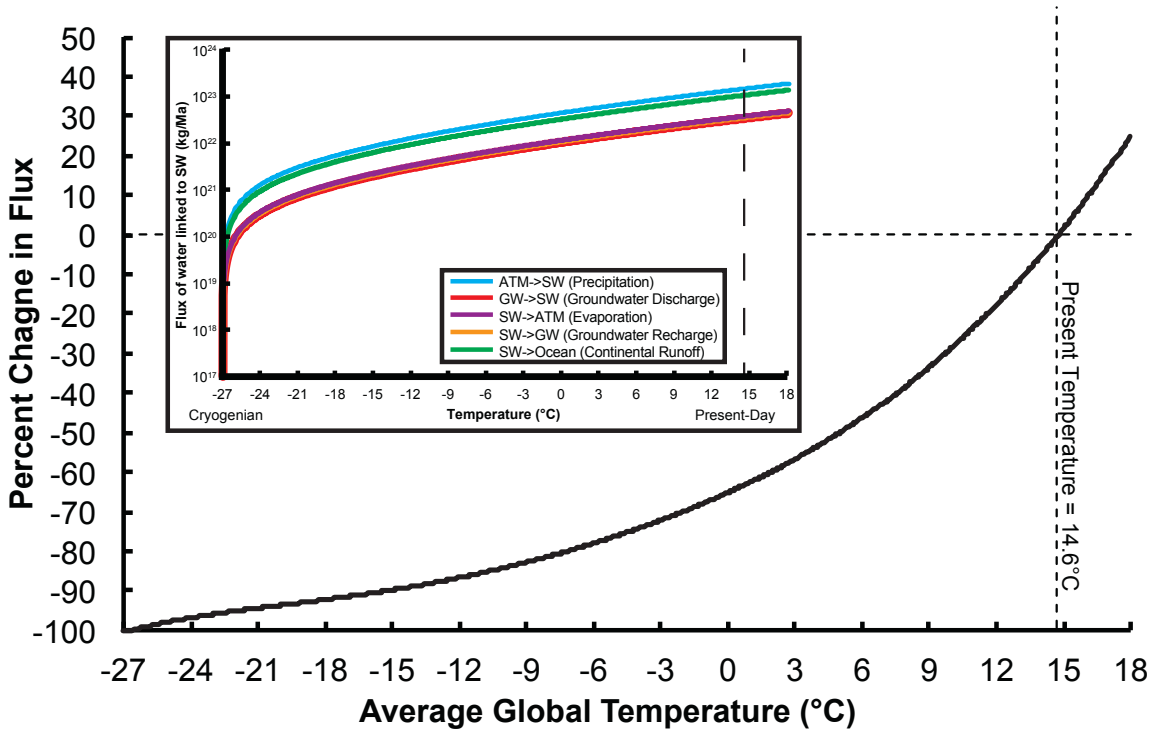

Figure 11: Relationship between global average temperature and fluxes of water into and out of the surface water reservoir, plotted as a percent change from modern values. All fluxes tied to the surface water reservoir change by the same relative amount as the size of the SW reservoir varies, mostly in response to variations in precipitation rates and exposed area of the continents not covered by ice. The inset shows the relationship between global average temperature and individual fluxes connected to the SW reservoir.

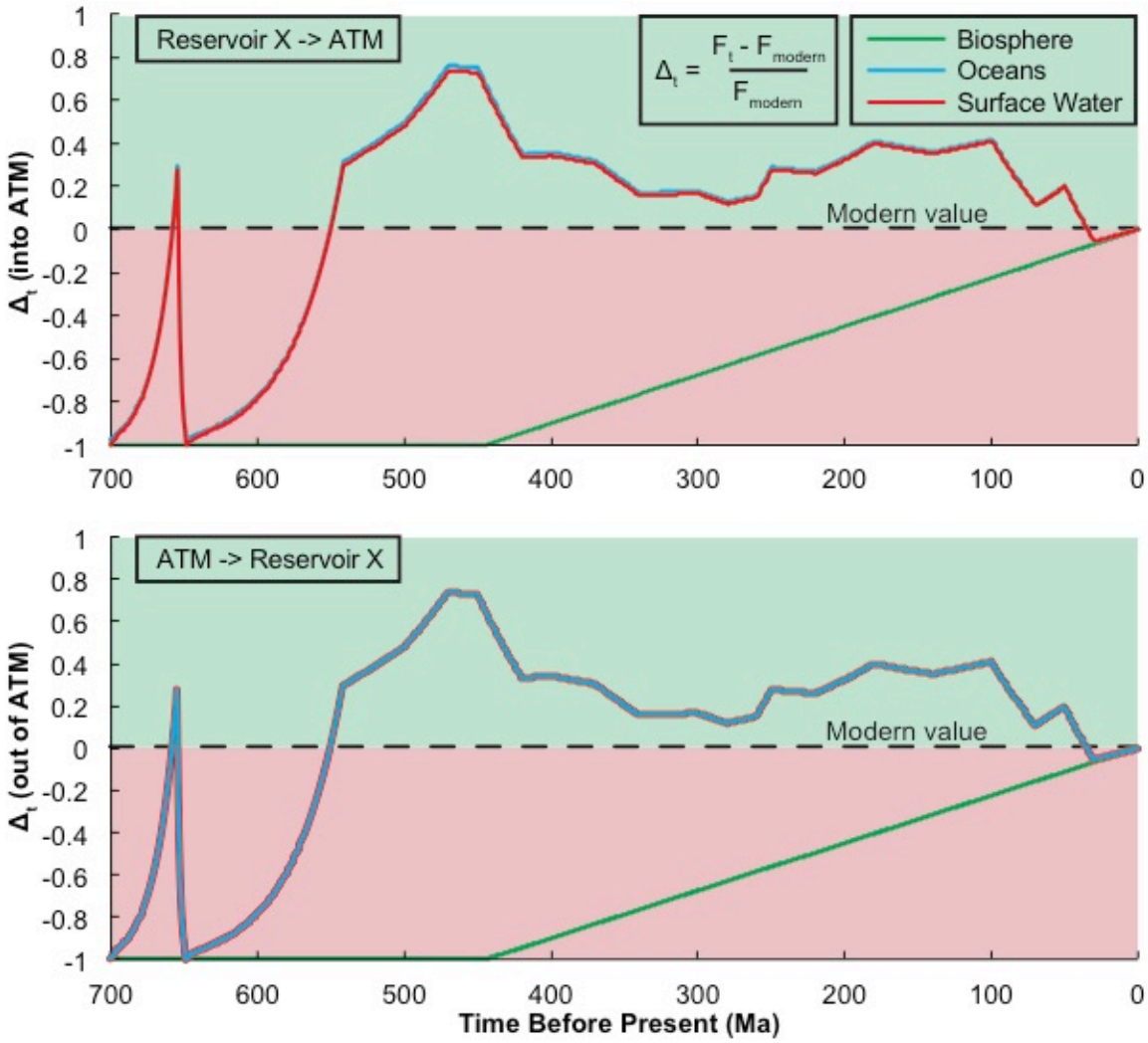

Figure 12: Variations in fluxes of water into and out of the atmosphere (ATM) reservoir, all calculated as the change in flux relative to the modern value.

1210 SW reservoirs. Thus, the amount of water transferred from the atmosphere to the oceans
1211 is related to the total amount of water transferred from the atmosphere to the Earth's
1212 surface, minus the amounts of water transferred directly from the atmosphere to the
1213 CRYO and SW reservoirs (Eqns. 21, 22, and 28), and each of these factors is in turn
1214 related to average global temperature (Fig. 13):

1215 $$F_{Ocean\ Pptn.,T} = F_{Total\ Pptn.,T} - F_{CRYO\ Pptn.,T} + F_{SW\ Pptn.,T} \quad (29)$$

1216 Accordingly, the modern flux of water from the atmosphere to the oceans is estimated to
1217 be 3.5×10^{17} kg/yr, consistent with previous estimates. The variation in the flux of water
1218 from the atmosphere to the oceans during the past 700 Ma is shown in Figure 12.
1219

1220 **8. Water fluxes from surface water and from the oceans to the atmosphere**

1221 Evaporation from the continental surface includes evaporation from standing bodies
1222 of fresh water such as lakes, rivers, streams and swamps. In most assessments of the
1223 hydrologic cycle, evaporation and transpiration rates from the continents have
1224 traditionally been combined into a single value referred to as evapotranspiration (Berner
1225 and Berner, 1987). Bodnar et al. (2013) separated the evaporation and transpiration fluxes
1226 and estimated a modern flux of water from SW to the atmosphere (evaporation) of
1227 6.4×10^{16} kg/yr. Recent studies have shown that the hydrogen isotopic composition (D/H)
1228 of meteoric waters and the average hydrogen isotopic composition of the atmosphere can
1229 be used to differentiate the amounts of water transferred to the atmosphere via
1230 transpiration and via surface water evaporation (Good et al., 2015). These workers
1231 determined that the amount of water evaporated from the continental surface to the
1232 atmosphere is ~26% of the total amount of water precipitated to the continents. Here, we
1233 use the estimated precipitation to the continents (1.28×10^{17} kg/yr) and the relationship

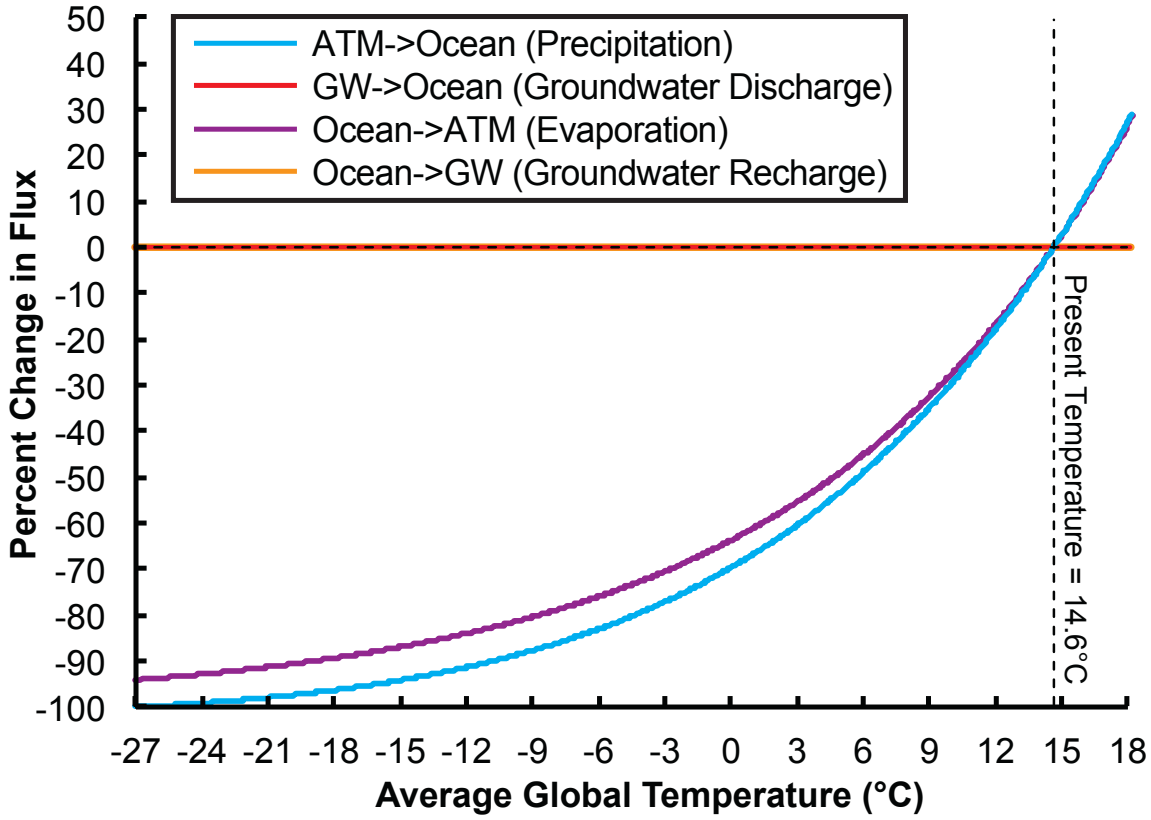

Figure 13: Relationship between the fluxes of water between the atmosphere and oceans (blue, purple) and the GW reservoir and oceans (red, orange) and global average temperature. See text for details.

between evaporation and precipitation reported in Good et al. (2015) to estimate that the modern annual amount of water transferred from the SW reservoir to the atmosphere is 3.34×10^{16} kg/yr, within an order of magnitude of previous estimates. Furthermore, we relate the flux of water evaporated from the SW reservoir to the atmosphere to the flux of water precipitated from the atmosphere to the continents (SW reservoir) (Eqn. 28) according to the proportions estimated by Good et al. (2015):

$$F_{SW\ Evaporation,T} = 0.2608 * F_{SW\ Pptn.,T} \quad (30)$$

The temperature dependence of the flux of water from the surface water reservoir to the atmosphere is shown in Figure 11, and the variation in this flux during the past 700 Ma is shown in Figure 12.

Evaporation from the oceans has traditionally been calculated as the "balance" of other fluxes in the hydrologic cycle, with previous workers estimating that 4.25×10^{17} kg/yr of water is transferred annually from the oceans to the atmosphere (Schlesinger, 1997; Reeburgh, 1997; Bodnar et al., 2013). In a manner similar to evaporation from the continents, temporal variations in the amount of water evaporated from the oceans are related to global average temperature and the total surface area of the oceans. Here, we estimate the flux of water from the oceans to the atmosphere as a "balance" of the other fluxes of water into and out of the atmosphere:

$$F_{Ocean\ Evaporation,T} = \left(F_{Total\ Pptn.,T} + F_{ATM\rightarrow BIOc,t}\right) - (F_{Sublimation,T} + F_{SW\ Evaporation,T} + F_{BIOc\rightarrow ATM,t}) \quad (31)$$

Recall that total precipitation includes precipitation from the atmosphere to the CRYO, SW, and ocean reservoirs. Here, the modern flux of water from the oceans to the atmosphere is 4.53×10^{17} kg/yr, consistent with previous estimates. The temperature dependence of the flux of water from the oceans to the atmosphere is shown in Figure 13,

and the variation in the flux of water from the oceans to the atmosphere during the past 700 Ma is shown in Figure 12.

9. Water flux from surface water (the continents) to the oceans

Water on the continental surface flows to the oceans via rivers and streams, and represents the dominant process that delivers solutes and sediment to the oceans. Previous workers produced consistent estimates of annual surface runoff, with a general consensus that ~3.6×10^{16} kg/yr flows from the SW reservoir (the continents) to the oceans (Berner and Berner, 1987; Drever, 1988; Bodnar et al., 2013; Good et al., 2015). Variations in surface runoff are influenced by changes in precipitation rate, surface topography, and the distribution and amount of vegetation on the continental surface (Otto-Bliesner, 1995; Berner, 1997). Berner and Berner (1987) described a relationship between surface runoff, precipitation and global average temperature and determined that the amount of runoff to the oceans increases as precipitation to the continents increases due to global warming. Other early climate models predicted a decrease in both continental precipitation and runoff with increases in temperature (Otto-Bliesner, 1995). Later workers observed that surface runoff increases by ~4% for every 1°C increase in average global temperature (Labat et al., 2004). The relationship between precipitation and runoff has been used to evaluate the role of surface runoff and continental weathering to changes in atmospheric CO_2 (Goddéris et al., 2014). Furthermore, it is widely accepted that the emergence and radiation of plant life during the Devonian stabilized soils and reduced physical weathering and runoff from the surface (Schumm, 1977; Johnsson, 1993; Algeo and Scheckler; 1998; Donnadieu et al., 2009; Le Hir et al., 2011).

As discussed above, the amount of water in the SW reservoir varies with the areal proportion of the continents not covered by ice. Furthermore, as the exposed surface area of the continents varies, the amount of water transferred from the atmosphere to the surface water reservoir also varies. An increase in exposed continental surface increases the amount of water transferred from the atmosphere to the continental surface and thus increases the amount of water that flows to the oceans as runoff. Furthermore, the amount of water evaporated into the atmosphere also increases as the amount of precipitation to the continents increases, and the portion of surface water taken up by plants varies in proportion to the size of the continental biosphere (see below). Here, the flux of water from the SW reservoir to the oceans varies with changes in the amount of water precipitated onto the continental surface (Eqn. 28), and the amounts of water removed from the SW reservoir by evaporation and uptake by land plants (Eqns. 30 and 38):

$$F_{Runoff,T} = F_{SW\ Pptn.,T} - F_{SW\ Evaporation,T} - F_{SW \rightarrow BIOc} \quad (32)$$

In the balanced model, the amount of water transferred from SW to the oceans today is 1.00×10^{17} kg/yr, which is an order of magnitude greater than previous estimates noted above. Note that the amount of water precipitated onto Earth's surface varies with changes in temperature, and the amount of runoff to the oceans varies as a function of precipitation onto the continents. Thus, we can describe changes in the amount of water transferred from the SW reservoir to the oceans as a function of temperature. The temperature dependence of the flux of water from the surface water reservoir to the oceans is shown in Figure 11, and the variation in the flux of water from the surface water reservoir to the oceans during the past 700 Ma is shown in Figure 14.

10. Water flux between surface water and groundwater

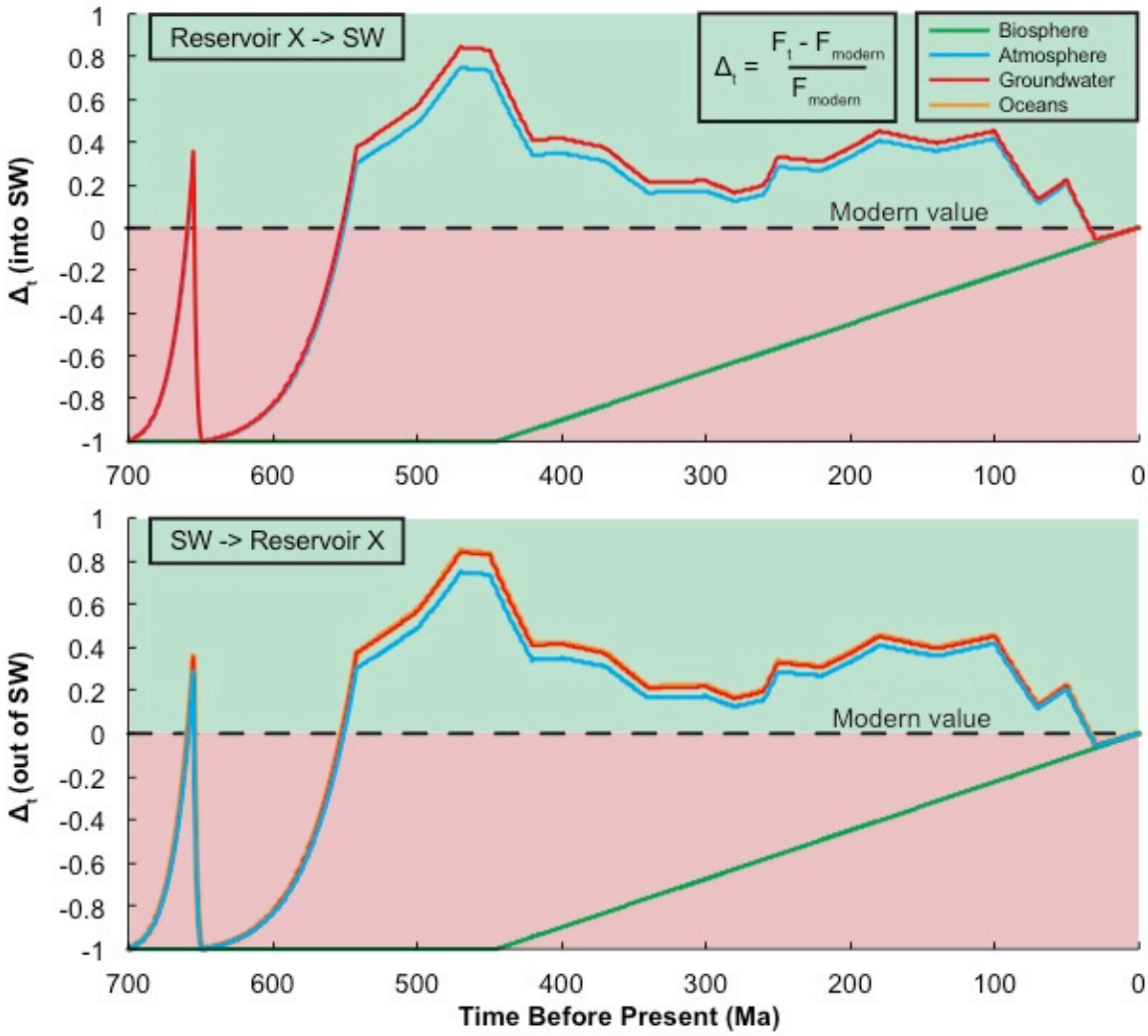

Figure 14: Variations in fluxes of water into and out of the surface water (SW) reservoir, all calculated as the change in flux relative to the modern value.

1305 It is generally accepted that surface recharge is the primary source of water flowing
1306 into the groundwater (GW) reservoir. Recent models of global groundwater recharge
1307 estimate that ~1.27×10^{16} kg/yr of water was transferred from surface waters into the
1308 global groundwater system from 1961 to 1990 (Döll and Fiedler, 2007). This value is
1309 consistent with the ~1.5×10^{16} kg/yr estimated by previous workers (Zekster and Loaiciga,
1310 1993; Bodnar et al., 2013). Here, the flux of water from SW to GW is calculated as a
1311 "balance" of the other fluxes of water into and out of the SW reservoir:

$$F_{SW\rightarrow GW,T} = \left(F_{Deglaciation,T} + F_{SW\ Pptn.,T} + F_{GW\rightarrow SW,T} + F_{BIOc\rightarrow SW,t}\right) -$$

1312 $$\left(F_{Glacial\ Advance,T} + F_{SW\ Evaporation,T} + F_{Runoff,T} + F_{SW\rightarrow BIOc,t}\right) \quad (33)$$

1313 This approach predicts that 3.35×10^{16} kg/yr of water is currently being transferred from
1314 the SW reservoir to the GW reservoir, within the same order of magnitude as previous
1315 estimates. The temperature dependence of the flux of water from the SW reservoir to the
1316 GW reservoir is shown in Figure 11, and the variation in this flux during the past 700 Ma
1317 is shown in Figure 14.

1318 In more humid and temperate environments in which gaining (or effluent) streams are
1319 common, water flows from the groundwater reservoir to springs, streams, and rivers and
1320 adds water to the SW reservoir. Although local and regional-scale GW and SW system
1321 models have been developed for specific areas, the global flux of water from GW to SW
1322 is uncertain. Previous workers have estimated that the flux of water from GW to SW is
1323 ~1/3 of the total annual amount of water transferred from SW to the oceans (Bodnar et
1324 al., 2013), and we adopt that estimate here:

1325 $$F_{GW\rightarrow SW,T} = 0.333 * F_{Runoff,T} \quad (34)$$

1326 Thus, the amount of water transferred from GW to SW today is 3.34×10^{16} kg/yr (i.e., 1/3
1327 of the flux to the oceans, which is 1.00×10^{17} kg/yr). This value is similar to the flux of

1328 water from SW to GW. The temperature dependence of the flux of water from the GW
1329 reservoir to the SW reservoir is shown in Figure 11 variation in the flux of water from the
1330 surface water reservoir to the groundwater reservoir during the past 700 Ma is shown in
1331 Figure 14.
1332
1333 **11. Water flux between the groundwater and the ocean reservoirs**
1334 Submarine groundwater recharge (SGR) describes the flow of seawater from the
1335 oceans to the coastal seabed through continental margins (Burnett et al., 2003; Moore,
1336 2010). It is logical to assume that the amount of water transferred from the oceans to
1337 coastal aquifers scales with the total length of continental coastline at any time.
1338 Moreover, it is well understood that the formation and breakup of supercontinents
1339 influences global coastline length, and reconstructions of continental configurations at
1340 various times during the Phanerozoic presented by Scotese (2001) may be used to
1341 produce "snapshots" of coastline length at various times during the Phanerozoic. During
1342 this time, landmass distribution has varied from periods when all of the landmasses on
1343 Earth were combined into a single landmass (e.g., supercontinents of Pangaea and
1344 Pannotia) to periods of time when multiple continents of various sizes are present (e.g.,
1345 the present distribution).
1346 Because the perimeters of the continents are highly irregular, the length of coastline
1347 corresponding to a landmass of given area is not well defined and is dependent upon the
1348 increments used in the measurement. This "coastal paradox" results in widely varying
1349 estimates of modern global coastal length, with an accepted estimate of 4.88×10^5 km
1350 ±27% (CIA WorldBook; NASA). The total coastline of a single supercontinent,
1351 intuitively, should be less than that of a similar-sized land area consisting of several

smaller continents; however, a supercontinent with a perimeter that is much more irregular than the modern continents could have a longer coastline. As such, the extent of coastline irregularity of such a supercontinent must be available to estimate paleo-coastline length, but this information is largely unknown.

The perimeter of an area with an irregular outer boundary can be described by its fractal dimension, a numerical index for characterizing fractal patterns or sets by quantifying their complexity as a ratio of the change in detail to the change in scale. Fractal Dimension (*FD*) is related to the measured perimeter (*P*) and area (*A*) of a shape according to Mandlebrot (1983):

$$FD = \frac{2 \ln (0.25 * P)}{\ln (A)} \quad (35)$$

whereby FD=1 indicates a shape with a smooth or regular outer boundary and FD=2 indicates a shape with a largely complex and irregular boundary.

We can estimate the perimeter (coastline length) of a Pangaea-like supercontinent by calculating the average fractal dimension of the modern continents and applying that calculated fractal dimension to a supercontinent with $A = 1.50 \times 10^8$ km^2 (the total area of all landmasses on Earth today). We ignore changes in sea level associated with supercontinent formation and breakup that occur when coastal areas are submerged or exhumed during the supercontinent cycle (c.f., Murphy and Nance, 2013). Using the areas and estimated perimeters of the modern-day continents (Table 4), we find that the average FD of the modern continents is ~1.151. A single landmass with an area of 1.5×10^8 km^2 and FD=1.151 has a perimeter of 2.04×10^5 km^2, or 58.2% less coastline than the modern continental configuration. We can also estimate the perimeter of a Pangaea-like supercontinent by describing continents as perfectly circular landmasses. Each continent is thus represented by a circle with a coastline corresponding to the

Continent	Area (km^2)	Perimeter (km)	FD	Ideal Cicrumference (km)
Eurasia	5.50×10^7	262300	1.245	26289.7
Africa	3.04×10^7	26000	1.019	19535.6
North America/ Greenland	2.47×10^7	295300	1.317	17621.1
South America	1.78×10^7	32700	1.079	14972.8
Antarctica	1.40×10^7	18000	1.022	13262.8
Australia/Oceania	8.53×10^6	71200	1.227	10350.9

Table 4: Areas and perimeters of Earth's major landmasses, their fractal dimensions (FD) calculated according to Eqn. 35, and the ideal circumference assuming that each continent has the shape of a circle.

circumference of a circle having an area equal to the continental area. We can then calculate the ratio of the circumference of the supercontinent ($Perimeter_{Super}$) to the sum of the circumferences of the individual continents ($Perimeter_{Multi}$) and use this ratio, combined with the known modern coastline ($Coastline_{Multi}$; 4.88x10^5 km), to estimate the coastline of the supercontinent ($Coastline_{Super}$; unknown) according to:

$$\frac{Perimeter_{Super}}{Perimeter_{Multi}} = \frac{Coastline_{Super}}{Coastline_{Multi}} \quad (36)$$

A circular supercontinent with an area of 1.50x10^8 km^2 has a circumference of ~43,416 km ($Perimeter_{Super}$). If each of the modern continental masses described above (Table 4) is represented by a separate circular landmass, the sum of the six circumferences is 102,033 km ($Perimeter_{Multi}$). Using these estimated values and the CIA/NASA average global coastal length ($Coastline_{Multi}$; 4.88x10^5 km), we find that the coastline of our theoretical supercontinent ($Coastline_{Super}$) is 2.08x10^5 km, or 57.4% less coastline than the modern estimate. A supercontinent with a coastline of 2.08x10^5 km and an area of 1.50x10^8 km^2 has a fractal dimension of ~1.153; this FD value is similar to the average FD value of the modern continents (discussed above).

Based on these results, we assume that during the period when Pangea was completely assembled (~200-300 Ma) the exchange of water between the groundwater and ocean reservoirs would have been reduced by 57% compared to modern values (Fig. 15). We further assume, based on plate reconstruction models, that starting at 200 Ma and continuing to the present, the number of continents and, therefore, the increase in coastline with time, has been linear from 57% at 200 Ma to the modern value today. Pangea began to assemble at about 480 Ma when Laurentia merged with other micro-continents. Owing to uncertainties about the timing of Rodina breakup and formation/breakup of Pannotia, we arbitrarily assume that pre-480 Ma the total coastline

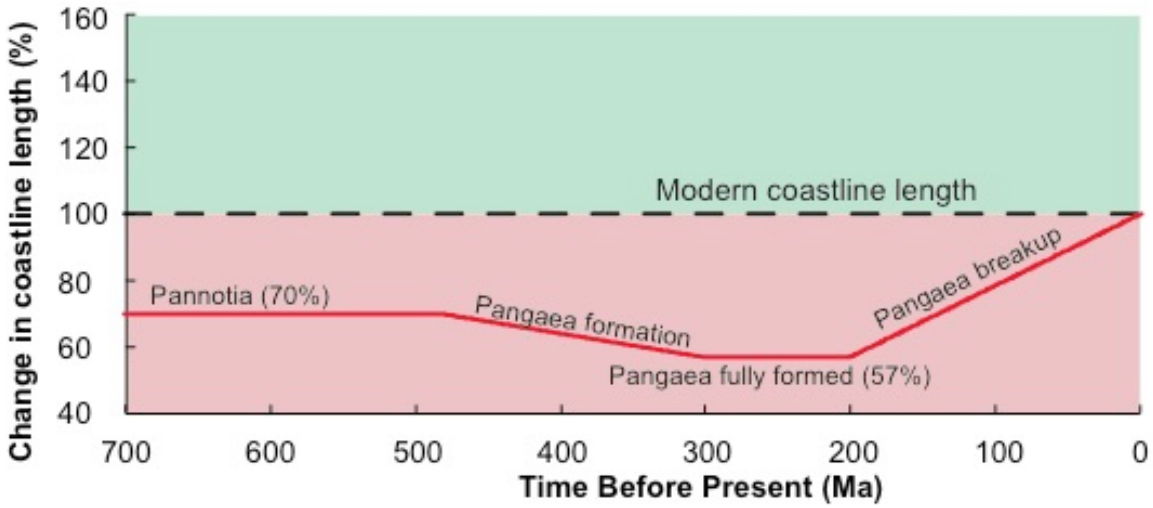

Figure 15: Change in length of global coastline during the past 700 Ma, relative to the estimated length of coastline today (Modern value).

1400 was intermediate between modern values and that associated with Pangea, and assume a
1401 value of 70% of the modern value between 700 and 480 Ma. Finally, we assume a linear
1402 change in coastline length between 480 and 300 Ma (Fig. 15).
1403 Based on the above discussion, we can estimate the amount of water exchanged
1404 between the oceans and GW reservoirs in the past as some fraction of the amount of
1405 water exchanged today. However, much uncertainty exists concerning the magnitude of
1406 submarine groundwater recharge (SGR) today. Previous workers have calculated SGR as
1407 a "balance" of other fluxes that are reasonably well constrained (Taniguchi et al., 2002;
1408 Bodnar et al., 2013). Bodnar et al. (2013) estimated that the modern flux of water from
1409 the oceans to GW is 2.6×10^{14} kg/yr. Here, we accept the estimate of Bodnar et al. (2013)
1410 for the modern flux and calculate the flux of water from the oceans to GW during the past
1411 700 Ma based on the relative difference in length of coastline today compared to the
1412 length in the past as shown in Figure 15. Applying these results to out model, the
1413 variation in the flux of water from the oceans to groundwater during the past 700 Ma is
1414 shown in Figure 16.
1415 Submarine groundwater discharge (SGD) represents the flow of water through
1416 continental margins from the coastal seabed into the ocean. Previous workers have
1417 identified hydraulic gradients between land and ocean related to tidal pumping and wave
1418 activity as the primary mechanism driving seawater circulation through coastal margins
1419 (Riedl et al., 1972; Nielsen, 1990; Burnett et al., 2003; Moore, 2010). Zekster and
1420 Loaiciga (1993) estimated an annual SGD flux of 2.4×10^{15} kg/yr, and Taniguchi et al.
1421 (2009) estimate fluxes ranging from 6.1-12.8×10^{16} kg/yr. Recent integrated radium tracer
1422 studies have been used to estimate a global SGD flux of 1.2×10^{17} kg/yr (Kwon et al.
1423 2014). These estimates, ranging over two orders of magnitude, highlight the large

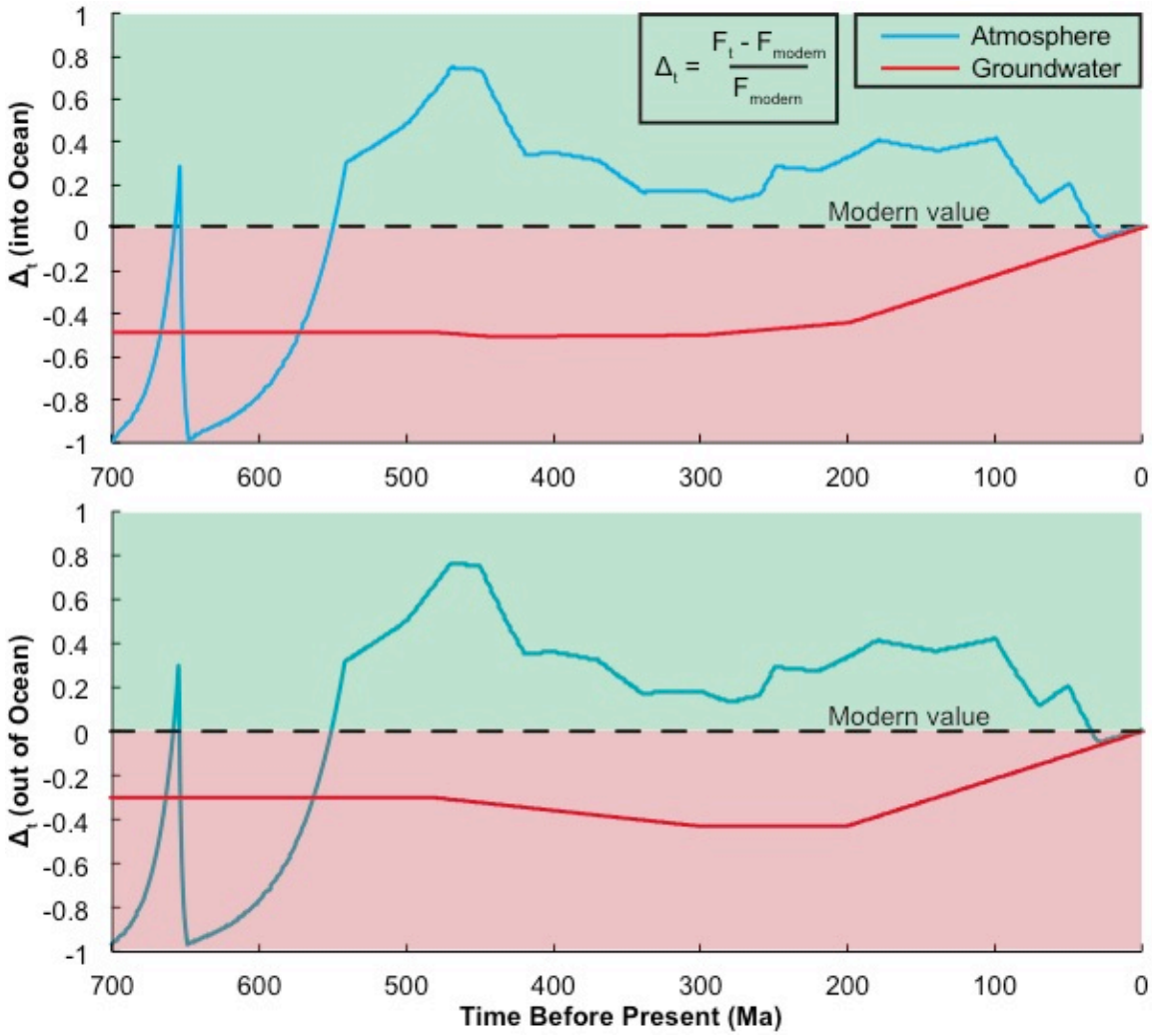

Figure 16: Variations in fluxes of water into and out of the ocean reservoir, all calculated as the change in flux relative to the modern value.

uncertainties associated with estimating SGD. Owing to these uncertainties, at any time in the past 700 Ma we calculate the GW-Ocean flux as a "balance" based on the other, better constrained, processes that transfer water into and out of the GW reservoir:

$$F_{SGD,T} = (F_{SW\rightarrow GW,T} + F_{SGR,T}) - F_{GW\rightarrow SW,T} \quad (37)$$

Accordingly, the modern flux of water from GW to the oceans is ~3.5×10^{14} kg/yr, which is similar to the flux of water from the oceans to the GW reservoir and is one order of magnitude lower than the value reported by Zekster and Loaiciga (1993) and three orders of magnitude less than that of Kwon et al. (2014). It is clear that development of more reliable models for the global water cycle today and in the past require better constraints on the processes associated with GW-Ocean interactions and the amounts of water transferred between these two reservoirs. Given these uncertainties, the variation in the flux of water from groundwater reservoir to the oceans during the past 700 Ma predicted by our model is shown in Figure 16.

12. Water fluxes from surface water (SW; continents) to the biosphere and from the biosphere to the atmosphere

Transpiration is the process by which plants absorb water through their root system, and use some portion of that water for photosynthesis ($CO_2 + H_2O = CH_2O + O_2$), and expel excess water vapor to the atmosphere from leaves, stems and flowers. Stated differently, transpiration is the flux of water from surface water through the continental biosphere (BIOc) and into the atmosphere. Approximately 99% of the surface water taken up by plants is evaporated to the atmosphere; the remainder is stored in plant biomass (Cummins, 2007; Bodnar et al., 2013).

1447 Previous workers have estimated a total flux of water from the continents to the
1448 atmosphere of 7.1×10^{16} kg/yr (Berner and Berner, 1987; Reeburgh, 1997). This reported
1449 flux from the continents includes soil moisture evaporation, transpiration, and polar ice
1450 sublimation. Later workers defined soil evaporation and transpiration as an
1451 "evapotranspiration" flux, ignoring evaporation from open surface water and ice caps
1452 (Trenberth, 2007; Ryu et al., 2011). Lawrence et al. (2007) estimate that 13-41% of
1453 reported evapotranspiration fluxes are due to transpiration. Recently, Good et al. (2015)
1454 used the hydrogen (D/H) isotopic compositions of continental meteoric waters to estimate
1455 that today plants transpire $55(\pm12)\times10^{15}$ kg/yr water to the atmosphere. Here, we adopt
1456 the estimate of Good et al. (2015). Furthermore, if the amount of water transpired to the
1457 atmosphere is 99% of all water taken up by plant biomass, then the modern flux of water
1458 from the SW reservoir to the continental biosphere is 5.56×10^{16} kg/yr.
1459 Owing to uncertainties regarding the total flora biomass on Earth and the average
1460 water uptake rate of plants at any time during the past 444 Ma, temporal variations in the
1461 amount of water transferred from the surface water reservoir to the continental biosphere
1462 are difficult to constrain. It is logical to assume that the amount of water uptake through
1463 roots of plants is related to flora biomass on Earth, i.e., as the biomass increases, the
1464 amount of water being extracted from the continental surface water reservoir by plants
1465 increases, and thus the rate of root water uptake increases. During the early Phanerozoic
1466 when plant life was absent from the continental surface (pre-444 Ma), movement of water
1467 from the surface water reservoir to the biosphere and from the biosphere to the
1468 atmosphere were not part of the hydrologic cycle. As discussed above and shown in
1469 Figure 5, we assumed a linear increase in the amount of biomass on the continents during
1470 the last 444 Ma. Therefore, we can relate the flux of water from the SW reservoir to the

biosphere at any time during the past 444 Ma to the modern flux of water from the SW reservoir to the biosphere using the calculated amount of wet biomass at that time:

$$F_{SW \rightarrow BIOc,t} = F_{SW \rightarrow BIOc,modern} * \frac{M_{BIOc,t}}{M_{BIOc,modern}} \quad (38)$$

The variation in the flux of water from the surface water reservoir to the continental biosphere during the past 700 Ma is shown in Figure 14. Figure 17 shows the relationship between the model chosen for growth of the continental biosphere during the past 444 Ma (as discussed above), and variations in fluxes of water between reservoirs. While the choice of growth model influences temporal variations in fluxes of water into and out of the biosphere, it has little impact on other reservoirs owing to the relatively small amount of water held in the biosphere reservoir.

As discussed above, the flux of water from the continental biosphere to the atmosphere represents 99% of the flux of water from the SW reservoir to the biosphere (Eqn. 38):

$$F_{BIOc \rightarrow ATM} = 0.99 * F_{SW \rightarrow BIOc} \quad (39)$$

The variation in the flux of water from the continental biosphere to the atmosphere during the past 700 Ma is shown in Figure 12.

13. Water flux from the biosphere to surface water

As plants grow they transfer water from the SW reservoir to the BIOc reservoir, and when the plants die, H_2O (and other nutrients) contained in biomass are surrendered back to the local ecosystem. Some of the water contained in expired plant material evaporates into the atmosphere, some is consumed by detritivores that promote plant decomposition, and some is returned to the SW reservoir. Here, owing to the lack of data and a defensible model to estimate the proportions of water evaporated to the atmosphere, consumed by

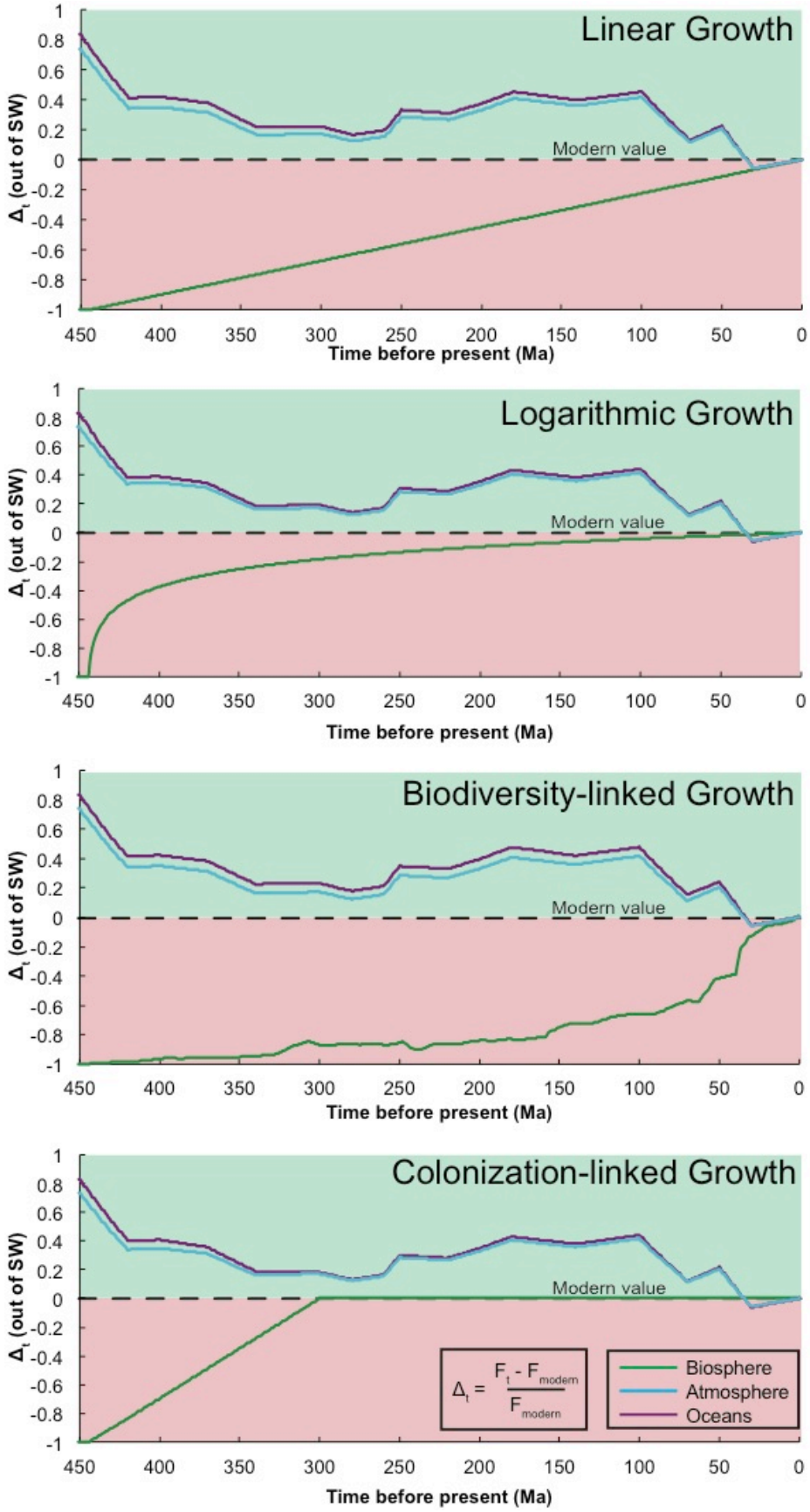
Linear Growth
Logarithmic Growth
Biodiversity-linked Growth
Colonization-linked Growth
Modern value
Δt (out of SW)
Time before present (Ma)
Δt = (Ft - Fmodern) / Fmodern
Biosphere
Atmosphere
Oceans

Figure 17: Variation in the flux of water between the surface water reservoir and the continental biosphere, atmosphere and ocean reservoirs for four different models for growth of the continental biosphere (amount of biomass) during the past 444 Ma. (A) Linear increase in the amount of water in the continental biosphere from 444 Ma to the present. (B) "Mass optimization" logarithmic function whereby the amount of water in the continental biosphere rapidly increases early in the Phanerozoic, followed by a more gradual increase to the present value. (C) The amount of water in the biosphere increases in proportion to biodiversity (data from Benton, 1993). (D) Amount of water in the biosphere following a "colonization forcing curve", whereby the amount of water is linked to the influence of the biosphere on other global chemical cycles (after Bergman et al., 2004). Fluxes of water from the SW reservoir to the ATM and Ocean reservoirs are primarily driven by temporal variations in global average temperature and are not significantly affected by the growth model used.

other organisms during decomposition, and transferred to the SW system, we assume that all water contained in the living BIOc is transferred to the SW reservoir when an organism on the continents dies. This simplifying assumption has little impact on the overall hydrologic cycle because the total amount of water lost from the continental biosphere each year as a result of plant death (9×10^{13} kg/yr) represents only about 0.02% of the total amount of water transferred into the atmosphere from all reservoirs today, and only about 0.07% of the total amount of water transferred into the surface water reservoir from all other reservoirs today. Bodnar et al. (2013) estimated that the modern flux of water from BIOc to the SW reservoir is 9×10^{13} kg/yr, and we adopt this value here.

As discussed above, we assume that the amount of wet biomass in the continental biosphere increases linearly from 0.0 kg at 444 Ma to the present value of 2.9×10^{15} kg. Accordingly, variations in the amount of water transferred from the continental biosphere to the surface water reservoir scale in proportion to the rate of increase of biomass during the past 444 Ma. Thus, the flux of water from the biosphere to the SW reservoir at any time during the past 444 Ma is related to the modern flux of water from the biosphere to the SW reservoir and the proportion of biomass at that time relative to the modern biomass:

$$F_{BIOc\rightarrow SW,t} = F_{BIOc\rightarrow SW,modern} * \frac{M_{BIOc,t}}{M_{BIOc,modern}} \quad (40)$$

The variation in the flux of water from the continental biosphere to the surface water reservoir during the past 700 (444) Ma is shown in Figure 14.

14. Water flux from the atmosphere to the biosphere

Epiphytes (often referred to as air plants) and related plant species adsorb water directly from the atmosphere during photosynthesis, rather than taking in water through

their root system. Benzing (2004) reports that epiphytes have existed since the Carboniferous, although the exact timing of epiphyte appearance in the fossil record is uncertain. To our knowledge, the annual global rate of water uptake by modern epiphytes has not been estimated. Moreover, owing to ongoing discovery of new plant species, genera, and families (The Plant List, 2013), the proportion of epiphytes compared to all flora on Earth is uncertain. Furthermore, the rate of water vapor uptake by different epiphytic species varies significantly compared to the rate of soil moisture uptake. Bodnar et al. (2013) estimated that the amount of water removed annually from the atmosphere by modern epiphytes is 6.3×10^{13} kg/yr – this value is not based on any measured data but, rather, represents a "mass balance" estimate. Other fluxes linked to the BIOc reservoir (transpiration, root uptake, and plant death and decomposition) are reasonably well constrained (see above). Thus, estimating the amount of water vapor uptake as a "balance" based on other fluxes that are better constrained is reasonable. Following this logic, we estimate the flux of water from the atmosphere to the BIOc as a "balance" between the other fluxes of water into and out of the continental biosphere (Eqns. 38, 39, and 40):

$$F_{ATM\rightarrow BIOc,t} = (F_{BIOc\rightarrow SW,t} + F_{BIOc\rightarrow ATM}) - F_{SW\rightarrow BIOc,t} \quad (41)$$

The variation in the flux of water from the atmosphere to the continental biosphere during the past 700 Ma is shown in Figure 12.

15. Summary of variations in fluxes in the hydrologic cycle during the past 700 Ma

As described in detail above, most fluxes of water between reservoirs in the hydrologic cycle have varied significantly during the past 700 Ma. Moreover, because we assume that the total amount of water held in the six reservoirs that comprise the

exosphere remains constant, increases in one flux require decreases in one or more other fluxes to maintain a balanced system. Synergies and feedbacks between different reservoirs are shown schematically in Figure 18, where the total flux into and out of each reservoir during the past 700 Ma is shown. As such, increases in average global temperature (panel A) lead to increases in the total flux of water into the ATM, SW, GW and ocean reservoirs, and decrease in the total flux of water into the CRYO reservoir. With the exception of the continental biosphere reservoir, all total fluxes vary in concert with changes in average global temperature.

Summary and Discussion of the Evolution of the Hydrologic Cycle During the Past 700 Ma

As discussed above, the calculated amount of water in the CRYO reservoir is a function of the average global temperature (Eqn. 6) and increases in this reservoir correlate reasonably well with the major glaciation events (Fig. 8). In this study, global average temperatures obtained from models of the global carbon cycle at specific times during the past 700 Ma were used (Goddéris et al., 2014). Uncertainties in these paleo-temperature estimates will, therefore, be manifest in our results as uncertainty in those aspects of the hydrologic cycle that are most sensitive to temperature, such as waxing and waning of the cryosphere. For example, there is evidence for widespread glaciation during the late Ordovician (Brenchley et al., 2001), and the Paleocene-Eocene Thermal Maximum (PETM) (~56 Ma) is a brief greenhouse period associated with rapid atmospheric CO_2 increase when the planet had no polar ice (McInerney et al., 2011; Bowen et al., 2015). However, our model does not predict the presence of a CRYO reservoir during the late Ordovician (Fig. 8), whereas our model does indicate the

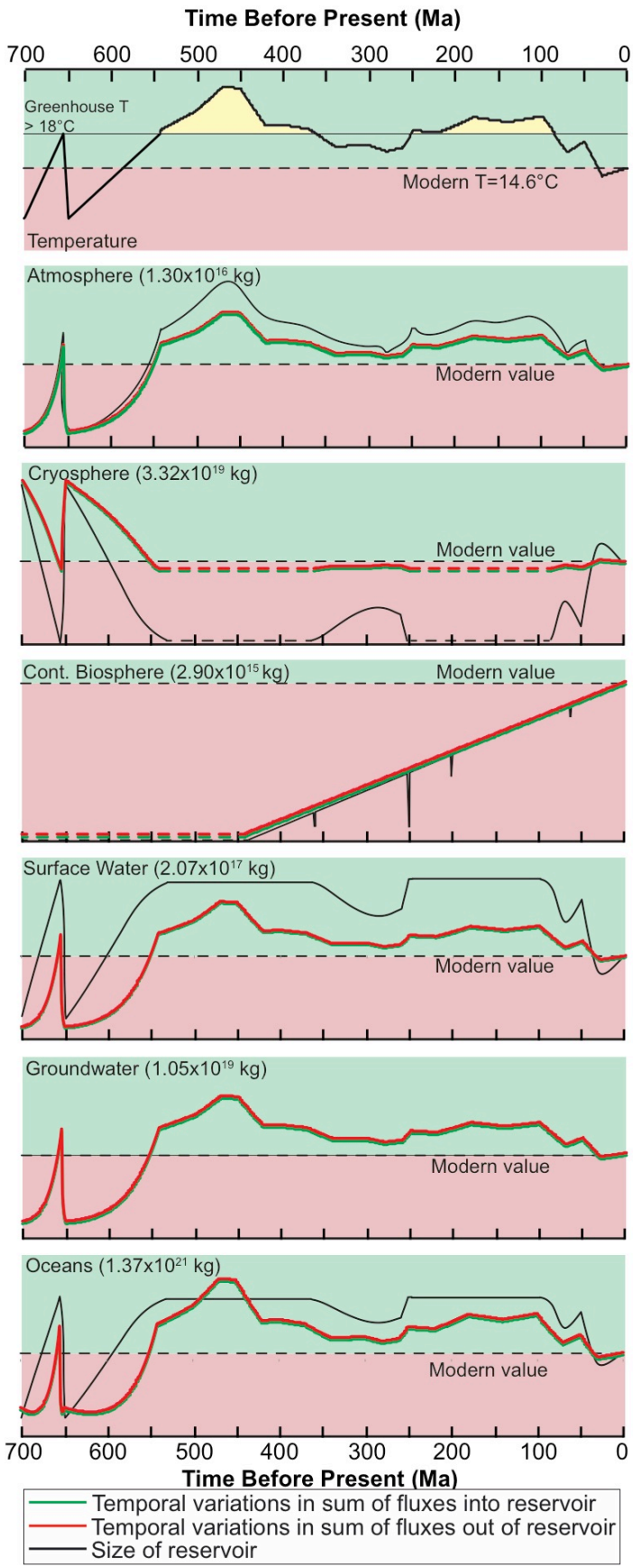
Time Before Present (Ma)
700
600
500
400
300
200
100
0
Greenhouse T
> 18°C
Modern T=14.6°C
Temperature
Atmosphere (1.30x10^16 kg)
Modern value
Cryosphere (3.32x10^19 kg)
Modern value
Cont. Biosphere (2.90x10^15 kg)
Modern value
Surface Water (2.07x10^17 kg)
Modern value
Groundwater (1.05x10^19 kg)
Modern value
Oceans (1.37x10^21 kg)
Modern value
Time Before Present (Ma)
Temporal variations in sum of fluxes into reservoir
Temporal variations in sum of fluxes out of reservoir
Size of reservoir

Figure 18: Summary of variations in fluxes between reservoirs of the hydrologic cycle during the past 700 Ma, all shown relative to the modern value. Note that departures from the modern line are schematic and are only intended to show the timing and direction of changes in fluxes and not the magnitude of the departures. The scale on the left side of each panel corresponds to the period from 700 to 540 Ma (pre-Phanerozoic) and the scale on the right side of each panel corresponds to the Phanerozoic (540 to 0 Ma). Note also that in some cases the positive and negative scales on the same side of individual panels are different in order to better emphasize variations in fluxes.

1567 presence of some permanent ice during the PETM. These results indicate that while
1568 waxing and waning of the CRYO reservoir may be mainly controlled by average global
1569 temperature, other factors such as organization and distribution of continents,
1570 topography, etc., that are unaccounted for in our model and not well documented in the
1571 literature also play a role. Importantly, these results provide incentives for paleo-climate
1572 researchers to consider other drivers that control the size of the CRYO reservoir. Higher
1573 resolution, short-term (<1-10 Ma) proxies for climate variations during the Phanerozoic
1574 would also allow more robust models to be developed to examine the effect of short-term
1575 temperature excursions.

1576 As the cryosphere expands across the oceans during global cooling, water is
1577 transferred from seawater to the ice phase, resulting in higher concentrations of all
1578 dissolved components in seawater. During snowball-Earth conditions, the concentrations
1579 of all aqueous species in seawater would be ~47% higher than in modern seawater,
1580 assuming that all water added to the cryosphere was removed from the oceans and that
1581 the total mass of all dissolved species in seawater remained constant (Angel et al., in
1582 prep). We note that a decrease in sea level associated with the expanding cryosphere
1583 would likely result in the formation of basins and lagoons that may lead to formation of
1584 evaporite deposits and remove solutes from seawater, though the extent to which this
1585 would influence seawater chemistry on a global scale is uncertain.

1586 During greenhouse periods, permanent ice melts and exposes the continental surface
1587 to weathering processes. Also, as the surface area of the continents increases, the total
1588 amount of precipitation onto the continents increases, subsequently increasing runoff to
1589 the oceans, assuming the flux of water from the atmosphere to the surface water reservoir
1590 remains constant. Furthermore, as discussed above, the loss of Arctic sea ice is linked to

1591 increased regional evaporation (Kopec et al., 2016) and the increase in evaporation, in
1592 turn, would be returned to the Earth's surface in the form of precipitation to the oceans,
1593 CRYO, and the SW reservoir, leading to a further increase in surface runoff to the oceans
1594 (Bintanja and Selten, 2014). Feedbacks linked to the retreat of glaciers and the melting of
1595 polar ice produce variations in the amounts of water and other materials transferred to the
1596 oceans and likely play a major role in temporal variations in global ocean chemistry
1597 (Angel et al., in prep).

1598 The dilution and enrichment of chemical species due to the exchange of water
1599 between oceans and CRYO reservoirs may impact marine organisms that rely on specific
1600 seawater conditions for survival. For example, the seasonal freezing of sea ice locally
1601 produces highly saline brines, which inhibits marine primary production (Gleitz et al.,
1602 1995). As such, during the onset of snowball-Earth conditions the latitudinal extension of
1603 polar ice caps would eventually reach tropical zones where primary producers thrive.
1604 Thus, we would expect to see a decrease in marine primary production corresponding to
1605 lower global average temperatures and associated changing seawater chemistry. It is
1606 possible that near-complete inhibition or destruction of marine life could occur as a result
1607 of global glaciation. However, although primitive pre-Cambrian life did exist on Earth,
1608 the most recent snowball-Earth event (the Marinoan) occurred before the Cambrian
1609 Explosion. There has been extensive study of the effect of snowball-Earth conditions on
1610 the marine biosphere that discuss major trends in microorganism biodiversity as
1611 influenced by changes in mean ocean temperature and ocean chemistry (e.g. Corsetti et
1612 al. 2006; Olcott et al. 2005; Riedman et al. 2014). Owing to the relatively small influence
1613 of the marine biosphere on the whole-Earth hydrologic cycle, variations in marine
1614 biodiversity are beyond the scope of this work.

There is extensive debate regarding the scale and timing of the freezing and melting of permanent ice during greenhouse-glacial period transitions, and recent studies suggest that polar ice exists in "flickering" pulses millions of years before the formation of permanent ice caps (Scher et al., 2011). Other workers suggest that the transition from extensive permanent ice to full snowball conditions (as average temperature decreases from 0° to -27°C) occurs very quickly, within tens of thousands of years (Hyde et al., 2000; Goddéris et al., 2003). Moreover, anthropogenic influence on the Earth system complicates our understanding of pre-human hydrologic processes. Based on modern rates of polar ice melting and sea level rise, it is suggested that all of Earth's ice will melt within tens of thousands of years, if not sooner, due to anthropogenic influences on climate and energy added to the atmosphere and ocean currents (Grénier et al., 2015). Modern worst-case scenario models of Earth's climate suggest that the rate of melting is accelerating (Cox et al., 2000).

Today, the oceans contain 13.7×10^{20} kg of water, and model results suggest that the total has varied from a maximum of ~14.0×10^{20} kg during greenhouse conditions, to a minimum of 9.64×10^{20} kg during snowball earth conditions, corresponding to paleo-oceans containing from 2.4% more water to 32% less water than the amount in the oceans today. As the amount of H_2O contained in the oceans varies, so does relative sea level. If all the ice present today were to melt and increase the amount of water in the oceans by 2.4%, sea level would rise by ~80 m (Poore et al., 2001). This rise in sea level would reduce the size of exposed continental area by about 15.6%. However, as the ice melts, new continental area is exposed. Today, ~10% of the land surface (~14.8×10^6 km^2) is covered by permanent ice (http://water.usgs.gov/edu/watercycleice.html), and for each square kilometer of permanent ice that melts (assuming a uniform thickness of ice of 0.94

km), sea level rises by 2.33×10^{-6} m and ~0.29 square kilometers of new continental surface is exposed. Today, about ~34% of the world's population live in areas that would become submerged if all permanent ice were to melt (Cohen and Small, 1998).

Conversely, as the amount of polar ice increases, sea level would fall and expose more continental area. However, this is offset by the fact that more of the continental area is covered by ice (and therefore not exposed) as the amount of ice increases. For each square kilometer of permanent ice that forms on the planet's surface, ~0.29 square kilometers of exposed continental surface is lost. Moreover, upon reaching snowball Earth conditions, the entire continental landmass would be covered by ice, regardless of the change in sea level as ocean water is sequestered in permanent ice. Stronger constraints on submarine topography during the Phanerozoic during snowball Earth and extremely cold climate conditions are necessary to better understand the influences of ice coverage and sea level regression on the amount of exposed continental landmass.

Transfer of water into and out of the CRYO reservoir involves interactions between CRYO and the oceans, atmosphere and surface water reservoirs. For every 1°C change in average global temperature, 9.76×10^{18} kg of water is transferred into or out of the CRYO reservoir. Thus, as temperature decreases and the CRYO reservoir grows, the amount of precipitation from the atmosphere to the CRYO increases owing to the increase in surface area of the CRYO reservoir. At the same time, the amount of water transferred from the CRYO to the atmosphere through sublimation increases owing to the increase in ice surface area. Similarly, as the CRYO reservoir grows in response to decreasing average global temperature, the annual flux of water from the CRYO to oceans increases because a larger amount of ice is at latitudes that are within the "seasonal melting range". In a similar manner the flux from the oceans to the CRYO reservoir increases with decreasing

1663 average temperature. Thus, as the size of the cryosphere grows overall with decreasing
1664 temperature, the effect of the cryosphere on local ocean chemistry increases as a larger
1665 amount of water is removed and added to the ocean during seasonal freeze/melting
1666 episodes. This, in turn, leads to significant annual local fluctuations in ocean chemistry
1667 that would likely exert increasing environmental stresses on the local marine ecosystem.
1668 Unlike the cryosphere-ocean interactions described above, as global average
1669 temperature decreases and the CRYO reservoir grows, the flux of water from the CRYO
1670 to the surface water reservoir decreases, as does the flux from the SW reservoir to the
1671 CRYO (Fig. 17). This occurs mostly as a result of the decrease in exposed continental
1672 surface as ice expands and covers the land surface.
1673 The amount of water transferred from the atmosphere to the CRYO reservoir varies
1674 from zero during interglacial (greenhouse) periods of the Phanerozoic to a maximum of
1675 3.54×10^{16} kg/yr at ~609 Ma (Fig. 10), owing to competing effects of temperature and
1676 reservoir surface area. Global precipitation increases as global average temperature
1677 increases. Conversely, the surface area of the CRYO reservoir increases as global
1678 temperature decreases. Thus, as average temperature decreases, the flux of water from the
1679 atmosphere to the planet's surface decreases but the proportion of the surface covered by
1680 ice increases such that the total amount of water transferred from the atmosphere to the
1681 cryosphere increases. Thus, as temperature increases from -27°C to ~-10.5°C, the amount
1682 of water transferred from the atmosphere to the cryosphere increases (Fig. 9) because the
1683 effect of surface area of ice on the flux is greater than that of increasing temperature. At -
1684 10.5°C, a "tipping point" is reached (Fig. 9) whereby the decreasing area of permanent
1685 ice has a greater effect on total flux than does the effect of increasing temperature. Thus,
1686 as temperature increases from -10.5°C to 18°C, even though the rate of precipitation is

increasing in response to increasing temperature, the total amount of water transferred from the atmosphere to the CRYO reservoir decreases because the surface area of the cryosphere has decreased sufficiently to counter the effect of increased precipitation. At temperatures >18°C, polar ice is does not exist and the CRYO reservoir is removed from the hydrologic cycle; hence, the flux of water from the atmosphere to the CRYO reservoir is zero.

The amount of water transferred from the CRYO to the ATM via sublimation varies from zero during greenhouse periods of the Phanerozoic to a maximum of ~2.65×10^{21} kg/Ma at 650 and 700 Ma (Figs. 10. 17). The sublimation flux to the atmosphere varies in a manner similar to the fluxes of water between the ocean and the cryosphere (discussed below), whereby the amount of water transferred decreases as global average temperature increases (Fig. 9). As discussed above, the primary control on the amount of water transferred from the cryosphere to the atmosphere via sublimation is the surface area of the cryosphere, which varies as a function of global average temperature. As such, when the surface of the Earth is completely covered by glacial and polar ice (snowball-earth, 650 and 700 Ma), the sublimation flux is at its maximum value. At temperatures >18°C, the CRYO reservoir is removed from the hydrologic cycle and the flux of water from the CRYO reservoir to the atmosphere is zero.

The flux of water from the oceans to the CRYO reservoir varies from zero during interglacial periods of the Phanerozoic to a maximum of 1.99×10^{23} kg/Ma at 650 and 700 Ma when the amount of water in the CRYO reservoir is at the maximum of 4.39×10^{20} kg (Fig. 10) and the rate of change of average global temperature with time is greatest (Fig. 8A). As discussed above, the flux of water from the oceans to CRYO decreases as global average temperature increases and the total amount of water in the CRYO reservoir

1711 decreases in response to increasing temperature (Eqn. 24, Figs. 7, 8). During snowball-
1712 Earth conditions, the oceans would be completely covered in ice and seasonal
1713 freeze/thaw variations do not occur (Hyde et al., 2000). Some workers, however, propose
1714 that relatively warmer seas existed at the equator, even during snowball-Earth conditions
1715 (Pierrehumbert, 2005). This "slushball" hypothesis would allow for seasonal variations in
1716 sea ice extent and transfer of water between the oceans and the cryosphere at extremely
1717 low global average temperatures.

1718 The amount of water transferred from the CRYO reservoir to the oceans varies from
1719 zero during interglacial periods of the Phanerozoic to a maximum of 2.23×10^{23} kg/Ma at
1720 700 Ma when the amount of water in the CRYO reservoir is 4.39×10^{20} kg. The flux of
1721 water from the oceans to CRYO is balance-calculated and decreases as global average
1722 temperature increases (Eqn. 25). This trend is similar to that of water transfer from the
1723 CRYO reservoir to the oceans (Fig. 10). As discussed above, the possibility of equatorial
1724 "slushball" seas allows for seasonal variations in sea ice extent, and exchange of water
1725 between the cryosphere and oceans may occur at extremely low average global
1726 temperatures.

1727 The flux of water from the CRYO reservoir to the SW reservoir decreases with
1728 decreasing temperature as the area of exposed continental surface decreases, and varies
1729 from zero during interglacial periods of the Phanerozoic to a maximum of
1730 4.40×10^{20}kg/Ma during interglacial/glacial period transitions when global average
1731 temperature is ≥18°C, at which point the amount of water in the CRYO reservoir is zero
1732 (Fig. 10). The flux of water from the CRYO reservoir to the oceans increases with
1733 increasing global average temperature until greenhouse conditions are reached and no
1734 polar ice exists on Earth.

1735 The amount of water transferred from the SW reservoir to the CRYO reservoir varies
1736 from zero during interglacial periods of the Phanerozoic to a maximum of 4.43×10^{20}
1737 kg/Ma at interglacial/glacial period transitions. Variations in the amount of water in the
1738 CRYO reservoir due to rapid glaciation and deglaciation during the Cryogenian
1739 significantly increase the amount of water transferred from the SW reservoir to the
1740 CRYO reservoir.
1741 As the area of exposed continental surface area decreases during expansion of the
1742 cryosphere, the amount of water in the SW reservoir is reduced, as well as the amounts of
1743 water transferred into and out of the SW reservoir. We link the glacial coverage of the
1744 continents to variations in global average temperature (Fig. 4) and quantify the fluxes of
1745 water into and out of the atmosphere and SW reservoirs as a function of temperature
1746 (Figs. 9, 10). Studies suggest a lack of terrigenous sediment flux from Antarctic
1747 meltwater runoff at the onset of polar ice formation during the late Eocene (Scher et al.,
1748 2014). This observation is consistent with the assumption in our model that expansion of
1749 the cryosphere covers continental landmass and reduces runoff from the SW reservoir to
1750 the oceans (Fig. 14). It is logical to assume that glacial coverage of the continents also
1751 influences the movement of water between the atmosphere and the surface water
1752 reservoir in a similar manner. As ice covers the continents and the surface area of the
1753 continents exposed to the atmosphere decreases, total precipitation to the surface water
1754 reservoir (continents) decreases, and evaporation from surface water to the atmosphere
1755 also decreases. Thus, as global temperature decreases, the flux of water between the
1756 atmosphere and SW reservoir decrease (Fig. 12). The same is true for the fluxes of water
1757 between the atmosphere and the ocean (Fig. 12); as sea ice covers the oceans and the
1758 exposed surface area of the oceans decreases, total precipitation onto the oceans

1759 decreases, and the amount of water evaporated from the oceans to the atmosphere also
1760 decreases. Thus, as global temperature decreases, the flux of water between the
1761 atmosphere and ocean decrease (Figs. 12, 16, 18).

1762 As global temperature decreases and ice sheets expand, the surface area of the
1763 continents exposed to the atmosphere decreases (Fig. 4). The decrease in exposed
1764 continental surface area results in a decrease in the amount of water that precipitates onto
1765 the land (non-ice covered) surface, and this, in turn, reduces the amount of water that
1766 flows from the continents to the oceans as runoff. Thus, the flux of water from the SW
1767 reservoir to the oceans varies with the amount of exposed subaerial continental surface in
1768 response to changes in temperature (Figs. 14, 18). The flux of water from the SW
1769 reservoir to the oceans as runoff increases from 0.0 kg/Ma during snowball-Earth
1770 conditions (-27°C) when no subaerial continental surface is present, to 1.39×10^{23} kg/Ma
1771 during greenhouse conditions (18°C) when the continental surface is fully exposed (Figs.
1772 11, 14).

1773 As global average temperature increases and the total precipitation onto the
1774 continents increases, the amount of surface runoff to the oceans increases. The increased
1775 precipitation and runoff also lead to increased weathering and erosion, and the products
1776 of weathering/erosion are added to the surface water reservoir, both as dissolved species
1777 and transported sediment. As such, increasing global average temperature results in an
1778 increase in the amount of water and dissolved and solid materials transferred from the
1779 continents to the oceans. In our model we estimate the amount of sediment transported
1780 annually to the oceans during the Phanerozoic by examining variations in surface runoff.
1781 Today, surface runoff annually transfers $1.00\text{x}10^{17}$ kg of H_2O and ~20 billion tons
1782 ($18.1\text{x}10^{12}$ kg) of sediment to the oceans (Holeman, 1968). For comparison, at 573 Ma

(slushball earth conditions), ~28% of the continental surface was covered by ice and total precipitation onto the continents was commensurately decreased. As such, the amount of water transferred from the SW reservoir to the oceans ($5.05x10^{16}$ kg/yr) was ~50% less than the present value. Assuming that the relationship between surface runoff and sediment transport was the same as today, the amount of sediment annually transported into the oceans by rivers at 573 Ma would be ~10 billion tons ($9.07x10^{12}$ kg), or ~50% of the modern amount. Potential impacts on ocean chemistry and sediment accumulation rates of such variations in masses of sediment delivered to the oceans is considered elsewhere (Angel et al., in prep).

Surface runoff from the continents to the oceans not only transports sediments but also transports dissolved components that to a large extent control ocean chemistry. Dissolved components that are transported to the oceans in the largest amounts today by rivers are silica, bicarbonate, Ca, Na, Mg and Cl. Variations in surface runoff discussed can be related to changes in the amount (number of moles) of dissolved species annually transferred to the oceans during the Phanerozoic. Moreover, if the rate of input of dissolved species into the oceans increases (or decreases), and if the rate at which physical and chemical processes remove these components from seawater remains constant, then average residence times must change. Today, major dissolved chemical species in seawater have residence times that vary from thousands to millions of years (Table 5).

Marine organisms such as foraminifera and diatoms rely on dissolved bicarbonate and silica to produce protective tests (shells). The replacement (residence) times of H_4SiO_4 and HCO_3 are relatively short (<1 Ma), and variations in surface runoff could significantly affect the concentrations of both of these components that are critical to

Element	Seawater (mmol/kg)	River water (mmol/kg)	Seawater residence time (10^6 yr)
Cl	546.0	0.22	87
Na	468.0	0.26	55
Mg	53.1	0.17	13
SO_4	28.2	0.11	8.7
Ca	10.3	0.38	1.0
K	10.2	0.07	10
HCO_3	2.39	0.96	0.083
H_4SiO_4	0.0483	0.218	0.021

Table 5: The average major ion compositions of seawater and river water (after Livingstone, 1963; Holland, 1978). Residence times from Berner and Berner (1987).

biomineralization processes. An increase in surface runoff would increase the amount of H_4SiO_4 and HCO_3 transported to the oceans, which could result in a surge in marine primary productivity as forams and diatoms produce tests in bicarbonate and silica-rich water. Conversely, a decrease in surface runoff and concomitant decrease in H_4SiO_4 and HCO_3 transport could result in a decrease in primary productivity as seawater becomes increasingly bicarbonate and silica depleted.

Many geochemical processes that operate in the near-surface environment involve water or aqueous solutions that serve to mediate and promote these processes. As such, other global chemical cycles (e.g., carbon cycle, sulfur cycle, atmosphere oxygenation) that occur within the hydrosphere will also be affected by changes in the sizes of reservoirs within the hydrologic cycle and rates at which water is exchanged between reservoirs. A broader understanding of the interplay between the Earth's hydrologic cycle in deep time and other global chemical cycles will advance our knowledge concerning the evolution of the planet we live on. We encourage future work to identify and quantify specific factors or events that link the water cycle to other geochemical cycles, so that we may better understand the Earth system as a whole.

References

Aguilar-Islas, A. M., Rember, R. D., Mordy, C. W., & Wu, J., 2008, Sea ice‐derived dissolved iron and its potential influence on the spring algal bloom in the Bering Sea, Geophysical Research Letters, v. 35, p. 24.

Algeo, T. J., Scheckler, S. E., & Maynard, J. B., 2001, Effects of the Middle to Late Devonian spread of vascular land plants on weathering regimes, marine biotas, and global climate. Plants invade the land: evolutionary and environmental perspectives, Columbia University Press, New York, 213-236.

Algeo, T. J., & Scheckler, S. E., 1998, Terrestrial-marine teleconnections in the Devonian: links between the evolution of land plants, weathering processes, and marine anoxic events. Philosophical Transactions of the Royal Society of London B: Biological Sciences, v. 53(1365), p. 113-130.

Allison, I., 1996, Icebergs, in Schneider, S.H., ed., Encyclopedia of Climate and Weather: New York, Oxford University Press, v. 1, p. 426–427.

Alroy, J., 1998, Cope's rule and the dynamics of body mass evolution in North American fossil mammals. Science, v. 280(5364), p. 731-734.

Arnall, A., & Kothari, U., 2015, Challenging climate change and migration discourse: Different understandings of timescale and temporality in the Maldives, Global Environmental Change, v. 31, p. 199-206.

Ashkenazy, Y., Gildor, H., Losch, M., Macdonald, F. A., Schrag, D. P., & Tziperman, E., 2013, Dynamics of a Snowball Earth ocean, Nature, v. 495(7439), p. 90.

Ausich, W. I., & Peters, S. E., 2005, A revised macroevolutionary history for Ordovician–Early Silurian crinoids, Paleobiology, v. 31(3), p. 538-551.

Bala, G., Caldeira, K., Mirin, A., Wickett, M., Delire, C., & Phillips, T. J., 2006, Biogeophysical effects of CO_2 fertilization on global climate. Tellus B, v. 58(5), p. 620-627.

Bambach, R. K. (1993). Seafood through time: changes in biomass, energetics, and productivity in the marine ecosystem. Paleobiology, 19(03), 372-397.

Bambach, R. K., Knoll, A. H., & Wang, S. C., 2004, Origination, extinction, and mass depletions of marine diversity, Paleobiology, v. 30(04), p. 522-542.

Barry, R.G. and Chorley, R.J., 2009, Atmosphere, weather and climate, Routledge.

Bentley, C. R., & Giovinetto, M. B., 1992, Mass balance of Antarctica and sea level change. Wisconsin University-Madison Geophysical and Polar Research Center.

Benton, M. J., 1993, The Fossil Record 2, Chapman and Hall, London.

Benton, M. J., (1995, Diversification and extinction in the history of life, Science, v. 268(5207), p. 52-58.

Benton, M. J., & Twitchett, R. J., 2003, How to kill (almost) all life: the end-Permian extinction event, Trends in Ecology & Evolution, v. 18(7), p. 358-365.

Benzing, D.H., 2004, Vascular epiphytes. In: Lowman, M.D., Rinker, H.B. (Eds.), Forest Canopies. Elseiver Academic Press, MA, pp. 175–211.

Bergman, N. M., Lenton, T. M., & Watson, A. J., 2004, COPSE: a new model of biogeochemical cycling over Phanerozoic time, American Journal of Science, v. 304(5), p. 397-437.

Berner, E. K., & Berner, R. A., 2012, Global environment: water, air, and geochemical cycles, Princeton University Press.

Berner, R. A., 1994, GEOCARB II: A revised model of atmospheric CO_2 over Phanerozoic time, American Journal of Science, v. 294(1).

Berner, R. A., 1997, The rise of plants and their effect on weathering and atmospheric CO2, Science, v. 276(5312), p. 544-546.

Betzold, C., 2015, Adapting to climate change in small island developing states, Climatic Change, v. 133(3), p. 481-489.

Bintanja, R., & Selten, F. M., 2014, Future increases in Arctic precipitation linked to local evaporation and sea-ice retreat, Nature, v. 509(7501), p. 479-482.

Blackburn, T. J., Olsen, P. E., Bowring, S. A., McLean, N. M., Kent, D. V., Puffer, J., McHone, G., Rasbury, E.T., & Et-Touhami, M., 2013, Zircon U-Pb geochronology links the end-Triassic extinction with the Central Atlantic Magmatic Province, Science, v. 340(6135), p. 941-945.

Bliss, A. K., Cuffey, K. M., & Kavanaugh, J. L., 2011, Sublimation and surface energy budget of Taylor Glacier, Antarctica, Journal of Glaciology, v. 57(204), p. 684-696.

Bloetscher, F., & Romah, T., 2015, Tools for assessing sea level rise vulnerability, Journal of Water and Climate Change, v. 6(2), p. 181-190.

Bodnar, R. J., Azbej, T., Becker, S. P., Cannatelli, C., Fall, A., & Severs, M. J., 2013, Whole Earth geohydrologic cycle, from the clouds to the core: The distribution of water in the dynamic Earth system, Geological Society of America Special Papers, v. 500, p. 431-461.

Bond, D., Wignall, P. B., & Racki, G., 2004, Extent and duration of marine anoxia during the Frasnian–Famennian (Late Devonian) mass extinction in Poland, Germany, Austria and France, Geological Magazine, v. 141(02), p. 173-193.

Bounama, C., Franck, S., & Von Bloh, W., 2001, The fate of Earth's ocean, Hydrology and Earth System Sciences Discussions, v. 5(4), p. 569-576.

Bowen, G.J., Maibauer, B.J., Kraus, M.J., Röhl, U., Westerhold, T., Steimke, A., Gingerich, P.D., Wing, S.L. and Clyde, W.C., 2015, Two massive, rapid releases of carbon during the onset of the Palaeocene-Eocene thermal maximum, Nature Geoscience, v. 8(1), p.44-47.

Brenchley, P. J., Marshall, J. D., & Underwood, C. J., 2001, Do all mass extinctions represent an ecological crisis? Evidence from the Late Ordovician, Geological Journal, v. 36(3‐4), p. 329-340.

Burnett, W. C., Bokuniewicz, H., Huettel, M., Moore, W. S., & Taniguchi, M., 2003, Groundwater and pore water inputs to the coastal zone, Biogeochemistry, v. 66(1-2), p. 3-33.

CIA World Book: https://www.cia.gov/library/publications/the-world-factbook/ (accessed May 2015)

Claeys, P., Casier, J. G., & Margolis, S. V., 1992, Microtektites and mass extinctions-Evidence for a late Devonian asteroid impact, Science, v. 257(5073), p. 1102-1104.

Cohen, K.M., Finney, S., Gibbard, P.L., 2013, International Commission on Stratigraphy.

Cohen, J. E., & Small, C., 1998, Hypsographic demography: The distribution of human population by altitude, Proceedings of the National Academy of Sciences, v. 95(24), p. 14009-14014.

Cope, E. D., 1887, The origin of the fittest: essay on evolution, Appleton.

Cox, P. M., Betts, R. A., Jones, C. D., Spall, S. A., & Totterdell, I. J., 2000, Acceleration of global warming due to carbon-cycle feedbacks in a coupled climate model, Nature, v. 408(6809), p. 184-187.

Crisp, M. D., & Cook, L. G., 2011, Cenozoic extinctions account for the low diversity of extant gymnosperms compared with angiosperms, New Phytologist, v. 192(4), p. 997-1009.

Cummins, 2007, Biological Science (3 ed.), Freeman, Scott, p. 215

D'Hondt, S., Donaghay, P., Zachos, J. C., Luttenberg, D., & Lindinger, M., 1998, Organic carbon fluxes and ecological recovery from the Cretaceous-Tertiary mass extinction, Science, v. 282(5387), p. 276-279.

DiMichele, W. A., Pfefferkorn, H. W., & Gastaldo, R. A., 2001, Response of Late Carboniferous and Early Permian Plant Communities to Climate Change 1, Annual Review of Earth and Planetary Sciences, v. 29(1), p. 461-487.

Döll, P., & Fiedler, K., 2007, Global-scale modeling of groundwater recharge, Hydrology and Earth System Sciences Discussions Discussions, v. 4(6), p. 4069-4124.

Donnadieu, Y., Goddéris, Y., & Bouttes, N., 2009, Exploring the climatic impact of the continental vegetation on the Mezosoic atmospheric CO2 and climate history, Climate of the Past, v. 5(1), p. 85-96.

Drever, J. I., 1997, The geochemistry of natural waters, 3rd edition (Vol. 437), New Jersey: Prentice Hall.

DuToit, A.L., 1956, Geology of South Africa, Oliver and Boyd, Edinburgh, pp. 611

Dyurgerov, M. B., & Meier, M. F., 2005, Glaciers and the changing Earth system: a 2004 snapshot (Vol. 58), Boulder: Institute of Arctic and Alpine Research, University of Colorado.

Ehlers, J., & Gibbard, P. L., 2004, Quaternary glaciations-extent and chronology: part I: Europe (Vol. 2), Elsevier.

Erwin, D. H., 2000, The Permo-Triassic extinction, Shaking the Tree: Readings from Nature in the History of Life, 189.

Ewing, R. C., Eisenman, I., Lamb, M. P., Poppick, L., Maloof, A. C., & Fischer, W. W., 2014, New constraints on equatorial temperatures during a Late Neoproterozoic snowball Earth glaciation, Earth and Planetary Science Letters, .v 406, p. 110-122.

Fawcett, P. J., & Barron, E. J., 1998, The role of geography and atmospheric CO^2 in long-term climate change: Results from model simulations for the Late Permian to the Present, Oxford Monographs on Geology and Geophysics, v. 39, p. 21-38.

Fédération Aéronautique Internationale, 2012, 100 km Boundary for Astronauts: http://www.fai.org/icare-records/100km-altitude-boundary-for-astronautics (accessed September 2014).

Fetterer, F., K. Knowles, W. Meier, and M. Savoie., 2002, updated daily, Sea Ice Index, Boulder, Colorado USA: National Snow and Ice Data Center, http://dx.doi.org/10.7265/N5QJ7F7W: http://nsidc.org/data/seaice_index/

Finnegan, S., Bergmann, K., Eiler, J.M., Jones, D.S., Fike, D.A., Eisenman, I., Hughes, N.C., Tripati, A.K. and Fischer, W.W., 2011, The magnitude and duration of Late Ordovician–Early Silurian glaciation, Science, v. 331(6019), p.903-906.

Flessa, K. W., & Jablonski, D., 1985, Declining Phanerozoic background extinction rates: effect of taxonomic structure?, Nature, v. 313(5999), p. 216-218.

Frakes, L.A., Francis, J.E., Syktus, J.I., 1992, Climate Modes of the Phanerozoic, Cambridge University Press, Cambridge.

Franck, S., Bounama, C., Von Bloh. W., 2006, Causes and timing of future biosphere extinctions. Biogeosciences, European Geosciences Union, v. 3 (1), p.85-92.

Gash, J. H., Nobre, C. A., Roberts, J. M., & Victoria, R. L., 1996, Amazonian deforestation and climate, John Wiley & Sons Ltd.

Gernon, T. M., Hincks, T. K., Tyrrell, T., Rohling, E. J., & Palmer, M. R., 2016, Snowball Earth ocean chemistry driven by extensive ridge volcanism during Rodinia breakup, Nature Geoscience, v. 9(3), p. 242-248.

Gleick, P. H., 1996, Water resources Encyclopedia of climate and weather, v. 2, p. 817-823.

Gleitz, M., vd Loeff, M. R., Thomas, D. N., Dieckmann, G. S., & Millero, F. J., 1995, Comparison of summer and winter inorganic carbon, oxygen and nutrient concentrations in Antarctic sea ice brine, Marine Chemistry, v. 51(2), p. 81-91.

Goddéris, Y., Donnadieu, Y., Nédélec, A., Dupré, B., Dessert, C., Grard, A., & Francois, L. M., 2003, The Sturtian 'snowball' glaciation: fire and ice, Earth and Planetary Science Letters, v. 211(1), p. 1-12.

Goddéris, Y., Donnadieu, Y., Le Hir, G., Lefebvre, V., & Nardin, E., 2014, The role of palaeogeography in the Phanerozoic history of atmospheric CO 2 and climate, Earth-Science Reviews, v. 128, p. 122-138.

Good, S. P., Noone, D., Kurita, N., Benetti, M., & Bowen, G. J., 2015, D/H isotope ratios in the global hydrologic cycle, Geophysical Research Letters, v. 42(12), p. 5042-5050.

Graham, A., 2011, The age and diversification of terrestrial New World ecosystems through Cretaceous and Cenozoic time, American Journal of Botany, v. 98(3), p. 336-351.

Grénier, P., De Elia, R., & Chaumont, D., 2015, Chances of Short-Term Cooling Estimated from a Selection of CMIP5-Based Climate Scenarios during 2006–35 over Canada, Journal of Climate, v. 28(8), p. 3232-3249.

Gulbranson, E. L., Montañez, I. P., Schmitz, M. D., Limarino, C. O., Isbell, J. L., Marenssi, S. A., & Crowley, J. L., 2010, High-precision U-Pb calibration of Carboniferous glaciation and climate history, Paganzo Group, NW Argentina, Geological Society of America Bulletin, v. 122(9-10), p. 1480-1498.

Hallam, A., 1985, A review of Mesozoic climates, Journal of the Geological Society, v. 142(3), p. 433-445.

Halverson, G. P., Hoffman, P. F., Schrag, D. P., Maloof, A. C., & Rice, A. H. N., 2005, Toward a Neoproterozoic composite carbon-isotope record, Geological Society of America Bulletin, v. 117(9-10), p. 1181-1207.

Hanna, E., Huybrechts, P., Steffen, K., Cappelen, J., Huff, R., Shuman, C., Irvine-Fynn, T., Wise, S. and Griffiths, M., 2008, Increased runoff from melt from the Greenland Ice Sheet: a response to global warming, Journal of Climate, v. 21(2), p.331-341.

Harris, T. M., 1976, Two neglected aspects of fossil conifers, American Journal of Botany, p. 902-910.

Hawkings, J.R., Wadham, J., Tranter, M., Lawson, E., Sole, A., Cowton, T., Tedstone, A.J., Bartholomew, I., Nienow, P., Chandler, D. and Telling, J., 2015, The effect of warming climate on nutrient and solute export from the Greenland Ice Sheet, Geochemistry Perspectives Letters, v. 1, p.94-104.

Helm, V., Humbert, A., & Miller, H., 2014, Elevation and elevation change of Greenland and Antarctica derived from CryoSat-2, The Cryosphere, v. 8(4), p. 1539-1559.

Herrmann, A. D., Haupt, B. J., Patzkowsky, M. E., Seidov, D., & Slingerland, R. L., 2004, Response of Late Ordovician paleoceanography to changes in sea level, continental drift, and atmospheric pCO 2: potential causes for long-term cooling and glaciation, Palaeogeography, Palaeoclimatology, Palaeoecology, v. 210(2), p. 385-401.

Holeman, J. N., 1968, The sediment yield of major rivers of the world, Water Resources Research, v. 4(4), p. 737-747.

Holland, S. M., & Patzkowsky, M. E., 2009, The stratigraphic distribution of fossils in a tropical carbonate succession: Ordovician Bighorn Dolomite, Wyoming, USA, Palaios, v. 24(5), p. 303-317.

Hone, D. W., & Benton, M. J., 2005, The evolution of large size: how does Cope's Rule work?, Trends in Ecology & Evolution, v. 20(1), p. 4-6.

Hönisch, B., Ridgwell, A., Schmidt, D. N., Thomas, E., Gibbs, S. J., Sluijs, A., Zeebe, R., Kump, L., Martindale, R.C., Greene, S.E., & Kiessling, W., 2012, The geological record of ocean acidification Science, v. 335(6072), p. 1058-1063.

Hyde, W. T., Crowley, T. J., Baum, S. K., & Peltier, W. R., 2000, Neoproterozoic 'snowball Earth'simulations with a coupled climate/ice-sheet model, Nature, v. 405(6785), p. 425-429.

Intergovernmental Panel on Global Climate, 2007, Climate change 2007: The physical science basis. Agenda, v. 6(07), p. 333.

Jablonski, D., & Chaloner, W. G., 1994, Extinctions in the fossil record [and discussion], Philosophical Transactions of the Royal Society of London B: Biological Sciences, v. 344(1307), p. 11-17.

Janssens, I., & Huybrechts, P., 2000, The treatment of meltwater retention in mass-balance parameterizations of the Greenland ice sheet, Annals of Glaciology, v. 31(1), p. 133-140.

Johnsson, M. J., 1993, The system controlling the composition of clastic sediments, Geological Society of America Special Papers, v. 284, p. 1-20.

Kallmeyer, J., Pockalny, R., Adhikari, R. R., Smith, D. C., & D'Hondt, S., 2012, Global distribution of microbial abundance and biomass in subseafloor sediment, Proceedings of the National Academy of Sciences, v. 109(40), p. 16213-16216.

Kalnay, E., Kanamitsu, K., Kistler, R.,Collins, W.,Deaven, D., Gandin, L., Iredell, M., Saha, S., White, G., Woollen, J., Zhu, Y., Chelliah, M., Ebisuzaki, W., Higgins, W., Janowiak, J., Mo, K.C., Ropelewski, C., Wang, J., Leetmaa, A., Reynolds, R., Jenne, R., & Joseph, D., 1996, The NCEP/NCAR 40-Year Reanalysis Project, Bulletin of the American Meteorological Society, v. 77(3), p. 437–471.

Kingsolver, J. G., & Pfennig, D. W., 2004, Individual-level selection as a cause of Cope's rule of phyletic size increase, Evolution, v. 58(7), p. 1608-1612.

Kopec, B. G., Feng, X., Michel, F. A., & Posmentier, E. S., 2016, Influence of sea ice on Arctic precipitation, Proceedings of the National Academy of Sciences, v. 113(1), p. 46-51.

Kozlowski, R., & Greguss, P., 1959, Discovery of Ordovician land plants. Acta Palaeontologica Polonica, 4(1).

Kwon, E. Y., Kim, G., Primeau, F., Moore, W. S., Cho, H. M., DeVries, T., Sarmiento, J.L., Charette, M.A., & Cho, Y. K., 2014, Global estimate of submarine groundwater discharge based on an observationally constrained radium isotope model, Geophysical Research Letters, v. 41(23), p. 8438-8444.

Labat, D., Goddéris, Y., Probst, J. L., & Guyot, J. L., 2004, Evidence for global runoff increase related to climate warming, Advances in Water Resources, v. 27(6), p. 631-642.

Lawrence, M. G., 2005, The relationship between relative humidity and the dewpoint temperature in moist air: A simple conversion and applications, Bulletin of the American Meteorological Society, v. 86(2), p. 225-233.

Lawrence, D. M., Thornton, P. E., Oleson, K. W., & Bonan, G. B., 2007, The partitioning of evapotranspiration into transpiration, soil evaporation, and canopy evaporation in a GCM: Impacts on land-atmosphere interaction, Journal of Hydrometeorology, v. 8(4), p. 862-880.

Le Hir, G., Donnadieu, Y., Goddéris, Y., Meyer-Berthaud, B., Ramstein, G., & Blakey, R. C., 2011, The climate change caused by the land plant invasion in the Devonian, Earth and Planetary Science Letters, v. 310(3), p. 203-212.

Lefebvre, V., Servais, T., François, L., & Averbuch, O., 2010, Did a Katian large igneous province trigger the Late Ordovician glaciation?: A hypothesis tested with a carbon cycle model, Palaeogeography, Palaeoclimatology, Palaeoecology, v. 296(3), p. 310-319.

Lenton, T. M., Daines, S. J., Mills, B., & Boyle, R. A., 2014, Co-evolution of Eukaryotes and Ocean and Atmosphere Oxygenation in the Neoproterozoic and Paleozoic Eras, AGU Fall Meeting Abstracts v. 1, p. 05.

Liao, J., Huey, L.G., Liu, Z., Tanner, D.J., Cantrell, C.A., Orlando, J.J., Flocke, F.M., Shepson, P.B., Weinheimer, A.J., Hall, S.R. and Ullmann, K., 2014, High levels of molecular chlorine in the Arctic atmosphere, Nature Geoscience, v. 7(2), p.91-94.

Liu, S. C., Fu, C., Shiu, C. J., Chen, J. P., & Wu, F., 2009, Temperature dependence of global precipitation extremes, Geophysical Research Letters, v. 36(17).

Livingstone, D.A., 1963, Chemical composition of rivers and lakes, United States Geological Survey.

Lowe, P. R., & Ficke, J. M., 1974, The computation of saturation vapor pressure (No. ENVPREDRSCHF-TECH-PAPER-4-74). Naval Environmental Prediction Research Facility, Monterey, CA.

Lund, D. C., Asimow, P. D., Farley, K. A., Rooney, T. O., Seeley, E., Jackson, E. W., & Durham, Z. M., 2016, Enhanced East Pacific Rise hydrothermal activity during the last two glacial terminations, Science, v. 351(6272), p. 478-482.

Luthcke, S.B., Zwally, H.J., Abdalati, W., Rowlands, D.D., Ray, R.D., Nerem, R.S., Lemoine, F.G., McCarthy, J.J. and Chinn, D.S., 2006, Recent Greenland ice mass loss by drainage system from satellite gravity observations, Science, v. 314(5803), p.1286-1289.

Lyons, W. B., Dailey, K. R., Welch, K. A., Deuerling, K. M., Welch, S. A., & McKnight, D. M., 2015, Antarctic streams as a potential source of iron for the Southern Ocean,Geology, v. 43(11), p. 1003-1006.

Mahan, K. H., Wernicke, B. P., & Jercinovic, M. J., 2010, Th–U–total Pb geochronology of authigenic monazite in the Adelaide rift complex, South Australia, and implications for the age of the type Sturtian and Marinoan glacial deposits, Earth and Planetary Science Letters, v. 289(1), p. 76-86.

Mandlebrot, B. B., 1984, The fractal geometry of nature, Macmillan.

Martin, R. E., 1996, Secular increase in nutrient levels through the Phanerozoic: implications for productivity, biomass, and diversity of the marine biosphere, Palaios, v. 209-219.

Martin, H. A., 2006, Cenozoic climatic change and the development of the arid vegetation in Australia, Journal of Arid Environments, v. 66(3), p. 533-563.

McElwain, J. C., & Punyasena, S. W., 2007, Mass extinction events and the plant fossil record, Trends in Ecology & Evolution, v. 22(10), p. 548-557.

McGhee, G. R., 1988, The Late Devonian extinction event: evidence for abrupt ecosystem collapse, Paleobiology, v. 14(03), p. 250-257.

McGhee, G. R., 2001, Late Devonian extinction, Palaeobiology II, v. 223-226.

McInerney, F. A., & Wing, S. L., 2011, The Paleocene-Eocene Thermal Maximum: a perturbation of carbon cycle, climate, and biosphere with implications for the future, Annual Review of Earth and Planetary Sciences, v. 39, p. 489-516.

McMenamin, M. A., & McMenamin, D., 1994, Hypersea, New York.

Meier, M. F., & Bahr, D. B., 1996, Counting glaciers: use of scaling methods to estimate the number and size distribution of the glaciers of the world, In Glaciers, Ice Sheets and Volcanoes: A Tribute to Mark F. Meier: CRREL Special Report, v. 96, p. 89-94.

Mii, H. S., Grossman, E. L., & Yancey, T. E., 1999, Carboniferous isotope stratigraphies of North America: Implications for Carboniferous paleoceanography and Mississippian glaciation, Geological Society of America Bulletin, v. 111(7), p. 960-973.

Moore, W. S., 2010, The effect of submarine groundwater discharge on the ocean, Annual Review of Marine Science, v. 2, p. 59-88.

Müller, R. D., Sdrolias, M., Gaina, C., Steinberger, B., & Heine, C., 2008, Long-term sea-level fluctuations driven by ocean basin dynamics, Science, v. 319(5868), p. 1357-1362.

Murphy, J. B., & Nance, R. D., 2013, Speculations on the mechanisms for the formation and breakup of supercontinents, Geoscience Frontiers, v. 4(2), p. 185-194.

National Research Council, 2001, Basic research opportunities in earth science, National Academy Press, Washington DC, USA.

New, M., Lister, D., Hulme, M., & Makin, I., 2000, A high-resolution data set of surface climate over global land areas, Climate Research v. 21, p. 1-25.

Nielsen, P., 1990, Tidal dynamics of the water table in beaches, Water Resources Research, v. 26(9), p. 2127-2134.

NOAA National Climatic Data Center, 2015: http://www.ncdc.noaa.gov/

Oerlemans, J., Anderson, B., Hubbard, A., Huybrechts, P., Johannesson, T., Knap, W.H., Schmeits, M., Stroeven, A.P., Van de Wal, R.S.W., Wallinga, J. and Zuo, Z., 1998, Modelling the response of glaciers to climate warming, Climate dynamics, v. 14(4), p.267-274.

Ohmura, A., & Reeh, N., 1991, New precipitation and accumulation maps for Greenland, Journal of Glaciology, v. 37(125), p. 140-148.

Otto-Bliesner, B. L., 1995, Continental drift, runoff and weathering feedbacks: Implications from climate model experiments, Journal of Geophysical Research, v. 100(D6), p. 11-537.

Parkinson, C.L., 1996, Sea Ice, in Schneider, S.H., ed., Encyclopedia of Climate and Weather: New York, Oxford University Press, v. 2, p. 669–675.

Peters, S. E., 2006, Genus extinction, origination, and the durations of sedimentary hiatuses, Paleobiology, v. 32(03), p. 387-407.

Pierrehumbert, R. T., 2005, Climate dynamics of a hard snowball Earth.Journal of Geophysical Research: Atmospheres, v. 110(D1).

Pierrehumbert, R. T., Abbot, D. S., Voigt, A., & Koll, D., 2011, Climate of the Neoproterozoic, Annual Review of Earth and Planetary Sciences, v. 39(1), p. 417.

Pimentel, D., Harvey, C., Resosudarmo, P., & Sinclair, K., 1995, Environmental and economic costs of soil erosion and conservation benefits, Science, v. 267(5201), p. 1117.

Pollard, D., & Kasting, J. F., 2004, Climate‐ice sheet simulations of neoproterozoic glaciation before and after collapse to Snowball Earth, The Extreme Proterozoic: Geology, Geochemistry, and Climate, p. 91-105.

Poore, R.Z., Williams, R.S., Jr., and Tracey, Christopher, 2000, Sea level and climate: U.S. Geological Survey Fact Sheet 002–00, 2 p.: https://pubs.usgs.gov/fs/fs2-00/.

Poore, R.Z., Williams, R.S., Jr., and Tracey, C., 2000, Sea level and climate: U.S. Geological Survey Fact Sheet 002–00: https://pubs.usgs.gov/fs/fs2-00/

Poorter, L., Bongers, F., Aide, T. M., Zambrano, A. M. A., Balvanera, P., Becknell, J. M., Boukili, V., Brancalion, P.H., Broadbent, E.N., Chazdon, R.L., & Craven, D., 2016, Biomass resilience of Neotropical secondary forests, Nature, v. 530(7589), p. 211-214.

Prave, A. R., 1999, Two diamictites, two cap carbonates, two δ13C excursions, two rifts: the Neoproterozoic Kingston Peak Formation, Death Valley, California, Geology, v. 27(4), p. 339-342.

Reeburgh, W. S., 1997, Figures summarizing the global cycles of biogeochemically important elements, Bulletin of the Ecological Society of America, v. 78(4), p. 260-267.

Reynolds, R.W., N.A. Rayner, T.M. Smith, D.C. Stokes, and W. Wang, 2002, An improved in situ and satellite SST analysis for climate, Journal of Climate, v. 15, p. 1609-1625.

Retallack, G. J., Metzger, C. A., Greaver, T., Jahren, A. H., Smith, R. M., & Sheldon, N. D., 2006, Middle-Late Permian mass extinction on land, Geological Society of America Bulletin, v. 118(11-12), p. 1398-1411.

Riedl, R. J., Huang, N., & Machan, R., 1972, The subtidal pump: a mechanism of interstitial water exchange by wave action, Marine Biology, v. 13(3), p. 210-221.

Ronov, A. B., 1982, The Earth's sedimentary shell (quantitative patterns of its structure, compositions, and evolution): The 20th VI Vernadskly Lecture, March 12, 1978, International Geology Review, v. 24(12), p. 1365-1388.

Ryu, Y., Baldocchi, D.D., Kobayashi, H., Ingen, C., Li, J., Black, T.A., Beringer, J., Gorsel, E., Knohl, A., Law, B.E. and Roupsard, O., 2011, Integration of MODIS land and atmosphere products with a coupled‐process model to estimate gross primary productivity and evapotranspiration from 1 km to global scales, Global Biogeochemical Cycles, v. 25(4).

Saltzman, M. R., & Young, S. A., 2005, Long-lived glaciation in the Late Ordovician? Isotopic and sequence-stratigraphic evidence from western Laurentia, Geology, v. 33(2), p. 109-112.

Schaller, M. F., Wright, J. D., & Kent, D. V., 2011, Atmospheric pCO_2 perturbations associated with the Central Atlantic magmatic province, Science, v. 331(6023), p. 1404-1409.

Scher, H. D., Bohaty, S. M., Zachos, J. C., & Delaney, M. L., 2011, Two-stepping into the icehouse: East Antarctic weathering during progressive ice-sheet expansion at the Eocene–Oligocene transition, Geology, v. 39(4), p. 383-386.

Scher, H. D., Bohaty, S. M., Smith, B. W., & Munn, G. H., 2014, Isotopic interrogation of a suspected late Eocene glaciation, Paleoceanography, v. 29(6), p. 628-644.

Schlesinger, W.H., 1997, Biogeochemistry: An analysis of global change, 2nd edition: San Diego, California, Academic Press, 588 p.

Schmittner, A., Yoshimori, M., & Weaver, A. J., 2002, Instability of glacial climate in a model of the ocean-atmosphere-cryosphere system, Science, v. 295(5559), p. 1489-1493.

Schulte, P., Alegret, L., Arenillas, I., Arz, J. A., Barton, P. J., Bown, P. R., Bralower, T.J., Christeson, G.L., Claeys, P., Cockell, C.S., & Collins, G. S., 2010, The Chicxulub asteroid impact and mass extinction at the Cretaceous-Paleogene boundary, Science, v. 327(5970), p. 1214-1218.

Schumm, S. A., 1977, The fluvial system (Vol. 338), New York: Wiley.

Scotese, C. R., 2001, PALEOMAP Project: http://www.scotese.com (accessed May 2014).

Sepkoski Jr, J. J., 1993, Ten years in the library: new data confirm paleontological patterns, Paleobiology, p. 43-51.

Sepkoski Jr, J. J., 1994, Extinction and the fossil record, Geotimes, v. 39(3), p. 15.

Sheehan, P. M., 2001, The late Ordovician mass extinction, Annual Review of Earth and Planetary Sciences, v. 29(1), p. 331-364.

Shiklomanov, I. A., 1993, World Fresh Water Resource, In: Gleick, PH (Ed.) Water crisis: A guide to world fresh water resources.

Shukla, J., Nobre, C., & Sellers, P., 1990, Amazon deforestation and climate change, Science, v. 247(4948), p. 1322-1325.

Smith, A. B., 2007, Marine diversity through the Phanerozoic: problems and prospects, Journal of the Geological Society, v. 164(4), p. 731-745.

Sole, R. V., & Newman, M., 2002, Extinctions and biodiversity in the fossil record—volume two, the earth system: biological and ecological dimensions of global environment change, Encyclopedia of Global Environmental Change, p. 297-391.

Soreghan, G. S., & Giles, K. A., 1999, Amplitudes of late Pennsylvanian glacioeustasy, Geology, v. 27(3), p. 255-258.

Sun, Y., Solomon, S., Dai, A., & Portmann, R. W., 2007, How often will it rain?, Journal of Climate, v. 20(19), p. 4801-4818.

Swanson-Hysell, N. L., Rose, C. V., Calmet, C. C., Halverson, G. P., Hurtgen, M. T., & Maloof, A. C., 2010, Cryogenian glaciation and the onset of carbon-isotope decoupling, Science, v. 328(5978), p. 608-611.

Taniguchi, M., Burnett, W. C., Cable, J. E., & Turner, J. V., 2002, Investigation of submarine groundwater discharge, Hydrological Processes, v. 16(11), p. 2115-2129.

Taniguchi, M., Shimada, J., Fukuda, Y., Yamano, M., Onodera, S. I., Kaneko, S., & Yoshikoshi, A., 2009, Anthropogenic effects on the subsurface thermal and groundwater environments in Osaka, Japan and Bangkok, Thailand, Science of the total environment, v. 407(9), p. 3153-3164.

Tardy, Y., Nkounkou, R. R., & Probst, J. L., 1989, The global water cycle and continental erosion during Phanerozoic time (570 my), American Journal of Science, v. 289, p. 455-483.

Trenberth, K. E., Caron, J. M., & Stepaniak, D. P., 2001, The atmospheric energy budget and implications for surface fluxes and ocean heat transports, Climate dynamics, v. 17(4), p. 259-276.

Trenberth, K. E., Dai, A., Rasmussen, R. M., & Parsons, D. B., 2003, The changing character of precipitation, Bulletin of the American Meteorological Society, v. 84(9), p. 1205-1217.

Trenberth, K. E., & Smith, L., 2005, The mass of the atmosphere: A constraint on global analyses, Journal of Climate, v. 18(6), p. 864-875.

United States Geological Survey, 2016, Ice, Snow, and Glaciers: The Water Cycle: http://water.usgs.gov/edu/watercycleice.html

Visser, J. N. J., 1987, The palaeogeography of part of southwestern Gondwana during the Permo-Carboniferous glaciation, Palaeogeography, Palaeoclimatology, Palaeoecology, v. 61, p. 205-219.

Wagnon, P., Ribstein, P., Francou, B., & Pouyaud, B., 1999, Annual cycle of energy balance of Zongo glacier, Cordillera Real, Bolivia. Journal of Geophysical Research: Atmospheres, v. 104(D4), p. 3907-3923.

Willett, K.M., Dunn, R.J.H., Thorne, P.W., Bell, S., De Podesta, M., Parker, D.E., Jones, P.D. and Williams Jr, C.N., 2014, HadISDH land surface multi-variable humidity and temperature record for climate monitoring, Climate of the Past, v. 10(6), p.1983-2006.

Whitman, W. B., Coleman, D. C., & Wiebe, W. J., 1998, Prokaryotes: the unseen majority, Proceedings of the National Academy of Sciences, v. 95(12), p. 6578-6583.

Young, S. A., Saltzman, M. R., Ausich, W. I., Desrochers, A., & Kaljo, D.. 2010, Did changes in atmospheric CO_2 coincide with latest Ordovician glacial–interglacial cycles?, Palaeogeography, Palaeoclimatology, Palaeoecology, v. 296(3), p. 376-388.

Zachos, J. C., Dickens, G. R., & Zeebe, R. E., 2008, An early Cenozoic perspective on greenhouse warming and carbon-cycle dynamics, Nature, v. 451(7176), p. 279-283.

Zekster, I. S., & Loaiciga, H. A., 1993, Groundwater fluxes in the global hydrologic cycle: past, present, and future, Journal of Hydrology, v. 144, p. 405-427.

Zheng, F. L., 2006, Effect of vegetation changes on the soil erosion on the Loess Plateau, Pedosphere, v. 16(4), p. 420-427.

Zimen, K. E., & Altenhein, F. K., 1973, The future burden of industrial CO_2 on the atmosphere and the oceans, Zeitschrift für Naturforschung A, v. 28(11), p. 1747-1752.

Appendix 1: Flowchart of the interactions of parameters, reservoirs, and fluxes within the numerical model (See also Fig. 1).